

# UNIVERSITY OF PADUA

Department of ICEA





UNIVERSITY OF PADUA

—  
DEPARTMENT ICEA

—  
MSc LEVEL DEGREE IN  
ENVIRONMENTAL ENGINEERING

—  
THESIS:

BIOGAS DRAINAGE LAYER FOR  
NONHAZARDOUS WASTE LANDFILL COVER:  
A CONTRIBUTION TO IMPROVE THE  
TRADITIONAL GEOTECHNICAL DESIGN  
APPROACH

Supervisor: PROF. MARCO FAVARETTI

Co-supervisor: DOTT. ING. STEFANO BUSANA

Student: SIMONA ALBERATI

A. A. 2014-2015



**INDEX**

CHAPTER 1: INTRODUCTION	1
1.1 Landfill typology	2
1.2 Final cover system of nonhazardous waste landfill	4
1.3 Function and principal characteristics of the final cover	5
CHAPTER 2: DETERMINATION OF THE HYDRAULIC CONDUCTIVITY OF THE BIOGAS DRAINAGE LAYER	6
2.1 Final landfill slope stability analysis and determination of maximum allowable biogas pressure	7
2.2 Estimating landfill gas flux	10
2.3 Correlation between the biogas pressure and hydraulic conductivity	12
2.4 Correlation between hydraulic conductivity and grain size	12
2.5 Determination of biogas transmissivity and hydraulic conductivity of the biogas drainage layer for the Torretta landfill case study	13
CHAPTER 3: DETERMINATION OF THE GRAIN SIZE DISTRIBUTION OF THE BIOGAS DRAINAGE LAYER	20
3.1 General information about filters	20
3.1.1 Filters of granular materials	21
3.1.2 Filters of synthetic materials	23
3.2 An empirical method for evaluating the grain size compatibility	24
3.3 An empirical method for evaluating the internal stability of the material	26
3.4 Grain size distribution curve of the biogas drainage layer	26
3.1.1 Grain size distribution of municipal solid waste	27
3.1.2 Grain size distribution and internal stability of the foundation layer	28
3.1.3 Grain size distribution and internal stability of the biogas drainage layer	29

CHAPTER 4: ANALYSIS OF THE LOADS ACTING ON THE BIOGAS DRAINAGE LAYER	32
4.1 Permanent loads . . . . .	32
4.2 Variable loads . . . . .	33
4.3 Actions analysis and modes of grain breakage . . . . .	37
CHAPTER 5: INTRINSIC CHARACTERISTICS OF GRANULAR MATERIALS	40
5.1 Definition of grains quality . . . . .	42
5.2 Determination of the tests used to define the mechanical resistance of the aggregates . . . . .	44
5.2.1 Los Angeles abrasion test . . . . .	45
5.2.2 Aggregate impact test . . . . .	47
5.2.3 Aggregate crushing test . . . . .	47
5.3 Correlation between the bulk indexes and the mechanical resistance . . . . .	49
CHAPTER 6 : INFLUENCE OF GRAIN BREAKAGE ON THE MECHANICAL BEHAVIOR OF GRANULAR MATERIAL	52
6.1 Triaxial test: methods and purpose . . . . .	53
6.2 Effect of grain breakage on the constitutive law . . . . .	55
6.3 Parameter affecting the grain rupture . . . . .	58
CHAPTER 7 : EFFECT OF GRAIN BREAKAGE ON THE PARTICLE SIZE DISTRIBUTION	60
7.1 Particles breakage factors. . . . .	62
7.2 Correlation between particles breakage factor and the and other engineering parameters . . . . .	66

CHAPTER 8 : TESTS USED TO DETERMINE THE CHARACTERISTICS OF THE MATERIAL FORMING THE BIOGAS DRAINAGE LAYER	69
8.1 Criteria analyzed for evaluating the tests types	70
8.1.1 Permeability test	71
8.1.2 Mechanical resistance and grain size	71
8.1.3 Static load and deformation at failure	73
8.2 Types and characteristics of the chosen material	75
8.2.1 Characteristics of the sample classified as selected waste	75
CHAPTER 9 : ANALYSIS OF THE RESULTS OBTAINED BY LABORATORY TESTS	80
9.1 Procedure adopted for determining the mechanical resistance of the analyzed sample	81
9.1.1 Grain size distribution of the sample after 100 revolutions	82
9.1.2 Grain size distribution of the sample after 200 revolutions	84
9.1.3 Grain size distribution of the sample after 500 revolutions.	86
9.2 Mechanical resistance of the analyzed sample	88
9.3 Effect of the energy levels on the grain size distribution of the analyzed sample	89
9.4 Effect of grains breakage on the hydraulic conductivity of the analyzed sample	91
9.4.1 Determination of the particle breakage factors and their correlation with energy and hydraulic conductivity	93
CHAPTER 10 : CONCLUSIONS	96
REFERENCES	99









## ***CHAPTER 1: Introduction***

The legislative decree n.36 of 13 January 2003, implementation of the directive 1999/31/CE - Ordinary supplement n.40 of the Official Journal n. 59 of 12 March 2003- provides standards of design, construction and management of solid waste landfill. For what concern the final cover, this regulation establishes the minimum thickness and the relative functions of each strata. Paying attention to the gas collection layer, it is possible to observe that it must possess a thickness higher than or equal to 50 cm, and have to be protected from clogging. Nothing is specified about the types and the geotechnical characteristics of the materials used for this layer. Therefore to determine properties like permeability, grain size and mechanical resistance, it is suggested a study based on literature surveys and laboratory tests. Firstly, in order to guarantee the final landfill cover slope stability against potential overpressure generated by the biogas itself, it is assigned the minimum permeability of the biogas drainage layer. Considering the neighboring strata and the filter design criteria , it is evaluated the particles size distribution of the granular medium forming the biogas drainage layer. Then, in order to prevent modification of its skeleton it is carried out the internal stability analysis.

The efforts presents on the biogas drainage layer could alter the grain size and dimension of the material used and then, the required permeability for the biogas drainage layer. Indeed, during the installation of this layer and after the realization, through the compaction of the overlying hydraulic barrier, the material chosen could modify its external surface and hence, its mechanical resistance. This negative scenario is caused by grains breakage and, consequently, to the production of the fine fraction. Any change in grains size, due to crushing or disintegration, can affect the stability of the final cover. In fact, as mentioned above, the

reduction of the design permeability may generate biogas overpressure and it can induce migration or erosion phenomena towards the underlying foundation layer.

The protraction of this study wants to identify laboratory tests able to simulate the efforts induced by the installation of the biogas drainage and by the compaction of the material forming the overlying hydraulic barrier. After that, in order to assess if the breakage material is still suitable, it will be analyzed its new grain size distribution and its permeability.

According to this procedure, firstly, it will be determined the geotechnical requirements of the biogas drainage layer for a real case study: the nonhazardous municipal solid waste landfill of Torretta (Legnago ). Then, it will be analyzed the results obtained testing the material chosen for the over mentioned efforts.

Since, the biogas drainage layer is placed under the hydraulic barrier, is protected from water infiltration. Therefore, for its installation, it is not excluded the possibility to use a waste material, properly chosen and in compliance with the acceptability limits of the landfill in here considered.

## **1.1 Landfill typology**

In accordance with the article 2 of the legislative decree 36 of 2003, landfill means *“a waste disposal site for the waste onto or into land (i.e. underground), including: internal waste disposal site ( i.e. landfill where a producer of waste is carrying out waste disposal at the place of production), and a permanent site (i.e. more than one) which is used for temporary storage of waste )”*. Indeed, with the terms waste refers to *"any substance or object, which the holder disposes of, intends or is required to discard."*

In function of the accepted waste, each landfills shall be classified in one of the following classes:

- landfills for inert waste;
- landfills for non-hazardous waste;
- landfills for hazardous waste.

A landfill must be situated and designed so as to meet the necessary conditions for preventing pollution of the soil, groundwater or surface water and ensuring efficient collection of the leachate. Protection of soil, groundwater and surface water is to be achieved by the combination of a geological barrier and a bottom liner, during the operational/active phase; by the combination of the of a geological barrier, a bottom liner (during the operational/active phase by the combination of a geological barrier) and a top liner during the passive phase/post closure.

Landfill gas shall be collected from all landfills receiving biodegradable waste and it must be treated and used. If the gas collected cannot be used to produce energy must be flared. The collection, treatment and use of landfill gas shall be carried on in a manner which minimizes damages to, or deteriorations of the environment and risk to human health.

In order to ensure the isolation of the body waste from environmental media, it must be taken the following requirement:

- Surface water management system and water drainage and conveyance of;
- Bottom liner and lateral barrier;
- Leachate management and collection system;
- Landfill gas collection and removal systems (only for landfills where are disposed biodegradable waste);
- Final landfill cover system.

For environmental safeguards must be guaranteed efficiency and integrity control. Moreover, the maintenance of an appropriate slope is necessary to guarantee runoff.

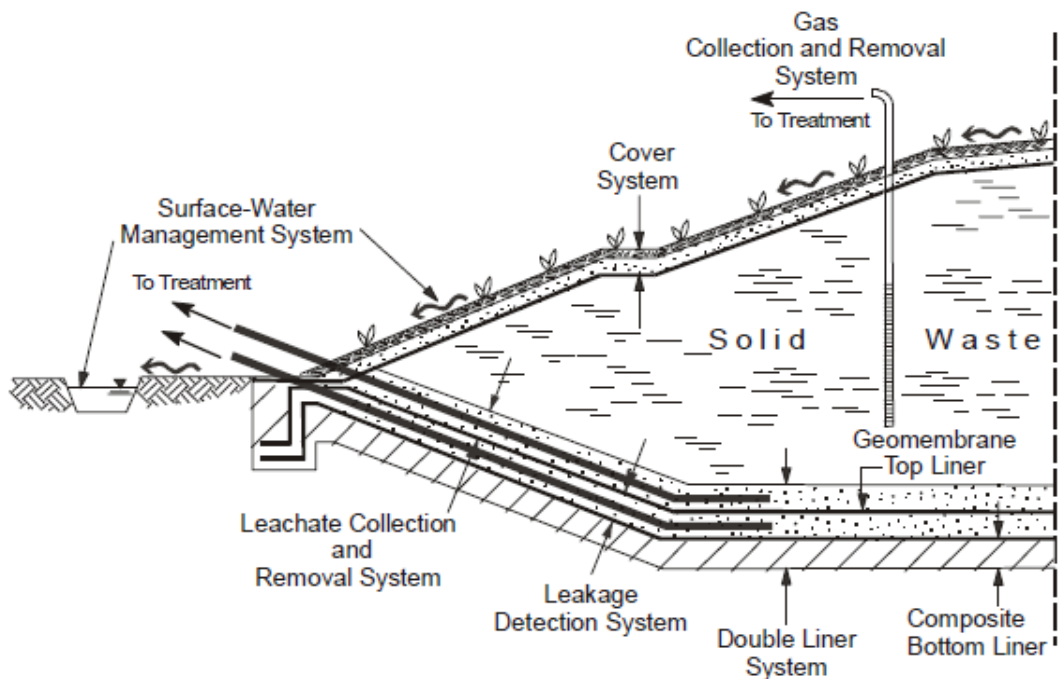


**Figure 1.1: Schematization of the landfill's technical requirements.**

## 1.2 Final cover system of a nonhazardous landfill waste

Final landfill cover system must meet the following criteria:

- Isolate the wastes from the environment;
- Minimize the infiltration of water;
- Reduce maintenance;
- Minimize the erosion phenomena;
- Resist to settling and localized subsidence phenomena.

Final cover for non-hazardous waste landfill must be carried out through a multilayered system, formed at least from the top to the bottom by the following layers (Figura 1.2):

- Surface layer with a thickness equal to or higher than one meter;
- Drainage layer with a thickness equal or higher than 50 cm and protected from clogging;
- Hydraulic barrier layer with a thickness equal to or higher than 50 cm, having hydraulic conductivity lower or equal to  $10^{-8}$  m/s or of equivalent characteristics;
- Gas collection and breaking capillary layer with a thickness equal to or higher than 50 cm and protected from clogging;
- Foundation layer to allow the correct installation of the overlying strata.

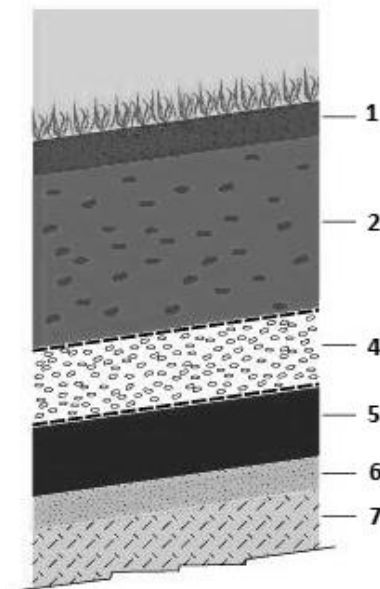


**Figure 1.2: Final cover system of nonhazardous landfill waste; from the top to the bottom: surface layer (1-2), drainage layer (3), hydraulic barrier (4), biogas collection layer (5), foundation layer(6).**

### 1.3 Function and principal characteristics of the final cover

The cover soil has the aim to protect the underlying layer and to promote vegetative growth for the environmental restoration. Generally, it is subdivided into two parts: the surface and protection layer. The first is designed in order to protect the cover against erosion by water and wind, be maintainable, and provide a growing medium for vegetation, if present. The second, instead, has the function to protect the underlying layers from erosion, exposure to wet-dry cycles, freeze-thaw cycles.

To prevent the formation of a hydraulic head and avoid increments of pore pressure between the surface layer and the mineral one, it is disposed a drainage layer formed by granular material and protected from clogging: at its upper interface it is placed a non-woven geotextile.

The function of the hydraulic barrier is to minimize percolation of water through the cover system by impeding infiltration into the barrier and by promoting storage or lateral drainage of water in the overlying layers. The material used must ensure a permeability lower than or equal to  $10^{-8}$  m/s and therefore, will be clay, silty-clay. This layer is lying through compaction in order to reduce permeability to an acceptable values and, to maintain excellent hydraulic requirements for most of the after-care procedures.

Gas collection layers may be necessary beneath cover system barriers for wastes that generate gas or emit volatile constituents. The presence of biogas flow can adversely affect the stability of the cover. Indeed, a possible failure of the latter, may facilitate the passage of water inside the body waste, with a consequent increase of the biogas and leachate production. Therefore, these layers are designed to have adequate in-plane gas transmissivity to convey gas to passive gas vents, active gas wells or trenches placed within the body waste. Consequently, it must be formed by draining material in order to allow adequate biogas diffusion, avoiding undesirable pore pressures. In accordance with the in force regulations, the biogas drainage layer must be protected from clogging induced by the erosion of fine particles of the overlying hydraulic barrier. As for drainage layer, it is set up a geotextile. In addition, the layer in question must perform the function of breaking capillary: in unsaturated conditions, the different particle size, produces capillary rise that are able to retain interstitial water.

The foundation layer is the bottom-most component of the cover system. The functions of the foundation layer are to provide grade control for cover system construction, adequate bearing capacity for overlying layers, a firm subgrade for compaction of overlying layers, a smooth surface for installation of overlying geosynthetics, and, in some applications, a buffer zone to reduce the potential effects of waste differential settlements on the cover system components.

## ***CHAPTER 2: Determination of the hydraulic conductivity of the biogas drainage layer***

In order to identify the hydraulic conductivity of the granular medium forming the biogas collection layer, will be used a correlation that bond it with the biogas transmissivity. This step, as shown later, is done through the concept of the intrinsic permeability, i.e. capacity of the soil to transmit a fluid.

The transmissivity is the ability of the medium to transmit a fluid that pass through it. It is obtained by the product between the thickness of the transmissive component and the hydraulic conductivity (i.e. rate at which the fluid can move through a permeable medium):

$$\psi = kf \cdot t \quad (2.1)$$

Where  $kf$  is the hydraulic conductivity for a porous medium and specific fluid [m/s],  $t$  thickness of the transmissive component[m] (i.e. thickness of the biogas drainage layer, section 1.2).

The biogas transmissivity is evaluated by using the methodology proposed by Thiel (1998), which wants to:

- perform a cover slope stability analysis in order to estimate the maximum allowable gas pressure, that results in an acceptable factor of safety;



- estimate the maximum gas flux that may need to be removed from below the landfill cover;
- design a biogas drainage system, consisting of a transmissive blanket gas drainage layer and intermittent highly-permeable strip drains, that will remove the gas at the estimated design flux rate.

In accordance with the Thiel methodology, to reduce the excess of pore gas pressure it is provided, in a final landfill cover, a blanked gas-drainage layer with highly permeable strip drains. Indeed, if the gas is not adequately vented, excess pore pressure may cause enough uplift below the hydraulic barrier and then, the cover veneer system can become unstable and slide down slope. The strip drains in turn would discharge the gas either to vents or an active gas collection system. They are a series of parallel trenches, more permeable than the biogas drainage layer, at regular spacing ( $D$ ) to allow the biogas to conveyed to the outlets (Figure 2.1). The introduction of this type of system is recommended as a prudent engineering measure for landfill final covers (R.Thiel, 1998).

### **2.1 Final landfill slope stability analysis and determination of maximum allowable biogas pressure**

Final landfill slope stability analysis is performed using the limit equilibrium method and considering the most simplest and conservative model: the infinite slope. The sliding mass is transitional, of constant thickness and, lower than the width of the cover. Moreover, it is planar, parallel to the slope and of infinite extension.

Since landfill cover is a geosynthetic-soil layered system constructed on a slope, (e.g. geomembranes, geosynthetic clay liners, and compacted clay layers), the failure surface occurs at the interface between the layers (Giroud et al. 1996). In the present case, considering the pore pressure exerted by the gas flux, it develops at the lower interface of hydraulic barrier. More specifically, evaluating that the biogas drainage layer must be protected from clogging, the most probable sliding surface occurs at the geosynthetic separation layer used for separating the hydraulic barrier and the biogas collection layer. Moreover, according to this observation and its position, the slope is dry or it contains only water retained by capillarity.

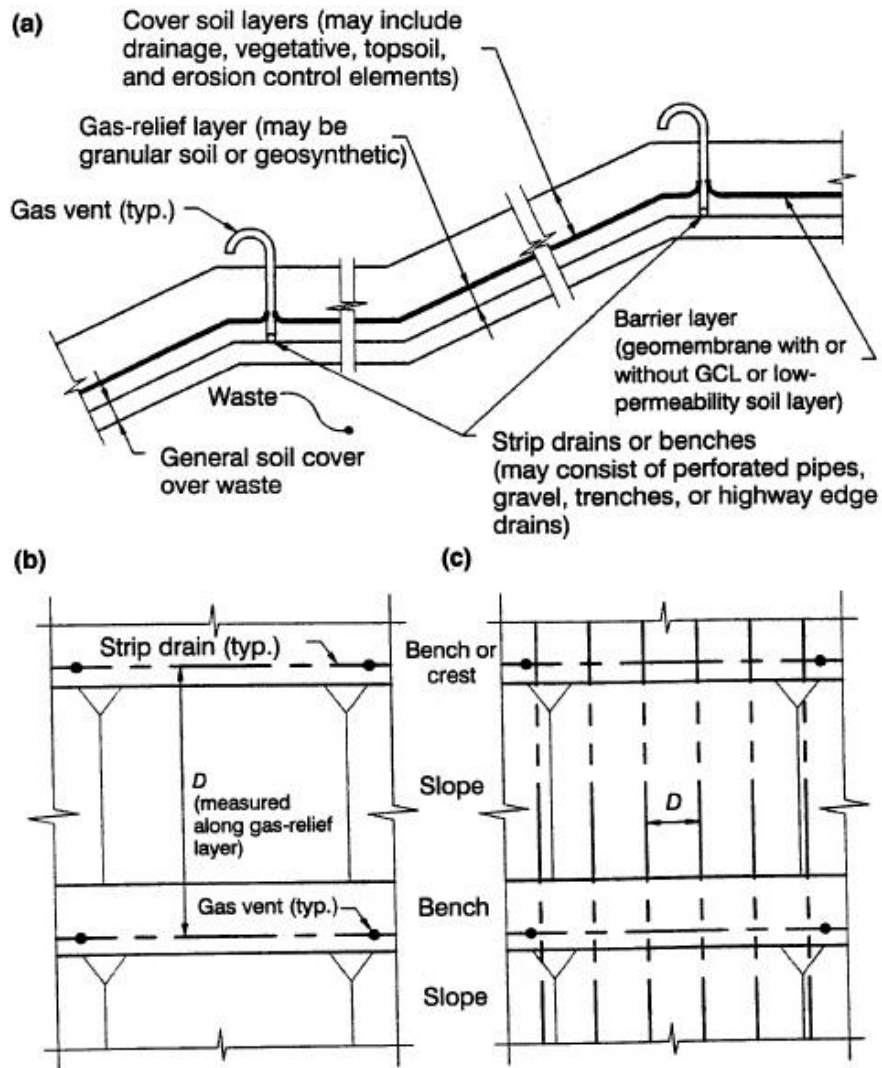


Figure 2.1: Schematic example of the final landfill cover composed by the strip drains (Thiel, 1998).

The slope stability evaluated determining the safety factor, coefficient by which the strength parameters can be reduced with the aim to lead the slope in a limit equilibrium condition along to a predetermined failure surface. The equation that characterizes this parameter is obtained doing the equilibrium limit on a vertical section, placed on the sliding surface, inclined of an angle  $\beta$ , having thickness  $b$ , height  $d$  and unit width (Figure 2.2). The applied forces are respectively the weight of the slice,  $W$ , and the pore gas pressure,  $u_g$ . The latter considered because, in the long term, can reduce the effective normal stresses developed on the failure surface.

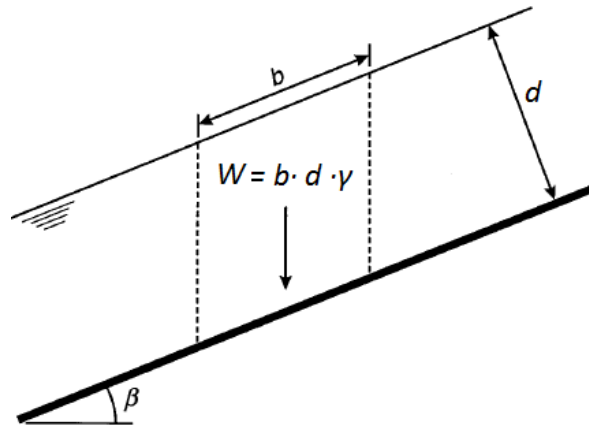


Figure 2.2: Identification of the vertical slice with a thickness  $b$ , height  $h$  and unit width.

Therefore, the factor of safety in term of effective stress can be calculated through the following expression:

$$FS = \frac{a' + (\gamma \cdot d \cdot \cos \beta - u_g) \tan \delta'}{\gamma \cdot d \cdot \sin \beta} \quad (2.2)$$

Where:  $h$  cover soil thickness above the biogas drainage layer and perpendicular to the slope;  $\gamma$ , average unit weight of cover soil above gas drainage layer;  $\beta$ , slope angle;  $u_g$ , gas pore pressure on lower side of gas drainage layer;  $a'$ , effective adhesion parameter for the lower geosynthetic interface;  $\delta'$ , effective friction parameter for the lower geosynthetic interface.

Assuming that the material properties and geometry are fixed for a specific project, the designer must select a minimum allowable factor of safety,  $FS_{allow}$ , and then calculate a maximum allowable gas pressure,  $u_{g-allow}$  (Thiel, 1998).

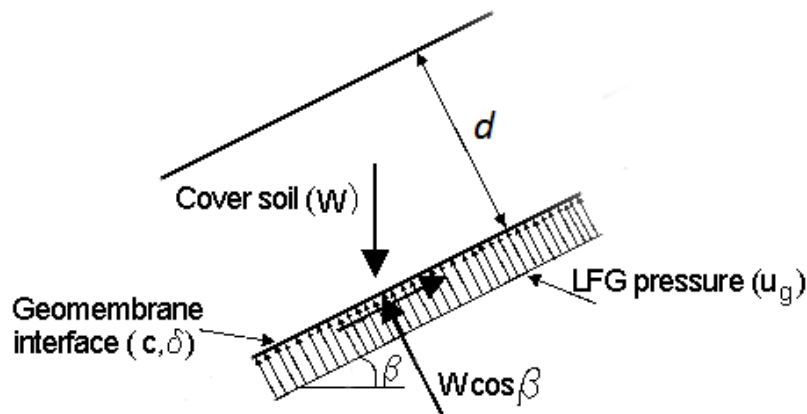


Figure 2.3: Identification of the forces acting on a sliding plane placed at the upper interface of the biogas drainage layer (R.Thiel, 1998).

## 2.2 Estimating gas flux

The mass flux of gas from the surface of a landfill will be site specific. It will also vary spatially and temporally at a given landfill. The amount of gas produced will depend on the waste type, age, temperature, moisture, barometric pressure, gas extraction or venting, etc. In the present case, empirical and simplistic method is used to estimate the mass flux, which assumes a gas generation rate per unit mass of waste. This parameter indicates the volume of biogas, at atmospheric pressure and ambient temperature, which is generated in a year from one kilogram of waste (Thiel, 1998). Therefore, the flux of biogas for unit surface ( $q_{LFG}$ ) can be calculated by using the following expression:

$$q_{LFG} \left[ \frac{m^3}{m^2 \text{ year}} \right] = rg \cdot H_{waste} \cdot \gamma_{waste} \quad (2.3)$$

Where:  $rg$  is the gas generation rate per unit mass of waste;  $H_{waste}$  and  $\gamma_{waste}$  are respectively the average height and unit weight of the waste.

The height of the waste is site dependent. For closures at municipal solid waste landfills on the west coast of the United States, where cell closure occurs at the end of a cell's life, Thiel (1999) has used a gas generation rate of  $0.1 \text{ ft}^3/\text{lb}/\text{yr}$  ( $6.24 \cdot 10^{-3} \text{ m}^3/\text{kg}/\text{yr}$ ) for purposes of cover design. The unit weight of waste is generally assumed close to  $0.8 \text{ ton}/\text{m}^3$  ( $8 \text{ kN}/\text{m}^3$ ).

## 2.3 Correlation between the biogas pressure and relative transmissivity

To obtain the landfill gas transmissivity, it is used a relationship that correlate the strip drain spacing ( $D$ ), the incoming gas flux rate ( $q_{LFG}$ ), and the pore gas pressure exerted in the gas collection layer ( $u_g$ ). This derivation is based on Darcy's law, which is applied to a fluid that flow in porous media in laminar flow regime. The derivation steps are the followings:

- Consider a unit-width surface area between strip drains. Ideally, the gas flow coming uniformly into the biogas drainage layer, is symmetric about the centerline between the strip drains and their half-distance,  $L$  ( $D/2$ ). The volume of gas being carried in the gas-drainage layer, would vary linearly from zero, at the centerline between the strip drains ( $x=L$ ), to a maximum value, at the beginning of the strip drains ( $x=0$ ) (Figure 2.4). The volume of gas per unit width can be written in terms of the gas flux as:

$$Q_{LFG} = (L - x) q_{LFG} \quad (2.4)$$

Where  $Q_{LFG}$  is gas discharge flow rate per unit width at any point  $x$  in the gas-drainage layer,  $L$  half distance between the strip drains,  $q_{LFG}$  flux of biogas for unit cover surface,  $(L-x)$  a unit-width surface area between strip drains.

- The flow in the gas-drainage layer can be assumed to follow Darcy's law (1856), which can be written in terms of the pressure gradient as follows:

$$\begin{aligned}
 Q_{LFG}(x) &= \left(\frac{kg}{\gamma g}\right) \cdot A \cdot \left(\frac{du}{dx}\right) = \left(\frac{kg}{\gamma g}\right) \cdot (t \cdot 1) \cdot \left(\frac{du}{dx}\right) = \\
 &= \left(\frac{kg \cdot t}{\gamma g}\right) \cdot \left(\frac{du}{dx}\right) = \left(\frac{\psi g}{\gamma g}\right) \cdot \left(\frac{du}{dx}\right)
 \end{aligned}
 \tag{2.5}$$

Where:  $kg$ , landfill gas permeability of the gas-drainage layer;  $\gamma g$ , the gas unit weight;  $A$ , cross-sectional flow or area which is obtained by the thickness of the layer ( $t$ ) times unit-width; and  $du/dx$  is the pressure gradient and  $\psi g$ , the landfill gas transmissivity.

Combining the relationship (2.4), (2.5) and solving the differential equation for  $x=0$  and  $x=L$ , corresponding respectively to the minimum and maximum gas pressure, the transmissivity of the gas drainage layer can be obtained by the following expression:

$$\psi_{LFG} = \frac{q_{LFG} \cdot \gamma g}{u_{g, max}} \cdot \frac{L^2}{2}
 \tag{2.6}$$

Where:  $\psi_{LFG}$  landfill gas transmissivity;  $q_{LFG}$  gas flux per unit surface obtained by using the Thiel (1998) empirical method;  $L$  half spacing between the strip drains;  $\gamma g$  the unit weight of the landfill gas;  $U_{g, max}$  the maximum allowable landfill gas pressure obtained fixing minimum safety of factor.

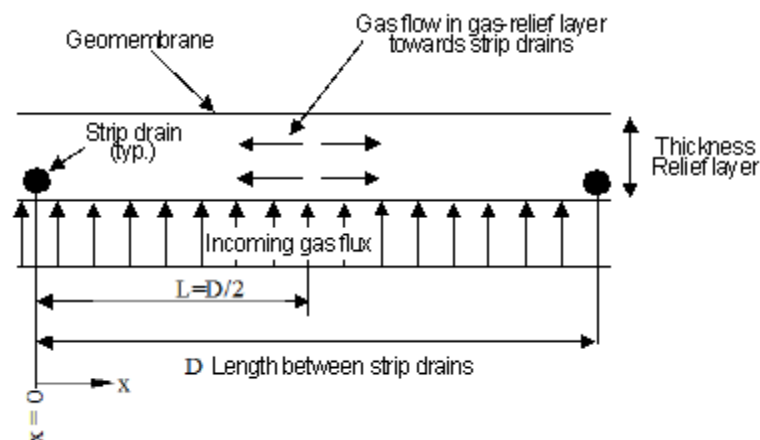


Figure 2.4: Diagram of strip drains operation, placed in the biogas drainage layer (R.Thiel, 1998).

### 2.3 Correlation between biogas and the hydraulic conductivity

To correlate biogas transmissivity and the hydraulic conductivity, it is used the Darcy's law (1856) in terms of intrinsic permeability, characteristic of the medium in question. Recalling equation (2.5), the flow rate for a specific fluid in a porous medium is:

$$Q = K \cdot \frac{\gamma_f}{\mu_f} \cdot i_f \cdot A \quad (2.7)$$

Where:  $Q$  flow rate;  $K$  intrinsic permeability;  $\gamma_f$  unit weight of the fluid;  $\mu_f$  dynamic viscosity of the fluid;  $i_f$  or  $dh/dx$  the fluid gradient, and  $A$  cross-sectional area of the flow medium.

The relationship between the standard civil engineering coefficient of permeability (i.e. hydraulic conductivity) and the intrinsic permeability, can be written as:

$$k_f = K \cdot \frac{\gamma_f}{\mu_f} \quad (2.8)$$

Where:  $k_f$  standard civil engineering coefficient of permeability for a given fluid and,  $K$  intrinsic permeability.

Since  $K$  is a constant factor dependent on the medium, the ratio between the coefficients of permeability for two different fluids can be determined as:

$$\frac{k_1}{k_2} = \frac{\mu_2}{\mu_1} \cdot \frac{\gamma_1}{\gamma_2} \quad (2.9)$$

Where:  $k_i$  is the standard civil engineering coefficient of permeability of a given fluid,  $\mu_i$  is the dynamic viscosity of the fluid, and  $\gamma_i$  is the unit weight of the fluid.

This relationship is obtained by using the Darcy equation (1856) and assuming that the same porous medium is crossed by two different fluids. In the present case, they are biogas and water (Thiel,1998). Using the previous equation, the design of a biogas drainage layer can now be accomplished by converting the required gas transmissivity into a required hydraulic (water) permeability as follow:

$$\psi_{H_2O} = \frac{\mu_{LFG}}{\mu_{H_2O}} \cdot \frac{\gamma_{LFG}}{\gamma_{H_2O}} \cdot \psi_{LFG} \quad (2.10)$$

Where:  $\psi_{LFG}$  gas transmissivity of the biogas drainage layer;  $\psi_{H_2O}$  transmissivity of the water;  $\gamma_i$ , unit weight of a give fluid;  $\mu_i$ , kinematic viscosity of a given fluid.

### 2.4 Correlation between hydraulic conductivity and particle size

Hydraulic conductivity ( $k_f$ ) can be estimated by particle size analysis of the interest sediment, using empirical equations. Some authors summarized several empirical methods from former studies, presenting the following general formula (Justine Odong, 2013):

$$kf = \frac{g}{\nu} \cdot C \cdot f(n) \cdot de^2 \quad (2.11)$$

Where:  $kf$ , hydraulic conductivity;  $g$ , acceleration due to gravity;  $\nu$ , kinematic viscosity;  $C$ , sorting coefficient;  $f(n)$ , porosity function, and  $de$ , effective grain diameter. The kinematic viscosity ( $\nu$ ) is related to dynamic viscosity ( $\mu$ ) and the fluid (water) density ( $\rho$ ).

In the present case, the equivalent diameter of the medium in question is determined using a relationships, that does not include the parameters characteristic of the soil, like the Hazen (1892) formula:

$$kf = 100 \cdot d10^2 \quad (2.12)$$

Where:  $kf$ , is hydraulic conductivity in [cm/s];  $d10$ , effective grain diameter represents the diameter in [cm] corresponding to a percentage in weight of 10% that is lower than, and  $100$  is the sorting coefficient. For applying this relationship, the effective diameter is in the range of 0.1 and 30 mm.

### 2.5 Determination of biogas transmissivity and hydraulic conductivity of the biogas drainage layer for the Torretta landfill case study

In the considered case study, the landfill final cover will be realized in accordance with existing legislation and, providing highly permeable strip drains within the gas collection layer as a preventive measure to avoid excess of pore gas pressure. Consequently, to obtain the biogas transmissivity it will be possible to apply the procedure proposed by Thiel (1998).

Applying equation (2.2), it is possible to obtain a linear relationship between the factor of safety (FS) and the biogas pressure (ug). In the present case, the maximum inclination of the cover is 1:2.5 (Table 2.2).

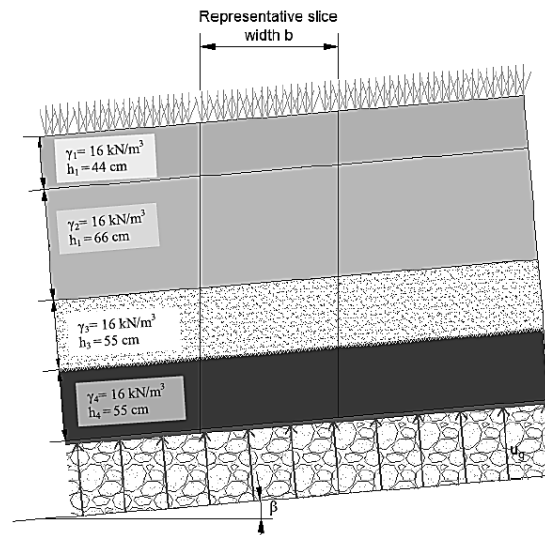
**Table 2.2: Characteristic of the slope.**

Slope characteristic	
slope	1:2,5
Inclination	40%
$\beta$	21.8°
cos $\beta$	0.93
sen $\beta$	0.37

The total thickness (d) of the layers placed above the sliding surface is equal to 2.2 m, as shown in table (2.3). The average unit weight of the strata above the biogas drainage layer is assumed equal to 16 kN/m<sup>3</sup>.

**Table 2.3: thickness of the layers forming the Torretta landfill final cover.**

<b>thickness d [m]</b>	
Surface layer	0,44
Protection layer	0,66
Drainage layer	0,55
Clay barrier	0,55
<b>TOTAL</b>	<b>2,20</b>

**Figure 2.5: Schematic representation of the slice analyzed for the limit equilibrium limit.**

At the lower interface of the hydraulic barrier to prevent clogging phenomena is placed a geosynthetic layer, capable of exerting the separation function. Therefore, the effective friction parameter between it and the biogas drainage, is determined through a reference TENAX catalog and it is assumed close to  $30^\circ$  (Figure 2.6). From a conservative point of view, the effective adhesion parameter is neglected. Hence, using all these values, it is possible to obtain a liner relationship between the factor of safety (FS) and the pressure of the biogas ( $u_g$ ), as:

$$FS = 1.44 - 0.048 u_g \quad (2.14)$$

When the pressure of the biogas is zero, in the absence of flow, the factor of safety is equal to 1.44. In agreement with the D.M. 11/03/1988, the slope stability is verified when the safety factor must be equal or greater than 1.3. According to this value, the maximum allowable pressure calculated by the proposed Thiel methodology is ( $U_{g,max}$ ) 3.2 kPa.



		BARRIER BENTO	QDRAIN	TEMATEX NW	BARRIER HDPE L	BARRIER HDPE AM	SABBIA	GHIAIA	TERRENO VEGETALE
Geocomposito bentonitico	BARRIER BENTO		18°/23°		9°/12°	28°/32°	28°/32°	30°/33°	24°/26°
Geocomposito drenante	QDRAIN	18°/23°			8°/14°	28°/32°	28°/32°	30°/33°	24°/26°
Geotessile tessuto non tessuto	TEMATEX NW				8°/14°	28°/32°	28°/32°	30°/33°	24°/26°
Geomembrana in HDPE liscia	BARRIER HDPE L	9°/12°		10°/12°			14°/18°		
Geomembrana in HDPE ad adherenza migliorata	BARRIER HDPE AM	28°/32°		28°/32°			25°/29°		
Sabbia	SABBIA	28°/32°		28°/30°	8°/14°	22°/25°			
Ghiaia	GHIAIA	30°/33°		32°/34°					
Terreno vegetale	TERRENO VEGETALE	24°/26°		24°/28°					

Figure 2.6 : Tenax chart.

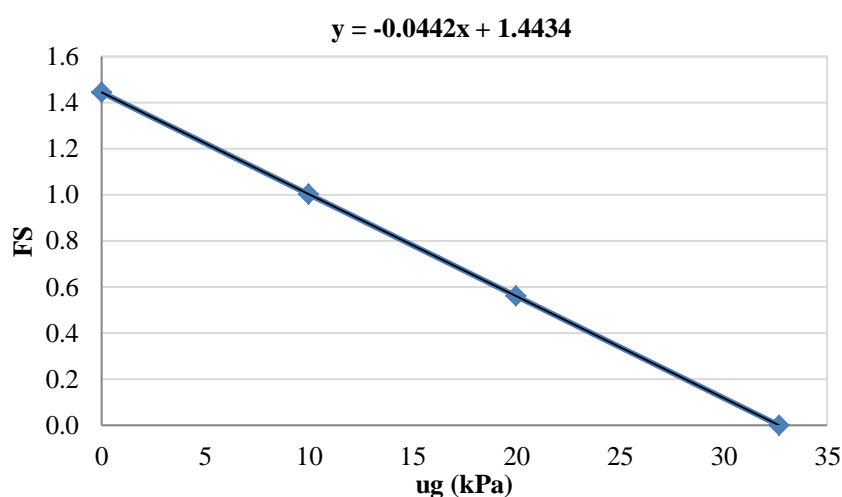


Figure 2.7: Trend between the factor of safety (FS) and the biogas pressure (ug): for FS equal to 1.3 the maximum allowable pressure 3.2 kPa.

By using the maximum allowable pressure and equation (2.6), it is possible to obtain the biogas transmissivity. However, before starting with this calculation, it is necessary to estimate the mass gas flux from the surface of landfill. For this purpose it is used the empirical relationship proposed by Thiel (1998), and

Assuming a gas generation rate equal to  $6.24 \cdot 10^{-3} \text{ m}^3/\text{kg}/\text{year}$ , an average waste unit weight of  $800 \text{ kg}/\text{m}^3$  and a height of the waste close to 20 m, the landfill gas flow for unit area is equal to  $99.84 \text{ m}^3/\text{m}^2/\text{year}$  ( $3.16\text{E-}06 \text{ m}^3 / \text{m}^2/ \text{sec}$ ).

In the present configuration, the vent system is composed by vertical wells placed at a distance of 25m. Taking into account that the strip drains are connected to them in order to have a single outlet point, the spacing will be the same. Then, using this parameter, the biogas flow, the half distance between strip drains and applying the equations 2.6, it is obtained a biogas transmissivity of  $9.752 \text{ E-}07 \text{ m}^2/\text{s}$ . This value is effective: allows the biogas flow in the porous medium in theoretical conditions. However, it should be noted that, between the reality and the schematic operational conditions there are some elements that tend to affect the transmissivity of the porous medium. For this reason, it is necessary to introduce a design transmissivity, obtained by increasing the effective one with a series of safety coefficients using the following expression:

$$\psi_{LFG,design} = \psi_{LFG,calc} \cdot FS \cdot RFin \cdot RFor \cdot RFcc \cdot RFbc \quad (2.15)$$

where  $\psi_{LFG,calc}$  represents the calculated transmissivity, and the  $\psi_{LFG,design}$  the design transmissivity incremented by the following parameters:

- $FS$  is the global safety factor that evaluates the uncertainties of the model used;
- $RFin$  is a factor that evaluates the reduction to intrusion;
- $RFor$  is a reduction factor that considers creep;
- $RFcc$  is a reduction factor for chemical intrusion;
- $RFbc$  is a factor reduction to biological clogging.

**Table 2.4: Factor of safety adopted in function of their range of variation.**

	<b>Range of variation</b>	<b>Adopted</b>
<b><math>FS</math></b>	2,0 ÷ 3,0	3,0
<b><math>RFin</math></b>	1,0 ÷ 1,2	1,1
<b><math>RFor</math></b>	1,1 ÷ 1,4	1,1
<b><math>RFcc</math></b>	1,0 ÷ 1,2	1,1
<b><math>RFbc</math></b>	1,2 ÷ 1,5	1,2

The maximum and minimum factors of safety are respectively equal to 2,64 ( $FStot,min$ ) and 9,072 ( $FStot,max$ ). In the present case are assumed the average values, except for the creep and the uncertainty of the model (Table 2.4). Indeed, for the first is used the lower limit because the layer is formed from granular material, while for the second it is assumed its maximum value. In this way, the FS adopted ( $FStot,design$ ) is equal to 4,792. Multiplying these coefficients for the prior biogas effective transmissivity, it is obtained the following design value:  $2.57\text{E-}06 \text{ m}^2/\text{s}$  for the minimum safety factor,  $8.85\text{E-}06 \text{ m}^2/\text{s}$  for maximum and  $4.67\text{E-}06 \text{ m}^2/\text{s}$  for the reference (figure 2.8).

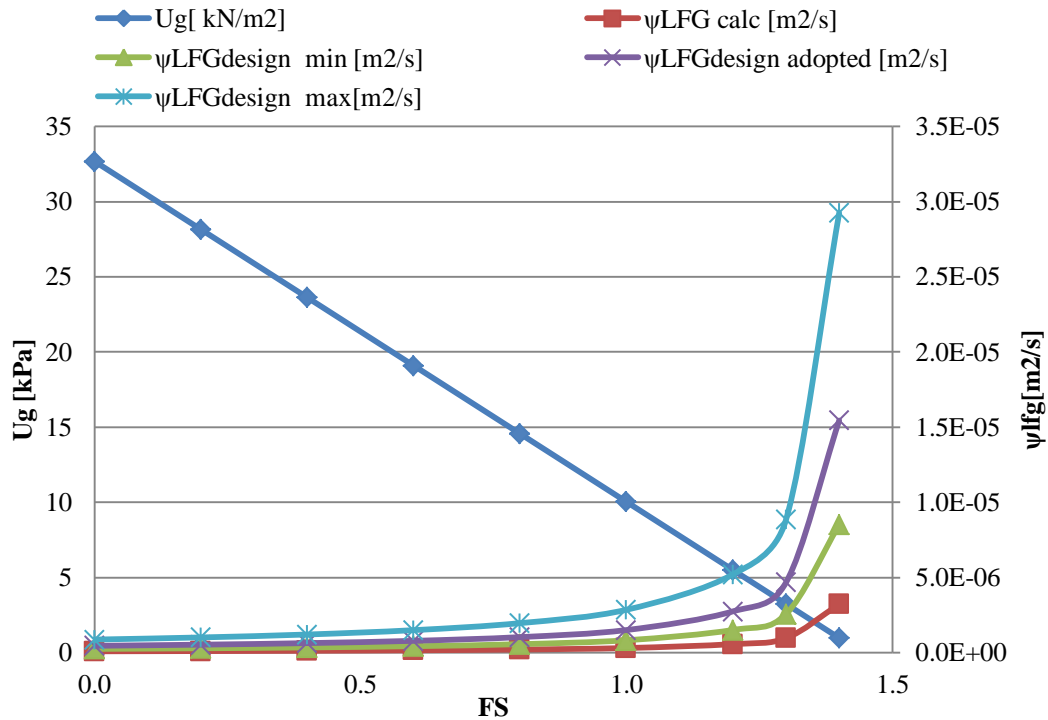


Figure 2.8 : Calculated and design biogas transmissivity  $\psi_{LFG}$  in function of the factor of safety (FS) and the biogas pressure exerted by the biogas ( $u_g$ ): for FS equal to 1.3,  $u_g$  is equal to 3.2 kPa and the reference transmissivity is equal to  $4.67E-06$  m<sup>2</sup>/s.

To convert into water transmissivity the biogas one, is used the expression (2.9). It is assumed that the biogas is composed by 45% of carbon dioxide and 55% of methane. By using these percentage, the unit weight of the biogas is equal to  $12.8 \text{ N/m}^3$ . The kinematic and dynamic viscosity of the fluid in exam are evaluated at atmospheric pressure and with a temperature equal to  $20^\circ$ .

Tabella2.5: Characteristic parameters of fluid at atmospheric pressure and with a temperature equal to  $20^\circ$ .

	Density ( $\rho$ ) [kg/m <sup>3</sup> ]	Unit weight ( $\gamma$ ) [N/m <sup>3</sup> ]	dynamic viscosity ( $\mu$ ) [N·s/m <sup>2</sup> ]	kynematic viscosity ( $\nu$ ) [m <sup>2</sup> /s]
Water	1000	9800	$1,01 \cdot 10^{-3}$	$1,01 \cdot 10^{-6}$
Air	1,28	11,8	$1,79 \cdot 10^{-5}$	$1,75 \cdot 10^{-5}$
Carbon dioxide	1,83	17,9	$1,50 \cdot 10^{-5}$	$8,21 \cdot 10^{-6}$
Methane	0,67	6,54	$1,10 \cdot 10^{-5}$	$1,65 \cdot 10^{-5}$
LFG (45% CH <sub>4</sub> - 55% CO <sub>2</sub> )	1,31	12,8	$1,32 \cdot 10^{-5}$	$1,01 \cdot 10^{-5}$

According the parameters reported in the table 2.5, the relationship between the biogas ( $\psi_{LFG}$ ) and water transmissivity ( $\psi_{H2O}$ ) is the following (Muskat,1937):

$$\psi_{H2O} = \frac{1,32 \cdot 10^{(-5)}}{1,01 \cdot 10^{(-3)}} \cdot \frac{12,8}{9800} \cdot \psi_{LFG} = 10 \psi_{LFG} \quad (2.16)$$

In accordance with the actual regulation, the thickness of the biogas drainage layer or, in this case of the transmission component, is equal to 55 cm. Consequently, the hydraulic conductivity must be higher than  $5.15E-05$  m/s in the case of FS minimum,  $1.77E-04$  m/s for the FS maximum and  $9.35E-05$  m/s for the FS adopted (figure 2.9). These values are the minimum allowable. Hence, in order to avoid excess of pore gas pressure, the hydraulic conductivity of the gas collection layer must be higher than  $10^{-4}$  m/s. According to this results, a coarse sand material can be suitable for the biogas drainage layer (Figure 2.10).

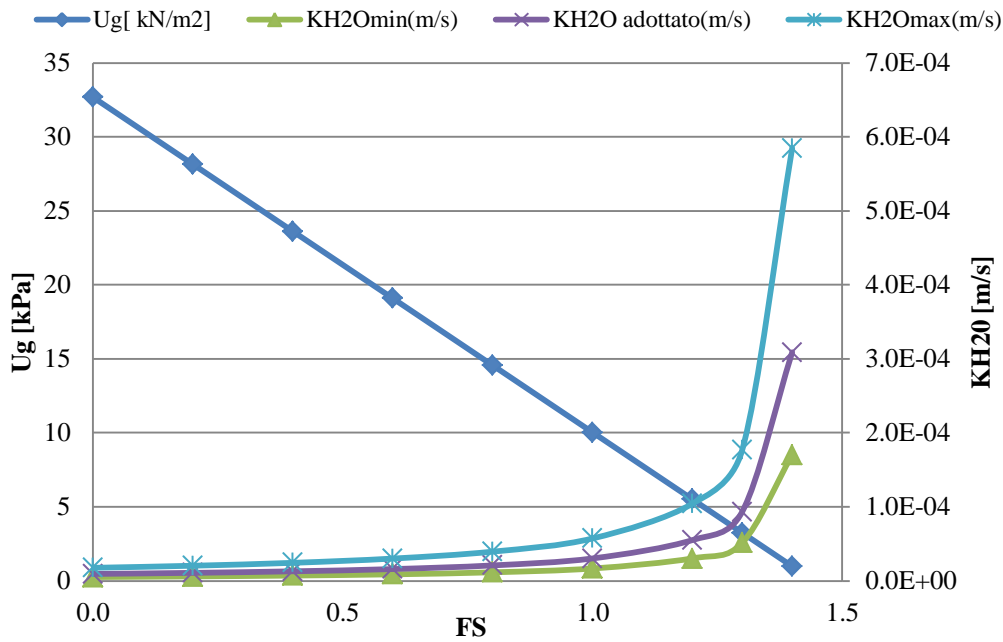


Figure 2.9 : Hydraulic conductivity  $K_{H_2O}$  of the biogas drainage layer in function of the factor of safety (FS) and the biogas pressure exerted by the biogas: for FS equal to 1.3,  $U_g$  is 3.2 kPa and the reference  $K_{H_2O}$  is equal to  $9.35 \cdot 10^{-5}$  m/s.

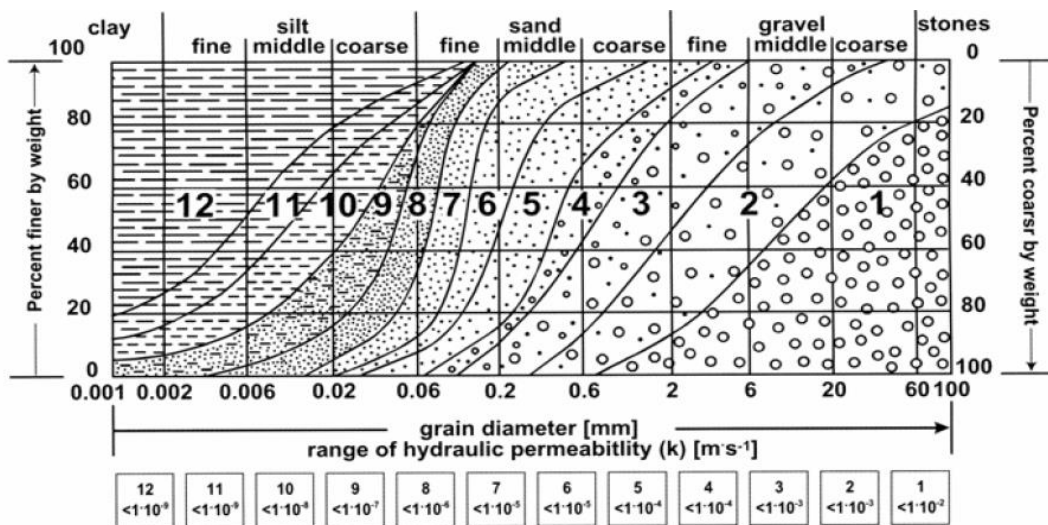


Figure 2.10: Range of variation of the hydraulic conductivity in grain size and grain size distribution (Algamir, 2005).

As reported in section (2.4), the Darcy law is used (1856) to obtain the correlation between the hydraulic conductivity of two fluids, which results to be valid only in laminar flow regime. To verify it is determined the number of Reynold. For sands, the motion is laminar if the Reynolds number should be less than 10 (Richardson, Thao, 2000):

$$Re = \frac{\rho \cdot v \cdot d}{\mu f} = \frac{v \cdot d}{\nu} \quad (2.17)$$

Where:  $\rho$  represents the fluid density,  $\nu$  kinematic viscosity  $\mu$  dynamic viscosity and  $v$  the fluid velocity and  $d$  the characteristic size of the surface through which the flow takes place.

Using the values of the biogas flow and the parameters listed in Table 2.5, it is possible to obtain a Reynolds number equal to 3.9, lower than 10 and therefore in laminar flow regime.

In order to determine the equivalent diameter associated to these hydraulic conductivity is used the Hazen formula (1892), reported in the section 2.5, and the results obtained is reported in table 2.7.

**Table 2.7: Minimum effective diameter (d10) in function of the hydraulic conductivity obtained.**

<b>kf [m/s]</b>	<b>d10 [mm]</b>
5.15E-05	0.07
1.77E-04	0.13
9.35E-05	0.1

## ***CHAPTER 3: Determination of the grain size distribution of the biogas drainage layer***

In accordance with Legislative Decree 36/2003, the biogas drainage layer must be protected from clogging (section 1.2). Therefore, shall be placed a separation material at the interface between the hydraulic barrier and the gas collection layer. In this way, the eroded particles induced by vibrations and seepage do not alter the hydraulic conductivity of the granular material forming the layer in question which, as shown in the chapter 2, is determined by the estimated biogas flow. To determine if this material has particle size distribution compatible with the underlying layers, it is used filter design criteria. In this way, and through the knowledge of the particle size of the underlying waste and foundation layer, it will be possible to define the grain size distribution of the biogas drainage layer.

### **3.1 General information about filters**

In the geotechnical engineering, filters are layers of materials having grains and voids sufficiently large to allow the passage of water and, small enough to prevent the migrations of fines particles through the interstices formed by the grains. They are used to prevent problems like piping and erosion and in many situations in which hydraulic gradients is very high; thus they are placed at the interface between coarse and fines materials and, in contact with surfaces that have different particle size.

Filters can be made of natural or synthetic materials. The latter, although capable of exerting the same properties of granular materials, has a limited durability, which can be accelerated in aggressive environments such as in a landfill. For these reasons, the synthetic filters are used in

situations where it is necessary to protect the material from possible occlusions. There are multiple models in the literature able to assess in detailed the design of the filter. In the interest of brevity it is used the simplest empirical models.

### 3.1.1 Filters of granular materials

This type of filters are generally characterized by granular material, like sand and gravel. The problems that arise in contact between two materials of different grain size, affected by seepage oriented towards the coarse-grained material and having high hydraulic gradient at the transition from one to another material, are two limit state conditions, defined as:

- *Clogging*: occurs when the pores of coarse material are gradually occluded by the particles of the finer material, until preclude its hydraulic efficiency (Figure 3.1 a);
- *Erosion*: occurs when the finer particles of the basic material completely pass through the pores of the coarse material. This phenomenon causes a progressive erosion of the base medium that can evolve to the formation of pipes inside the base material able to adversely affect the stability of the work (Figure 3.1 b);

The filters collapse when they are reached this limit state conditions (Moraci et. al., 1996). The design of a transition zone, in the literature conventionally known as filter, has the aim to deal with clogging and erosion conditions limit.

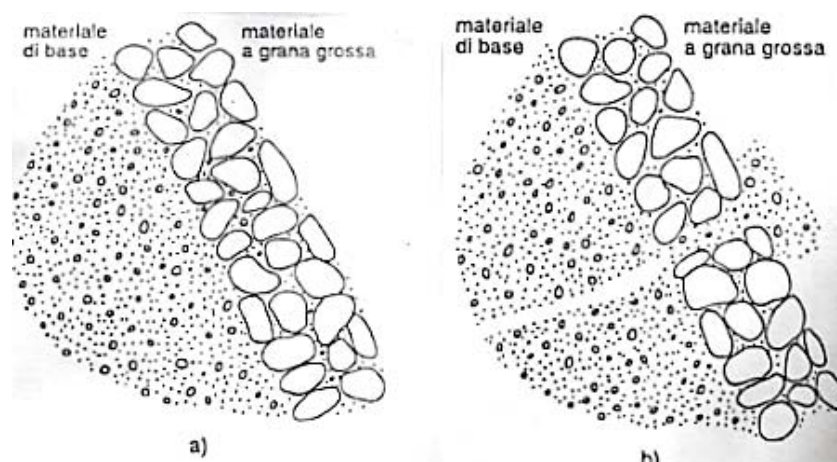


Figure 3.1: a) clogging; b) erosion (Colombo e Colleselli).

To prevent the limit state reported above, it is necessary to satisfy the following filter design criteria:

- *Clogging criterion*: the material forming the filter must be fine enough to prevent the adjacent finer material from piping or migrating into the filter material;
- *Permeability criterion*: the filter material must be coarse enough to carry water without any significant resistance;
- *Internal stability criterion*: the filter material must be stable, it means that the local particle size composition and permeability, under the drag action exerted by the fluid, must be preserved in order to do not suffer appreciable variation in time.

These design criteria are performed in order to evaluate the filter efficiency starting from the grain size distribution of the material. Indeed, most of the methods used in the design of filters formed by granular materials, is in function of the geometrical characteristics of the two materials that interact in the phenomenon.

The particle size distribution represents a curve in which grain size of the material is reported along the bottom and, the percent of a soil that is smaller than (“or passes”) each dimension is shown on the left side. This type of analysis is performed by using standard sieves, sized according to standard classification system. Obtained this curve, the material is described by parameters, which are (Harold N. Atkins):

- *Uniform coefficient ( $C_u$ )*: this value gives an indication of the shape of the curve and the range of particle sizes that a soil contains, especially in the more important fine part of the soil. Uniform coefficient is expressed as:

$$C_u = \frac{d_{60}}{d_{10}} \quad (3.1)$$

Where  $d_{60}$  and  $d_{10}$  are the grain size that only 60% and 10% of the grains are finer than. A material is uniform when the  $C_u$  is equal to 2, poor graded when  $C_u$  is lower than 6, well graded when  $C_u$  is higher than 15;

- *Coefficient of curvature ( $C_c$ )*: this is another measurement of the shape of the curve.

$$C_c = \frac{d_{30}^2}{d_{60} d_{10}} \quad (3.2)$$

Where  $d_{60}$ ,  $d_{30}$  and  $d_{10}$  are the grain size that only 60%, 30% and 10% of the grains are finer than.



### 3.1.2 Filters of synthetic materials

The filters of synthetic material were born with geosynthetic materials produced by the plastics and textiles industries. This category belong to nonwoven and woven geotextiles, which usually perform a filtering and separation function.

The limit states faced by these types of filters are the same seen for granular material, with the addition to the blinding limit state: the filter of geosynthetic material must be able to avoid accumulation of fine particles on the geotextile surface and hence, the formation of a low permeability zone which can increase pore pressure. For synthetic filter the internal stability criterion loses meaning, while clogging and permeability still have to be verified.

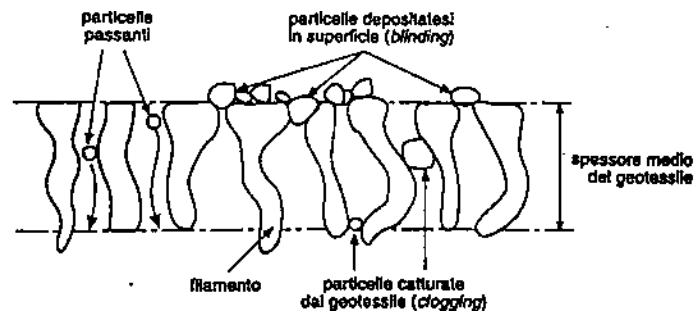


Figure 3.2: Blinding and clogging limit state (Colombo e Colleselli).

### 3.2 An empirical method for evaluating the grain size compatibility

The particle size compatibility are verified when permeability and clogging criterion is satisfied. In other words, the base material must have voids small enough to retain filter particles, and sufficiently large to allow the flow. Erosion and occlusion in a filter depends on different variables, often uncertain and difficult to quantify (Ruot, 2006). Consequently, is employed empirical or probabilistic models in order to verify the particle size compatibility, which are based on the dimensions, geometry and gradation of the material used. In the present case, for satisfying this criterion, is used the model proposed by Terzaghi (1922). This is empirical and bases on the grain size distribution curve of the material (figure 3.3).

Considering two materials placed in contact with each other, the clogging criterion wants to avoid the erosion of fine particles. For this purpose, the method proposed by Terzaghi compares the coarse fraction of the base material ( $d_{85_b}$ ), with the fine fraction of the filter material ( $d_{15_f}$ ):

$$\frac{d_{15_f}}{d_{85_b}} < 4 \quad (3.3)$$

Where  $d_{15_f}$  and  $d_{85_b}$  are the grain size corresponding to 15 and 85% passing, respectively, and can be obtained from the grain size curves of each material.

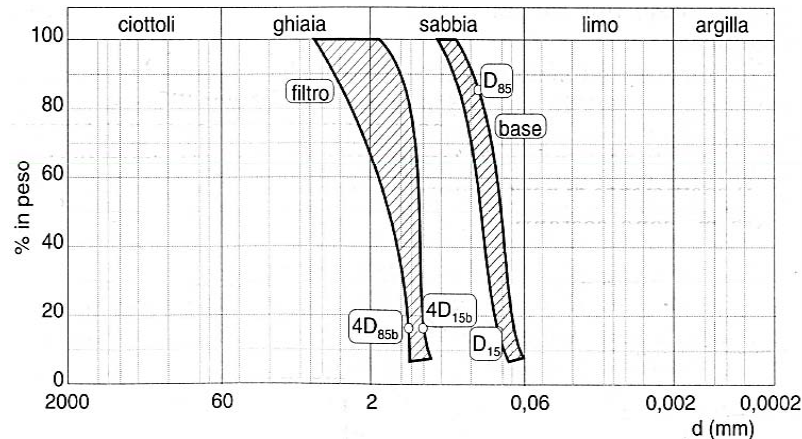


Figure 3.3 : Graphical representation of the Terzaghi methodology (1922) (Colombo e Colleselli).

This criterion should be applied not only to the filter material but also to the drainage layer. This will prevent migration of the subgrade material into the sub-base and the sub-base into the drainage layer.

The permeability criterion, instead, is formulated in order to avoid excess of pore water pressure. The permeability of the two materials must increase in the flow direction for allowing the flow (Graauw et al., 1984). Therefore, the filter must be maintained at least an order of magnitude higher than that of the base material (Moraci et al., 1996). The method proposed by Terzaghi compares the fine fraction of the base material ( $d_{15b}$ ), with the fine fraction of the filter material ( $D_{15f}$ ):

$$\frac{d_{15f}}{d_{15b}} > 4 \quad (3.4)$$

In which  $d_{15}$  is the grain size corresponding to 15% passing. This criteria need to be applied only to the filter or the sub-base. The drainage layer is so permeable and this criterion can certainly be satisfied.

### 3.3 An empirical method for evaluating the internal stability of the material

Material is defined internally stable when its skeleton does not affect modification. When finer soil particles (mobile particles) are moved through constrictions between larger soil particles (soil skeleton) by hydraulic or seepage forces, the material are considered unstable. In literature, this is described as suffusion (Chapuis, 1992). Usually, internally unstable material are those broadly graded soils with particles from silt or clay to gravel size, whose particle size distribution curves are concave upward, or gap graded soils (Wan e Fell, 2008). However, even materials which have a uniform particle size distribution curve can be internally unstable.

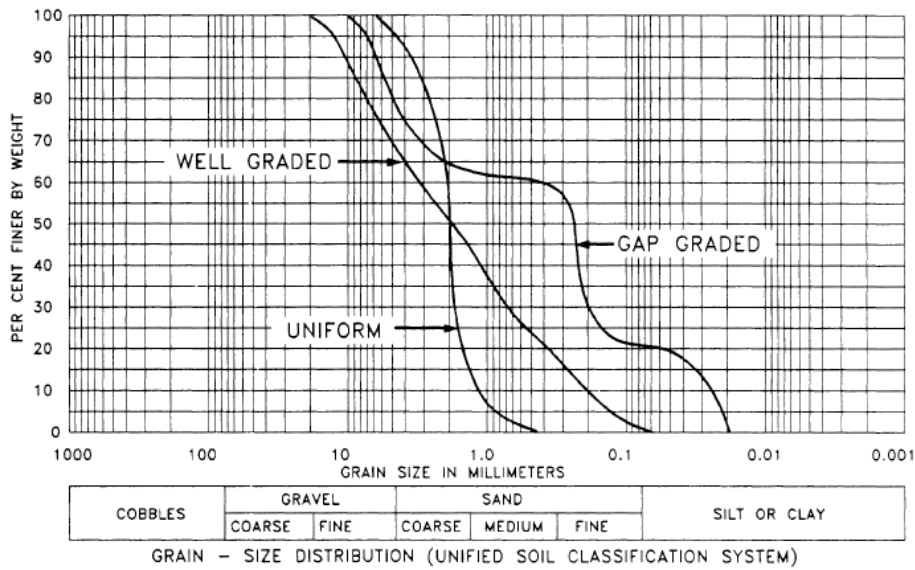


Figure 3.4: Grain size distribution curve: uniform, well graded and e gap graded; (Yun Zhou, 1998).

To assess the internal stability of a layer formed from granular material, there are several empirical methods. Among the many, it is focused the Kezdi (1979) and Kenney and Lau (1985) approach.

Kezdi (1979) proposed splitting up the grain size distribution of a soil into two distributions of the fine and coarse parts, and assessing the stability by Terzaghi’s well-known filter criterion applied to the two distributions:

$$\frac{d_{15f}}{d_{85b}} < 4 \text{ for each } d^* \tag{3.5}$$

Where  $d_{15f}$  grain diameter for which 15% of the grains by weight of the coarse soil are smaller; and  $d_{85b}$  grain diameter for which 85% of the grains by weight of the fine soil are smaller;  $d^*$  is a generic grain size by which the curve of the tested material is cutting.

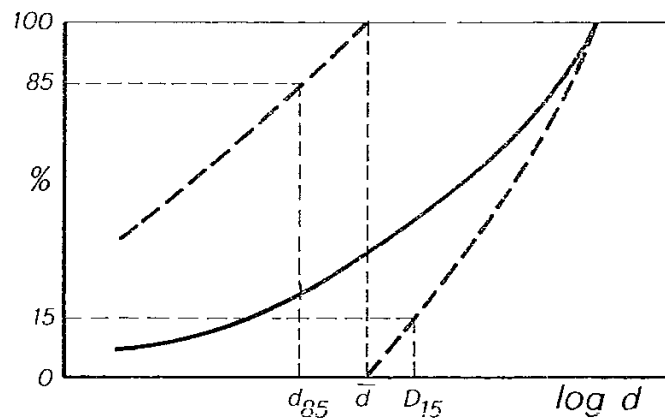


Figure 3.5 : Graphical interpretation of the Kezdi (1979) method (Musso e Federico,1983) .

Kenney and Lau (1985) proposed transforming the ordinary grain size distribution curve to a F-H diagram. Here F is the mass percentage of grains with diameters less than a particular grain diameter d and H is the mass percentage of grains with diameters between d and 4d. The soil will be considered as stable if, for  $F < 20$  or 30% the curve thus obtained is located above the critical line  $H=F$ . On the contrary, if some portion of this curve passes below the line  $H=F$ , the soil will be considered as unstable. According to Kenney and Lau (1986) the values of 20% applies to the widely graded soil in the range  $0.2 < F < 1$  and the values of 30% to the normally graded soils in the range of  $0.3 < F < 1$ .

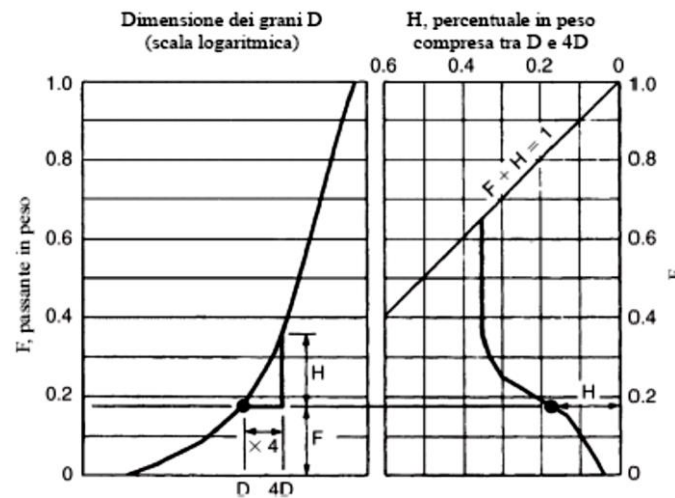


Figure 3.6: Graphical interpretation of the Kenney e Lau method (1986).

### 3.4 Grain size distribution curve of the biogas drainage layer

In accordance with the filter design criteria, reported in the section 3.2 and 3.3, the grain size distribution curve of the biogas drainage layer must be internally stable and compatible with the neighboring layers. The presence of a non-woven geotextile at the interface with the clay, allows us to exclude the upper layers from the calculations subsequently proposed. Therefore, to identify the curve in question, we will proceed by applying the Terzaghi (1922) empirical methods and considering as base materials the underlying waste. Contextually is identified the particle size distribution of the foundation layer, because it is placed between the biogas drain and waste (paragraph 1.2).

#### 3.4.1 Grain size distribution of the municipal solid waste

Municipal solid waste (MSW) is a mixture of wastes that are primarily of residential and commercial origin. Typically, they consist of: organic waste, paper, fabric, garden wastes, plastic, pieces of metal, rubber, glass, waste from demolition, slag and ash. The proportion of

these materials will vary from one site to another and also within a site. Life style changes, legislation, seasonal factors, pre-treatment and recycling activities result in a changing waste stream over time. Moreover, the composition of MSW varies from region to region and country to country (Dixon, 2004).

The particle size of the wastes are reduced over time due to the degradation processes that occur within the landfill. Therefore, the composition of the waste is identified as a function of the degree of aging (Figure 3.7). Consequently, because of their great variability is assigned them an area that describe the grain size distribution curve built on a semi-logarithmic plane, which varies from silt or clay to gravel size. A fresh MSW whose fill age is less than a few years would contain significant amounts of organic components with size larger than gravel (Hyun II, Borinara and Hong, 2011). Grain size distribution of the waste presents a uniform coefficient higher than 15, and then is considered well graded.

In the present case, wastes represent the base material. Then, for the filter design criteria, it is used the lower limit of the area that characterize the dimension of this material: the particles migration due to erosion is oriented toward the voids created by coarse particles forming the waste from clogging criterion.

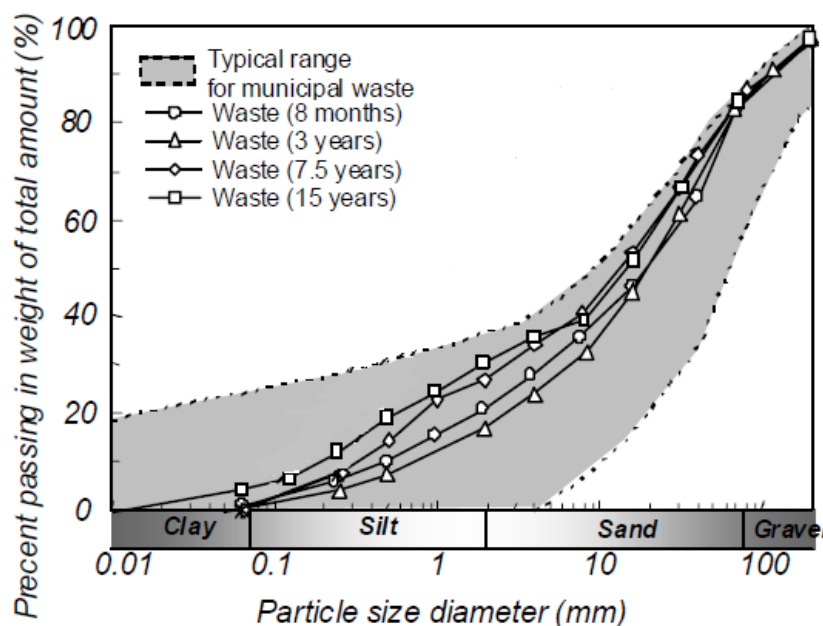


Figure 3.7: Grain size distribution curve of the municipal solid waste from Jessberger (1994); (Hyun II, Borinara and Hong, 2011).

### 3.4.2 Grain size distribution and internal stability of the foundation layer

As described in section 3.2 and 3.3, the grain size distribution curve of the foundation layer must be internally stable and compatible with the underlying waste. To prevent migration phenomena of fine particles forming this layer, it is necessary to apply the Terzaghi's clogging criterion. According to this method, the  $d_{15}$  of waste is approximately equal to 16 mm and hence, the  $d_{85}$  of the foundation layer must be greater than 4 mm, as shown in figure 3.7.

Applying the Terzaghi's permeability criterion, the  $d_{15}$  of the foundation layer should be less than 4mm. However, these layers are dry and not crossed by a water flow, then the use of this principle is only conservative.

In agreement with these observations, it is determined an indicative grain size distribution curve, that has  $d_{15}$  and  $d_{85}$  respectively equal to 4 and 20 mm (figure 3.8). It has an upwards concavity, is uniform and has no gaps, in other words, and according to the definitions reported in the section 3.3, is internally stable (Figure 3.9 e 3.10). Based on these results, the suitable material for the foundation layer consists of gravels.

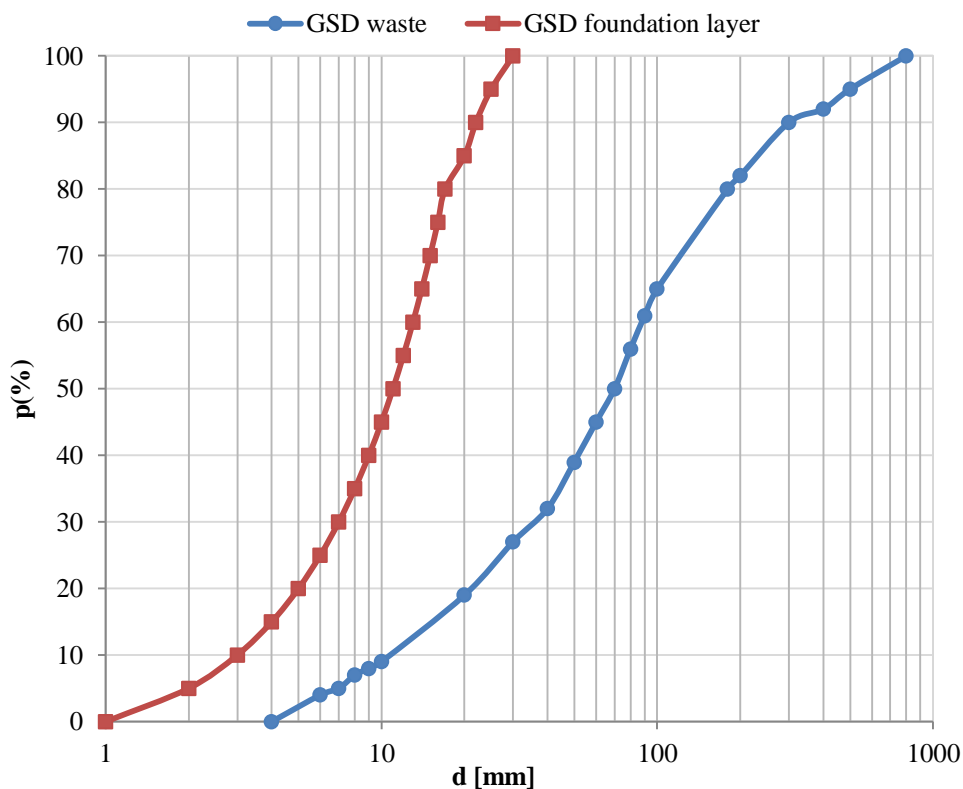


Figure 3.8: Graphical representations of the grain size distribution (GSD) of the foundation layer, compared with the GSD of the waste material.

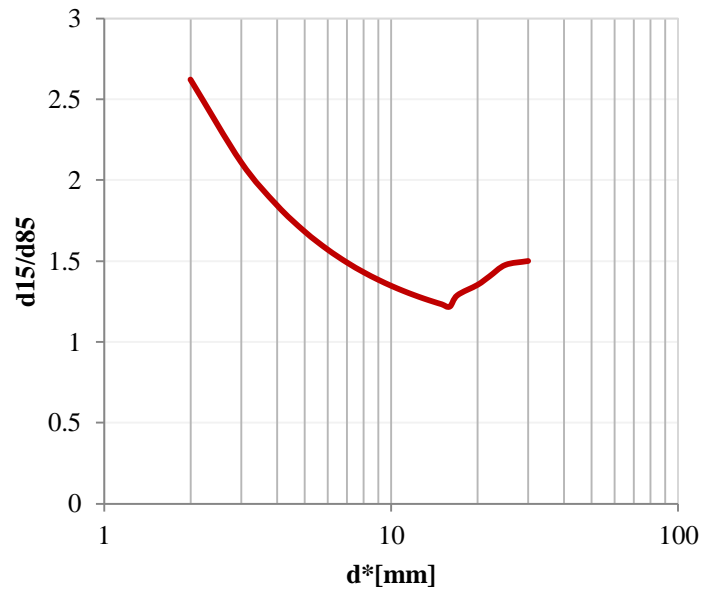


Figure 3.9: Internal stability results of the foundation layer obtained by using Kezdi procedure (1979);

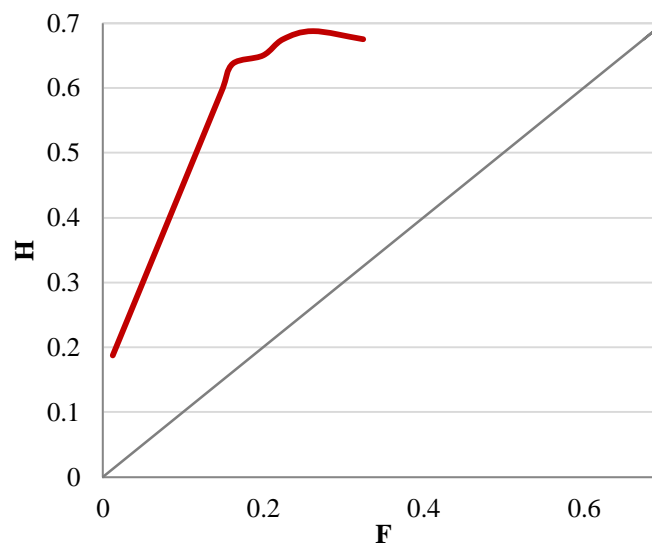


Figure 3.10: Internal stability results of the foundation layer obtained by using Kenney e Lau procedure (1986);

### 3.4.3 Grain size distribution and internal stability of the biogas drainage layer

Through the Thiel's procedure (1998), and the Hazen's formula (1892) it was possible to identify the minimum equivalent diameter ( $d_{10}$ ) of the biogas drainage layer (section 2.6). In particular, it must be greater than 0.1 mm and, in the present case, it represents an additional information by which it is possible to determine the grain size distribution curve of the biogas drainage layer.

Applying the Terzaghi's clogging criterion (section 3.2) and considering the worst case scenario, foundation layer formed by material that is homogeneous, uniform ( $C_u \leq 2$ ) and of size equal to 4 mm (section 3.4.2), the  $d_{85}$  of the drainage layer of the biogas should be greater than 1mm. This hypothesis is considered conservative and therefore applicable.

An example of the grain size distribution curves of the three layers is reported in figure 3.11. They identify the minimum order of magnitude of the material used. Indeed, as reported previously, the  $d_{85}$  of the foundation and biogas drainage layer, are respectively equal to 1 mm and 4 mm. Moreover, according to the definitions reported in the section 3.3, the curve of the biogas drainage layer is internally stable, as it shown in figure 3.12 and 3.13. Based on these results, the suitable material for the biogas drainage consists of coarse sand.

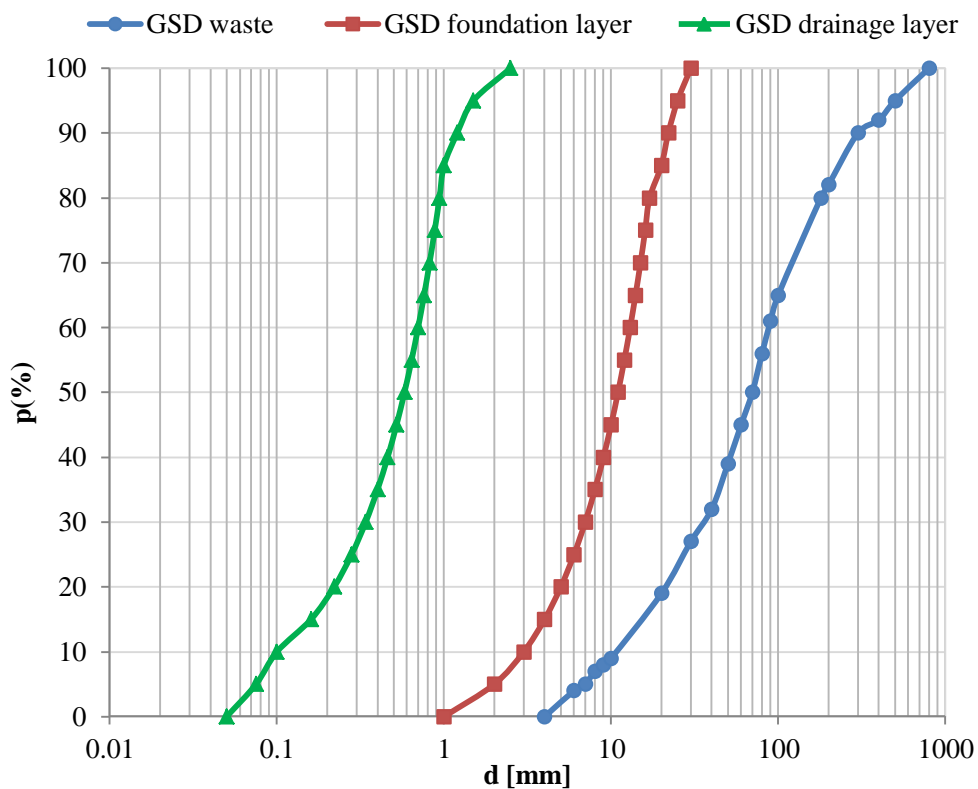


Figure 3.11: Graphical representations of the minimum grain size distribution (GSD) of the biogas drainage layer, compared with the GSD of the waste and the foundation layer.



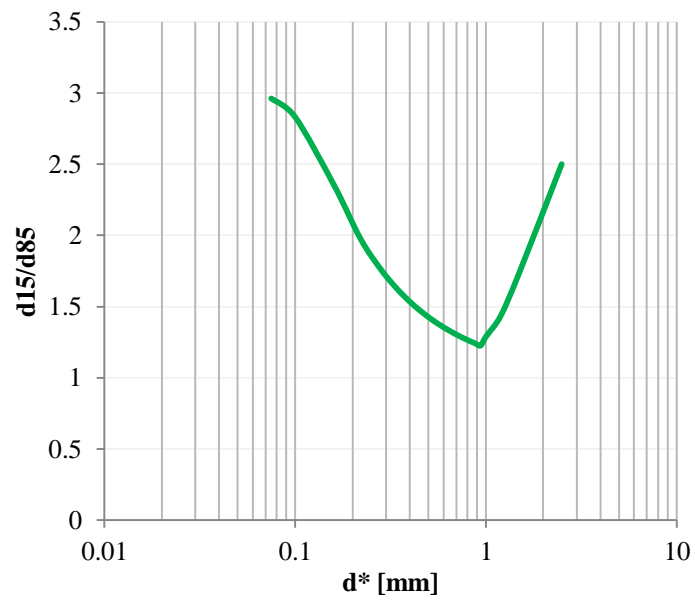


Figure 3.12: Internal stability results of the biogas drainage layer obtained by Kezdi procedure (1969);

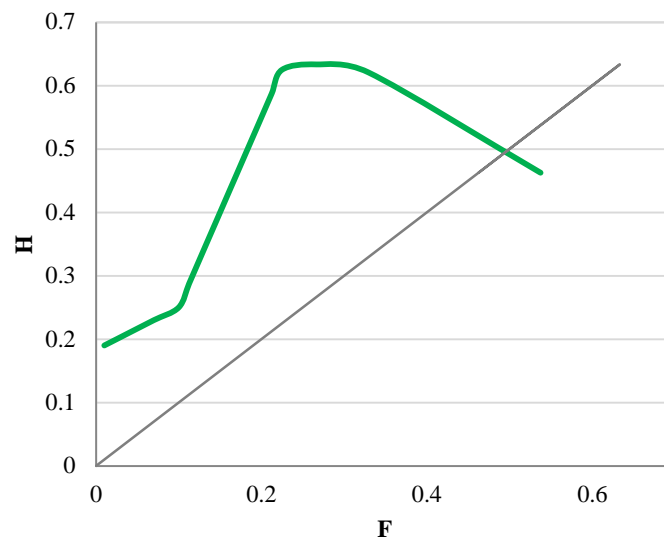


Figure 3.13: Internal stability results of the biogas drainage layer obtained by Kenney e Lau procedure (1985);

## ***CHAPTER 4: Analysis of the loads acting on the biogas drainage layer***

The actions present on the biogas drainage layer are different and classified in two main categories:

- *Permanent*, explicated throughout the entire useful life of the work:
  - static load induced by weight of the upper layers.
  
- *Variable*, presents during its installation:
  - due to vehicles used for the installation of the biogas drainage layer;
  - due to the energy transmitted by compactations means used for the realization of the hydraulic barrier.

The task of the granular material forming the biogas drainage layer is to resist to these actions.

### **4.1 Permanent loads**

According to the legislative decree 36/2003, the biogas drainage layer is placed at the base of the final landfill cover. For this reason, it must bear the weight of the upper layers, that is considered as a uniformly distributed load, of intensity calculated by the following relationship:

$$q \left[ \frac{kN}{m^2} \right] = \gamma \left[ \frac{kN}{m^3} \right] \cdot s [m] \quad (4.1)$$

Where  $q$  is the uniformly distributed load or weight for unit surface acting on the strata,  $\gamma$  is the average unit weight, and  $s$  is the thickness of the strata placed above the biogas drainage layer.

Table 4.1: characteristics of the layers forming the final landfill cover.

Cover layer	Height, h [m]	thickness, s [m]	$\gamma$ [kN/m <sup>3</sup> ]
<b>Protection layer</b>	1	1	17
<b>drainage</b>	0.66	1	16.5
<b>Hydraulic barrier</b>	0.55	1	20
<b>Biogas collection layer</b>	0.55	1	16.5

The characteristics parameters of the layers are reported in Table 4.1. For safety reasons, in this part of the work it is assumed an average unit weight of 20 kN/m<sup>3</sup>. Therefore, the uniformly permanent load acted on the biogas drainage layer is equal to 20 kPa.

## 4.2 Variable loads

The operating loads are due to the actions of the vehicles used for the installation and realization of the biogas drainage layer and, to the energy transmitted by compaction means for the laying of the hydraulic barrier.

- **Loads induced by work means**

During the realization of the biogas drainage layer, the material used is loaded into trucks, transported on landfill, tipped, compressed and spread by work means. The effect of these actions on the material can be translated as resistance to:

- Impacts due to falling;
- Fracturing due to crushing;
- Wear, abrasion and friction due to grains sliding induced by work means.

These dynamic efforts are being very aggressive in respect of the material. Therefore, before the realization of the biogas drainage layer it is necessary to evaluate their effect.

- **Loads induced by the compaction of the hydraulic barrier**

The third and last type of action is induced by the action transmitted through compaction of the above hydraulic barrier. In this case, this load is applied on a strata because the biogas drainage layer has been realized. Therefore, the material is confined and behaves as a continuum medium.

The hydraulic barrier has the aim to minimize and prevent water infiltration into the body waste. Consequently and in accordance with the legislative decree 36/2003, it must realize by using clayey or silty-clay material, suitably installed by compaction in order to:

- Decrease permeability;
- Increase shear strength;
- Reduce compressibility;
- Controlling shrinkage and swelling;
- Reduce the potential liquefaction.

The compaction is performed by impressing a certain energy, that depends on type, weight and power exerted by the means used. In the case of cohesive material is preferable to transmit a quasi-static load and working with sheep foot roller.

In specific, it means to work at low speed and high energy and pressure. The compaction takes place for successive layers of 20-30 cm and therefore, the layer in question must be compressed for determined intervals of time. Moreover, through the grains contact this pressure is transmitted in depth and redistributed over a greater area, i.e. load diffusion (Figure 4.1). Consequently, the laying of the first strata of the hydraulic barrier is the most onerous for the material forming the biogas drainage layer.

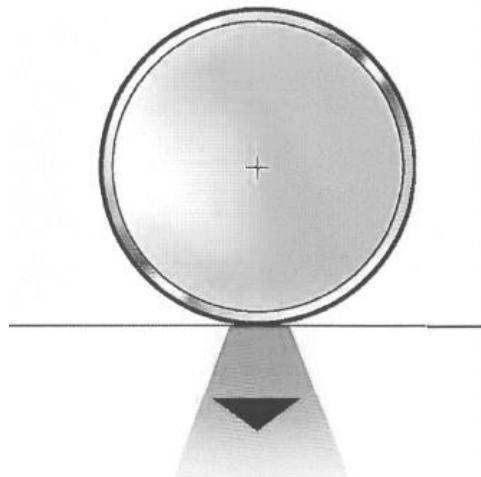


**Figure 4.1: Load diffusion induced by compaction.**

To evaluate the entity of the stresses transmitted by compaction means, for the realization of the hydraulic barrier on the biogas drainage layer, is used elastic theory usually applied to assess the soil-foundation interaction. Indeed, it is assumed that the means work induces the same vertical stresses of a foundation built on a ground.

The Boussinesq's method(1885) was the first used for this type of analysis. Through this model it is possible to determine the stresses produced by the application of a uniform force  $P$ , that acts perpendicular to an horizontal surface placed on a semi-infinite, homogeneous and isotropic solid. As said before, the solutions of this method are obtained by the elastic theory: when the load is removed any type of deformation or settlement produced is reversible.

The equation of the vertical stresses for a point  $N$ , located at depth  $z$  from the horizontal surface and at a distance  $r$  from the vertical, can be written in polar coordinates as:

$$\sigma_z = \frac{3P}{2\pi} \frac{z^3}{(z^2 + r^2)^{\frac{5}{2}}} = \frac{P}{z^2} I_\sigma \quad (4.2)$$

Where  $\sigma_z$  is the vertical stress for a point  $N$ , located at depth  $z$  from the horizontal surface and, at distance equal to  $r$  from the vertical surface, for a point  $a$  of application  $P$  (figure 4.2). The  $I_\sigma$  is the influence factor of vertical force and depends on the point in which you want to know the stress state.

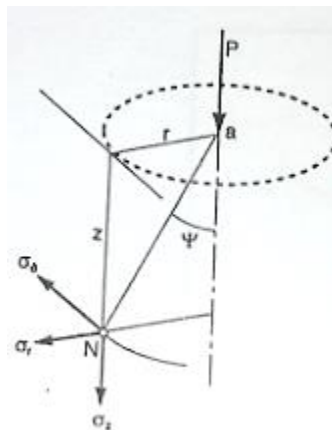


**Figure 4.2: Graphical representation of the Boussinesq model.**

In practical applications, it is used charts that are able to identify or provide, for different types of charged areas, the following data:

- The variation of the vertical stress  $q$  in function of the depth  $z$ , along axis or in the center of the loading area;
- The trend of the curves of equal pressure in a vertical cross section.

These data allow the determination of the vertical stresses distribution on any horizontal surfaces. In the present case, it is considered the Steinbrenner (1934) solution for a rectangular

footprint loading, which is representative of the pressure transmitted by the compactions means. For simplicity it is used the reference chart, through which it is possible to determine the vertical stress present at 30 cm depth (thickness of the first strata forming the hydraulic barrier) from the biogas drainage layer. To proceed with this calculation it is necessary to evaluate the pressure transmitted by the work means ( $q$ ) and the dimension of the sheep foot roller footprint, width ( $L$ ) and thickness ( $B$ ). Through these values it is possible to enter in the references Steinbrenner (1934) chart, which is shown in Figure 4.3, and define the pressure transmitted on the biogas drainage layer.

The most unfavorable loading condition for the biogas drainage layer is obtained when the  $L/B$  ratio tends to infinity and the  $z/B$  ratio tends to zero. This assumption is satisfied when the depth,  $z$ , is very small and the load width,  $L$ , is very large. Hence, as shown in the table 4.4, the ratio between the vertical stress ( $\Delta\sigma_z$ ) and the load ( $q$ ) is equal to 0.25.

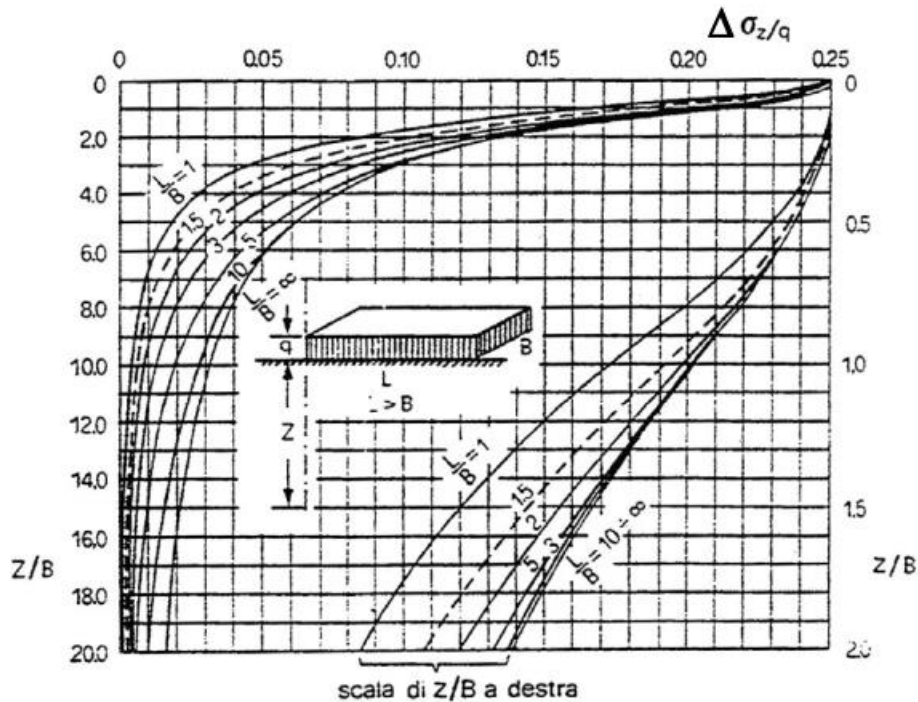


Figure 4.3: Steinbrenner chart (1934);

z/B	Valori di $\Delta\sigma_z/q$						
	L/B = 1.0	L/B = 1.5	L/B = 2.0	L/B = 3.0	L/B = 5	L/B = 10	L/B = $\infty$
0.00	0.2500	0.2500	0.2500	0.2500	0.2500	0.2500	0.2500
0.25	0.2478	0.2482	0.2483	0.2485	0.2485	0.2485	0.2485
0.50	0.2325	0.2378	0.2391	0.2397	0.2398	0.2399	0.2399
0.75	0.2060	0.2182	0.2217	0.2234	0.2239	0.2240	0.2240
1.00	0.1752	0.1936	0.1999	0.2034	0.2044	0.2046	0.2046
1.50	0.1210	0.1451	0.1561	0.1638	0.1665	0.1670	0.1670
2.00	0.0840	0.1071	0.1202	0.1316	0.1363	0.1374	0.1374
3.00	0.0417	0.0612	0.0732	0.0860	0.0959	0.0987	0.0990
4.00	0.0270	0.0383	0.0475	0.0604	0.0712	0.0758	0.0764
6.00	0.0127	0.0185	0.0238	0.0323	0.0431	0.0496	0.0521
8.00	0.0073	0.0107	0.0140	0.0195	0.0283	0.0367	0.0394
10.00	0.0048	0.0070	0.0092	0.0129	0.0198	0.0279	0.0316
15.00	0.0021	0.0031	0.0042	0.0061	0.0097	0.0158	0.0213
20.00	0.0012	0.0018	0.0024	0.0035	0.0057	0.0099	0.0159

Figure 4.4: Values of  $\Delta\sigma/q$  in function of z/B and L/B obtained from the Steinbrenner solution (1934);

Multiplying this value for the pressure applied by the sheep foot roller, it is possible to obtain the vertical stresses acting on the biogas drainage layer. More specifically, the load for unit surface transmitted by the compactions means ( $q$ ) varies between 1400 and 7000 kPa, and assume an higher value in function of the drum types. Consequently, the vertical stress ( $\sigma_z$ ) is respectively equal to 350 kPa and 1750 kPa.

### 4.3 Actions analysis and modes of grain breakage

Considering the results obtained in the previous sections (4.1 and 4.2), the material forming the biogas drainage layer will be subject, in the following sequence, to:

- Fracturing, attrition and wear induced by dynamic efforts due to grains contacts, sliding and impacts explicated during the installation;
- Compression induced by quasi-static load and static load, respectively for the compaction of the hydraulic barrier and for the weight of the overlying layers.

Table 4.2: Intensity of the static loads.

Load	Intensity (kPa)
Permanent	20
Quasi-Static	350-1750

Looking at table 4.2, it is noted that the load induced by the compaction means is more heavily than the weight transmitted by the overlying layers.

It is important to note that , in this case, it is not considered the property called "freezing", or ability of the layer to withstand frost and freeze-thaw cycles: in our climates the annual heat wave interests a layer of the order of 60 cm, below which the temperatures does not drop below 0°C. In the present case, the thickness of the layers placed above the biogas drainage layer is greater than 60 cm, and then the layer itself will never be subject to the above actions.

In each cases, the material can arrive at failure and can change the geotechnical requirements for which is chosen (sections 2.6 and 3.4). Due to mechanical actions, the grain breakage may classified according to three modes (Guyon and Troadec, 1994):

- *Fracture*: a grain breaks into smaller grains of similar sizes (i.e. splitting);
- *Attrition*: a grain breaks into one grain of a slightly smaller size and several much smaller ones;
- *Abrasion*: the result is that the granulometry remains almost constant but with a production of fine particles (lower than the effective size).

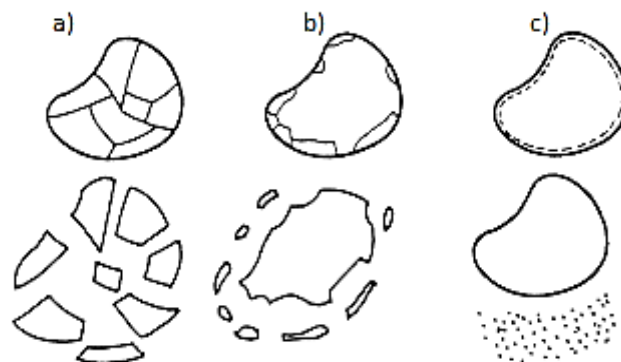


**Figure 4.5: Different modes of grain breakage: (a) fracture; (b) attrition; and (c) abrasion (Ali Daouadji et al, 2001).**

Hence, the splitting of grains corresponds to a mode of grain rupture by fracture; the rupture of sharp angles to the mode of rupture by attrition, whereas the rupture of micro asperities, during the sliding of grains, corresponds to the mode of rupture by abrasion. The latter may occur in the absence of notable fracture or attrition; for example, during cyclic tests of small stress intensity, as in a railroad ballast, for which grain size and grain size distribution do not change in significant proportion. Fracture and attrition can lead to significant changes in the grading curve and consequently, the mechanical properties of granular material can significantly change (Daouadji Ali et al, 2001).

Hence, the correlation between the loads and grain breakage is summarized in Table 4.3.



**Table 4.3: Correlation between the grain breakage and the associated actions;**

<b>Grain Breakage</b>	<b>Actions</b>	<b>Effect</b>
Fracture	Impacts Compression	Lead to significant changes in the grading curve;
Attrition	Sliding of the grains	Lead to significant changes in the grading curve;
Abrasion	Wear freeze-thaw	Lead to an increment of the fine fraction of the grading curve;

## CHAPTER 5: *Intrinsic characteristics of granular materials*

As explained in Chapter 4, the granular material formed the biogas drainage layer must possess a mechanical resistance through which withstand static and dynamic loads. Therefore, in this chapter, in order to define this characteristics will be reported literature studies.

Granular materials are defined as loose materials consisting of a set of discrete particles or grains including sand, gravel, rocks and aggregate, i.e. granular mineral particles used in construction or in combinations with various types of cementing material to form concretes or used alone as road bases, backfill, etc. Usually, they are classified in function of their dimension. Based on this property, they show different mechanical behavior. According to the AASTHO classification, are those having dimension higher than 0.075mm (Table 5.1).

**Table 5.1: Granular materials classification based on their dimensions; MIT (Massachusetts Institute of Technology), AASTHO (American Association of State Highway and Transportation Officials), AGI (Association geotechnical Italian) (Lancelotta, 1983).**

System	Gravel [mm]	Sand[mm]	Silt [mm]	Clay [mm]
MIT(1931)	60÷2	2÷0.06	0.06÷0.002	<0.002
AASTHO(1970)	75÷2	2÷0.075	0.075÷0.002	<0.002
AGI	> 2	2÷0.02	0.02÷0.002	<0.002
CP 2001 (1957)	60÷2	2÷0.06	0.06÷0.002	<0.002

The granular material resistance depends on the intrinsic characteristics of individual grains, such as shape, size, particle size distribution and its mechanical resistance.

- Shape

Flat particles, thin particles, or long, needle shaped particles break more easily than cubical particles (Harold N, Atkins). Increase in grain breakage depends also on the angularity of grains (shape factor). This may be due to a greater fragility of the contact points of small curvature radii and to the intensity of forces at contact points (Hardin, 1985; Ali Daouadji et al, 2001).

- Size

A bigger grain breaks easily than finer one. (Mitchell, 1993; Lee and Farhoomand, 1967). Smaller particles are generated from the larger ones along zones of lower strength. As the particle size increases, particle crushing also increases. Larger particles contain more flaws or defects and then, they have a higher probability of the defect being present in the particles that will break. As the breakdown process continues, there are fewer defects in the subdivided particles. Therefore, similar particles are less likely to fracture as they become smaller (Yamamuro and Lade (1996).

- Grain size distribution

Lower is the uniform coefficient of the material, higher is the grain breakage. Tested in the same mechanical conditions and for identical nature parameters except for the value of  $C_u$ , the well graded mixture presented very slight evolution in its grain size distribution in contrast to the badly graded mixture (Figure 5.1) (Ali Daouadji et al, 2001). Well-graded soils do not break down as easily as uniform soils. As the relative density increases, the amount of particle breakage decreases. Both these factors are based on the fact that with more particles surrounding each particle, the average contact stress tends to decrease (Yamamuro and Lade (1996). Densely graded aggregate layers also increase the strength developed: particles are locked together to a greater degree, aiding in the development of frictional resistance to shearing failures.

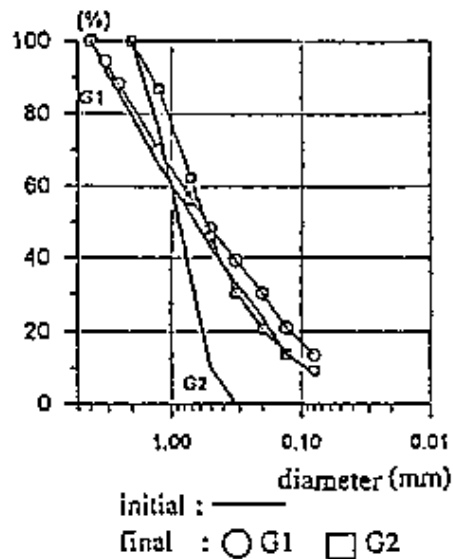


Figure 5.1: Evaluation of the influence of the uniform coefficient on the grain size distribution for two different material G1 and G2, having respectively  $C_u$  equal to 10 and 2 (Hicher et al., 1995) .

Table 5.1: Tests performed on granular material to determine some properties.

Properties	Test
Gradation	Sieve analysis
Hardness and Abrasion	Aggregates impact test- Los Angeles abrasion test
	Aggregates pressure test- Darry abrasion test
	Aggregates friction test- Deval abrasion test
Durability	Soundness test
Deleterious Substances	Petrographic analysis
	Sand equivalent test
Fines Content	Washed sieve analysis
Particle shape	Amount of thin or Elongated particles
Particle surface	Amount of crushed particles
Chemical stability	Reactivity - stripping

### 5.1 Definition of grains quality

In addition to the aforementioned parameters, it is important to consider other properties indicative of the mechanical strength of the material. They are:

- Hardness, abrasion or resistance to wear;
- Durability;
- Surface texture;
- Deleterious substances;

- Crushing strength;
- Soft and light weight particles.

They give an indication of quality of the material used.

- Hardness, Abrasion or resistance to wear

The hardness and abrasiveness of rocks depend on type and quality of the various constituents and, by the bonds between them. Hardness is defined as the penetration or deformation resistance of a body induced by external forces. It is expressed by a number that indicates the characteristics of the material plastic deformation. It is a concept related to the behavior of the material, rather than a fundamental property.

Abrasion is the superficial removal of material caused by repeated friction actions. Therefore, it indicates the ability of the material to resist wear or degradation phenomena. As hardness, it is associated to the mechanical behavior of the material.

- Durability

The durability of an aggregate particle shows its resistance to disintegration due to cycles of wetting and drying, heating and cooling, and especially freezing and thawing. Aggregates particles have pores, which often become saturated. Repeated cycles can cause the particles to break. This is especially dangerous with particles from sedimentary rocks, which usually have planes of weakness between layers.

- Shape and surface texture

Particle shape and surface texture affect the strength of the aggregate particles, the bond with cementing materials, and the resistance to sliding of one particle over another. Particles with rough, fractured faces allow a better bond with cements do rounded, smooth gravel particles. Rough faces on the aggregate particles also allow a higher frictional strength to be developed if some load would tend to force one particle to slide over an adjacent particle.

- Deleterious substances o fines

Deleterious substances are harmful or injurious materials. They include various type of weak or low-quality particles and coatings that are found on the surface of aggregates particles. Deleterious substances include organic coating; dust (material passing 0.0075 mms sieve), clay lumps, shale, coal particles, friable particles, etc. These substances may affect the strength of the

aggregate. Soft particles may be unsuitable where they may be exposed to abrasion, such as road surface.

- Crushing strength

Crushing strength is the compressive load that aggregate particles can carry before breaking. This trait is relatively important for most aggregate uses since aggregate strength of the asphalt or concrete mixture.

- Chemical stability

Chemical stability refers to specific problems due to the chemical composition of aggregate particles. The presence of material unstable influences the capacity of the material to maintain its properties.

## **5.2 Determination of the tests used to determine the mechanical resistance of the aggregates**

The grains or aggregate mechanical resistance is strictly correlated to the parent material. In the case of natural materials it is a function of the mineralogical composition, whereas for artificial materials it depends on different factors, like raw material, mixture or chemical component. Therefore, the history of its natural deposition, or the history of its fabrication for the artificial mixtures, can be a determining factor (Ali Daouadji et al, 2009).

Generally, an aggregate is a brittle material: achieved the maximum allowable stress arrives at failure without strain. Then, at some point, the material suddenly collapses or crushes. The grain or particle mechanical resistance is evaluated by the uniaxial compressive test and calculated as (Jaeger , 1967):

$$\sigma = \frac{F}{d^2} \quad (5.1)$$

where  $\sigma^f$  [kPa] is the single particle strength;  $F$  is the load at failure and  $d$  is the diameter of the grain (corrected or not from asperity crushing). Thus, as the size of the grains decreases due to crushing, the strength of the new grains increases (Ali Daouadji et al, 2009).

The mechanical resistance is strictly correlated with parameters such as hardness, durability and abrasion resistance. Indeed, it increases with the quality of the materials used (Al Harti,2001). Therefore, to determine this property can be performed laboratory tests, usually applied for evaluating the friction, wear, impact and crushing resistance. For the first three categories of

actions are used the Los Angeles abrasion test. In order to measure the resistance of an aggregate to crushing, under gradually applied compressive load, are applied the aggregate crushing test; while for assessing the resistance to sudden shock are performed the aggregate impact test (Al-Harti,2001). In general, they are used for determining the effects of frictional and compressive forces induced by pressure applied over the material. However, exist other tests able to evaluate the quality and the strength of the aggregates, like the Deval and Darry abrasion tests (Harold N.Atkins,2006).

Despite, they are time consuming and require large quantities of aggregates of specified grading, they are extremely useful in determining the quality of the aggregates (Al-Harti,2001). Indeed, aggregate is exposed to a number of physical and chemically degrading forces during processing, transporting, and construction. They must be tough and abrasion resistant to prevent crushing, degradation and disintegration when stockpiled, fed through an asphalt plant, placed with a paver, compacted with rollers, and subjected to traffic loadings. Aggregates, which do not have adequate toughness and abrasion resistance, may cause construction and performance problems (Ugur I., et. al. 2010).

The Los Angeles abrasion test, the aggregate impact test and the aggregate crushing test types of tests are destructive and then, the material modifies irreversibly its external surface (Al-Harti, 2001).

The result of these types of test is a bulk index value, that indicates the percentage by weight retained on a sieve, of size smaller than the dimension of the fraction analyzed. It is determined by sieve analysis: the mass index is equal to the material passing a sieve of standard dimension (2.36 or 1.7 mm), that is variable with the considered test ( Table 5.2). A crushing and degraded material presents values of these index very high (Ugur I., et. al. 2010). Shape, dimension, fine fraction and grain size distribution can be completely different for a given bulk index obtained from different materials: the results of these tests does not indicate the way in which the particles have decreased their size (Stenlid, 1996; Thörnvall, 1997).

**Table 5.2: Bulk indexes obtained for different test.**

<b>Test</b>	<b>Result</b>	<b>Material*</b>
Aggregate impact test	$AIV (\%) = \frac{[Mi - M_{2.36}]}{Mi} \cdot 100$	Retained on sieve 9.52mm and passing 12.70 mm
Los Angeles abrasion test	$LA (\%) = \frac{[Mi - M_{1.7}]}{Mi} \cdot 100$	Material retained on sieve of 19 mm or 7.5 mm
Aggregate crushing test	$ACV (\%) = \frac{[Mi - M_{2.36}]}{Mi} \cdot 100$	Retained on sieve 9.52mm(or 10mm) and passing 12.70 mm (or 14mm)

\*depend on the classification system

### 5.2.1 Los Angeles Abrasion test

The abrasion tests measure the wear resistance of rocks or aggregates by using an abrasive material, or for contact with another rock or metal. The result gives an indication of the hardness, toughness and the quality of the material. Simulates the effect induced by cyclic loading, freezing and thawing, and evaluates the degradation resistance by wear and abrasion. Is generally used to test the mechanical resistance of aggregates used for road foundations. Consequently, simulates the effect of vehicle loads for a time equal to the nominal lifetime of the work itself.

The Los Angeles test is performed using a sample having dimensions in a well-defined range and having a weight close to 5000g (Table 5.3). In accordance with the ASTM system, grain size must be within in one of the ranges reported in Table 5.3; while according to UNI 1097-2, the sample must be between 10 and 14 mm and also must meet one of the following requirements: between 60% and 70% passing through a sieve test 12.5mm; or between 30% and 40% passing through a sieve test by 11.2 mm.

Test samples were oven-dried at 105–110 °C for 24 hours and then cooled to room temperature before they were tested. After that it is placed in a drum with 11 steel balls (the abrasive charge) of weight between 400 and 450 grams. The drum was rotated for 500 revolutions at a rate of 30–33 rev/min and then the sample was sieved through the No. 12 sieve (1.7 mm). The amount of material passing the sieve, expressed as a percentage of the original weight, is the LA abrasion loss or percentage loss.

$$LA (\%) = \frac{[M_i - M_{1.7}]}{M_i} \cdot 100 \quad (5.2)$$

$M_i$  represents the initial mass,  $M_f$  the mass retained on a sieve of 1.7 mm.

**Table 5.3: The grain size composition of the sample for coarse aggregates smaller than 38 mm (ASTM).**

Size- in square mesh sieve (mm)		Weight classes in grams- Grain size composition			
Passing	Retained	A	B	C	D
38	25.4	1250±25	-	-	
25.4	19	1250±25	-	-	
19	13.2	1250±10	2500±10	-	
13.2	9.5	1250±10	2500±10	-	
9.5	5.6	-	-	2500±10	
5.6	4.7	-	-	2500±10	
4.7	2.3	-	-	-	5000±10
	Total	5000±10	5000±10	5000±10	5000±10



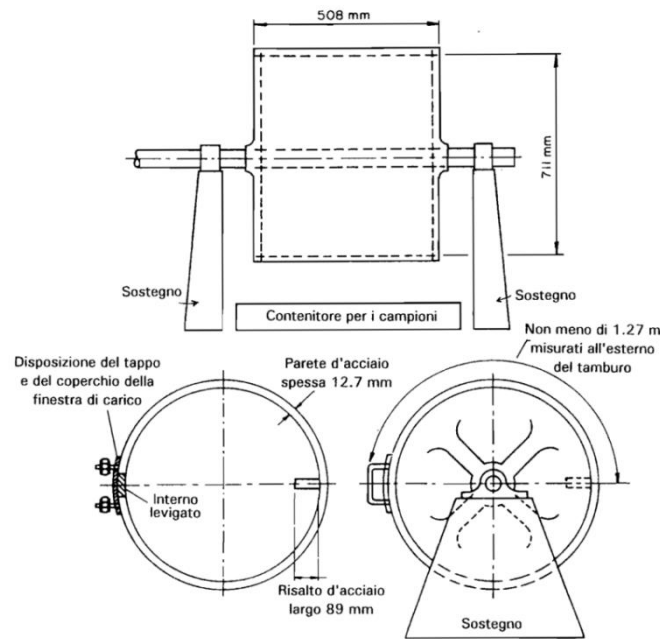


Figure 5.2: Los Angeles apparatus (ISRM,1998).

### 5.2.2 Aggregate impact test

Aggregate impact test is used to evaluate the resistance of the aggregate when subjected to a sequence of impact. The apparatus consists of a steel test mould with a falling hammer or weight as shown in Figure 5.3. The material used is aggregate passing a 12.70 mm sieve and retained on a 9.52 mm sieve. It shall be clean and dry (washed if necessary) but it must not be dried for longer than 4 hours nor at a temperature higher than 110 °C otherwise certain aggregates may be damaged. The crushed aggregate is sieved over a 2.36 mm sieve. The aggregate impact value (AIV) is fraction passing 2.36 mm:

$$AIV (\%) = \frac{[M_i - M_{2.36}]}{M_i} \cdot 100 \quad (5.3)$$

$M_i$  represents the initial mass,  $M_f$  the mass retained on a sieve of 2.36 mm.

### 5.2.3 Aggregate crushing test

Aggregate crushing test is used to evaluate the resistance of the aggregate when subjected to a pressure. The apparatus (Figure 5.4) consists of a case hardened steel cylinder 154 mm diameter and 125 mm high. It requires a compression testing machine capable of applying a force of up to 500 kN and which can be operated to give a uniform rate of loading so that this force is reached in 10 minutes. The material used is aggregate passing a 12.70 mm sieve and retained on a 9.52 mm sieve. It shall be clean and dry (washed if necessary) but it must not be dried for

longer than 4 hours nor at a temperature higher than 110 °C otherwise certain aggregates may be damaged. The crushed aggregate is sieved over a 2.36 mm sieve. The aggregate impact value (ACV) is fraction passing 2.36 mm:

$$ACV (\%) = \frac{[M_i - M_{2.36}]}{M_i} \cdot 100 \quad (5.4)$$

$M_i$  represents the initial mass,  $M_f$  the mass retained on a sieve of 2.36 mm.

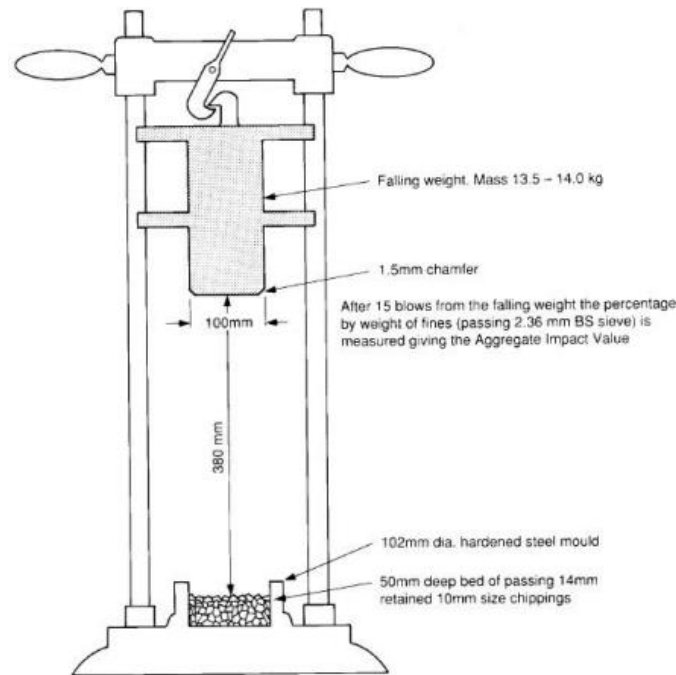


Figure 5.3: Aggregate Impact test apparatus (Miller,1993).

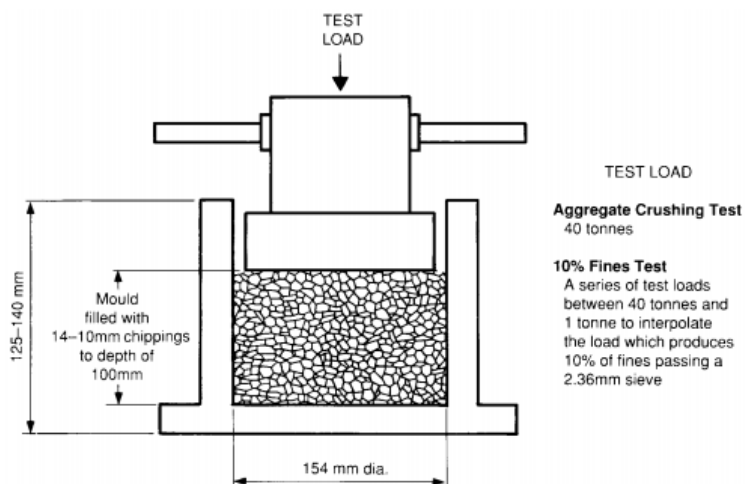


Figure 5.4: Aggregate Crushing test apparatus (Miller,1993).

### 5.3 Correlation between the bulk indexes and the mechanical resistance

The correlation between the bulk index, obtained through the standard tests referred in paragraph 5.2 , and the mechanical resistance of the material, leads to identify its ability to support the compressive stresses. In order to underline this relationship, it is reported results obtained from literature studies, that compare ACV, AIV and LA with indexes that represent the mechanical strength of the material. These relations are comparable because obtained by using materials of equivalent properties. The strength of the material is expressed as *Uniaxial compressive strength (UCS)* and *Point load index (Is)*. The first defines the compression resistance of the material, while the second, the tensile resistance expressed as a applied force at failure with the square diameter. Their correlation is linear (Figure 5.5). The factor for converting *Is* and *UCS* values vary between 17 and 39, depending on the degree of weathering of the tested rock samples. In the figure 5.6 is reported the trend between the bulk indexes and the uniaxial compressive strength. It is possible to observe that, increasing the applied load, ACV, AIV and LA, decreases: the degradation leads to a reduction of size, with a consequence increases of the compressive strength of the particles (equation 5.1). In other word, the hardness increase with the inverse of the diameter. Moreover, the curve fit is exponential o logarithmic and therefore, expressed by the following empirical relationship:

$$ACV (\%) = 78.82 - 11.73 \cdot \ln(UCS) \pm 2.69 \quad (5.5)$$

$$AIV (\%) = 78.47 - 11.87 \cdot \ln(UCS) \pm 2.97 \quad (5.6)$$

$$LA (\%) = 88.01 - 12.35 \cdot \ln(UCS) \pm 4.06 \quad (5.7)$$

Where: AIV, aggregate impact value; ACV, aggregate crushing value; LA Los Angeles abrasion index; UCS, uniaxial compressive strength in (MPa).

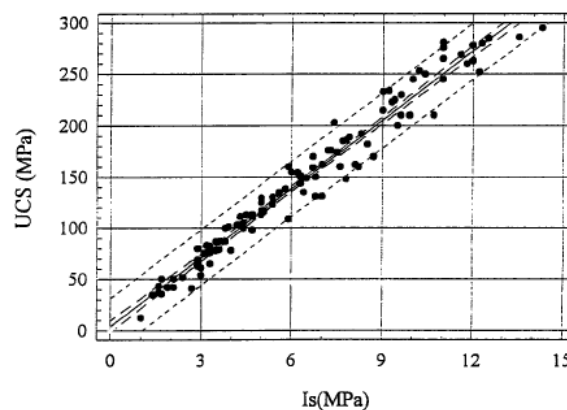
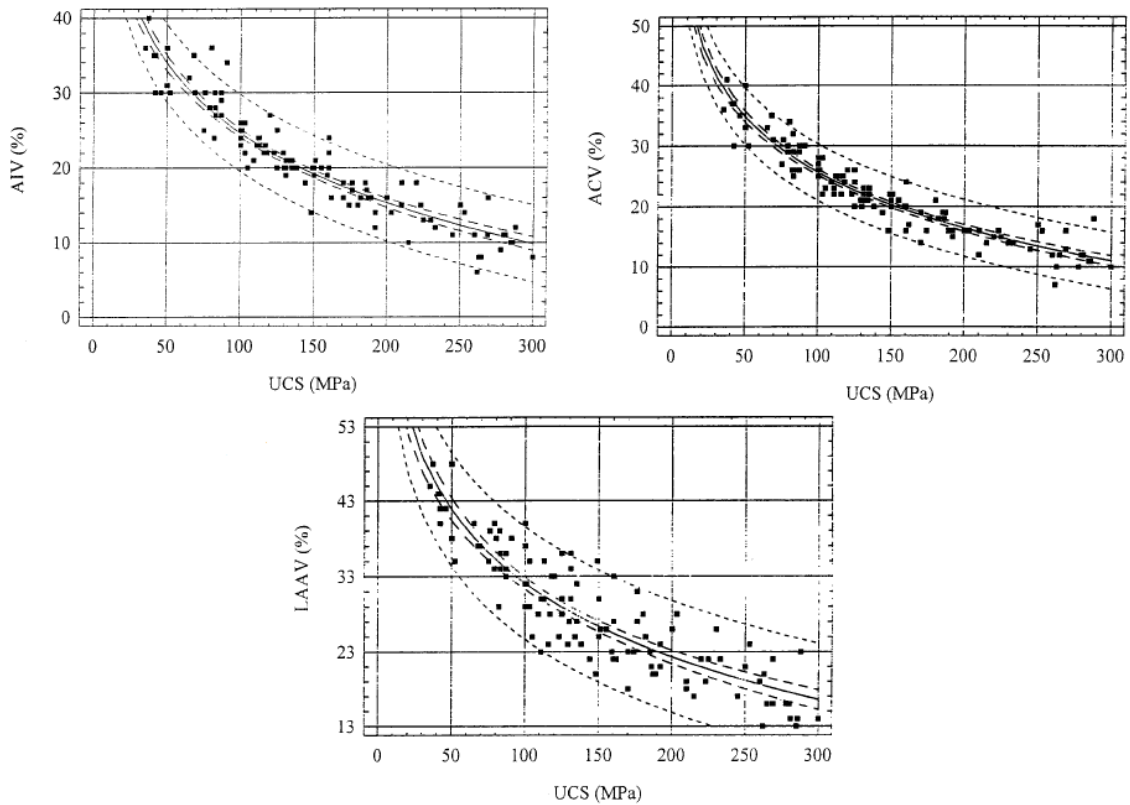


Figure 5.5 : Correlation between the tensile strength defined through the point load index (*Is*) and the compressive strength defined as Uniaxial compressive strength (UCS); (Al Harti, 2001).



**Figure 5.6 : Correlation between resistance to compression defined in terms of Point load index ( $I_s$ ) and Uniaxial compressive strength (UCS) and the mass indices LA, AIV and ACV (Al Harti, 2001).**

$$ACV (\%) = 43.08 - 12.32 \cdot \ln(I_s) \pm 2.42 \quad (5.8)$$

$$AIV (\%) = 42.20 - 12.41 \cdot \ln(I_s) \pm 2.79 \quad (5.9)$$

$$LA (\%) = 50.35 - 12.93 \cdot \ln(I_s) \pm 3.90 \quad (5.10)$$

Where: AIV, aggregate impact value; ACV, aggregate crushing value; LA Los Angeles abrasion index;  $I_s$ , tensile strength expressed as uniaxial Point load index (MPa).

These correlations have been obtained on different types of rocks and testing materials having the same properties. Figure 5.7 shows the results obtained by other authors. It is observed that they have the same order of magnitude and trend, hence they are comparable. Moreover, these relationships are extremely useful for determining the bearing capacity of a layer or a strata (i.e. road pavements). Indeed, if the particle shows a low LA and high UCS values, it supports the load without breakage: the material used has a good quality, hardness and abrasion resistance.

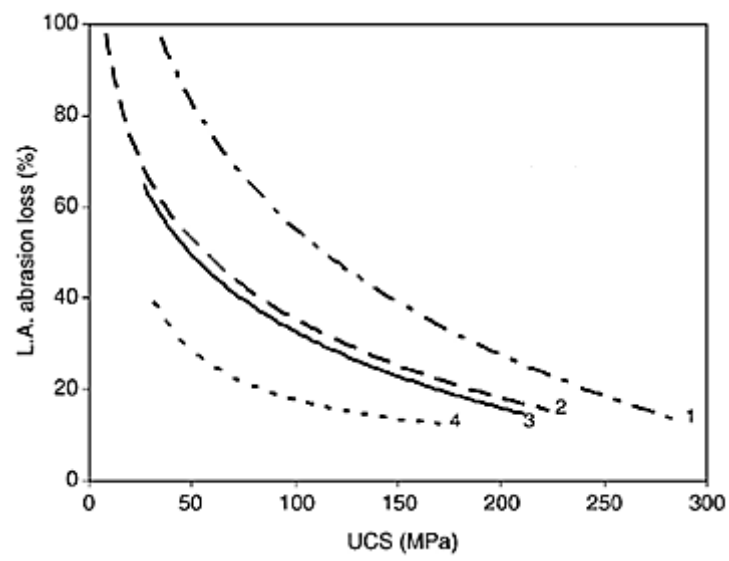


Figure 5.7 : Comparison between UCS and LA evaluated in several studies (S. Kahraman et. al., 2007).

## ***CHAPTER 6: Influence of grain breakage on the mechanical behavior of granular material***

As seen in section 4.3, the biogas drainage layer is compressed due to static loads, which can lead to rupture the material. This kind of action is transmitted to the material forming the biogas drainage layer identified as a continuous medium. Then, its resistance is associated with the mechanical behavior.

The mechanical behavior associated to granular materials is of complex determinations because functions on the representative parameters of the grains and those of the constitutive law, i.e. function that represents the maximum or ultimate stress of a granular material of the material (Ali Daouadji, 2000, Biarez and Hicher, 1994).

For determining the behavior of a medium under determined stress and strain conditions, are carried out cylindrical (improperly called triaxial), oedometric or uniaxial compression tests (Figure 6.1), those are representative of some real loading conditions. The result obtained from these tests is plotted in a plane in which the x axis it is shown the strain or volume change, while the y axis the stress. The first is represented by the void ratio ( $e$ ), calculated as the ratio between void and total volume occupied by material granular material. Stress, instead, is represented through the maximum principal stress difference ( $q$ ), compressive strength of the specimen, or isotropic component ( $p'$ ), mean effective stress applied on the sample. As seen above, if the material does not have adequate intrinsic parameters, when subjected to actions of different nature can arrive at failure. In the present case, considering the continuum medium, the effect of this action is evaluated on the particles size distribution of the material, identified through the variation in the coefficient of uniformity ( $C_u$ ).

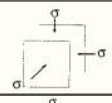
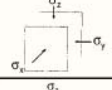
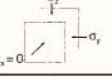
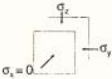
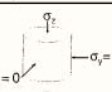
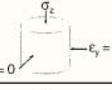
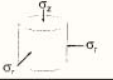
CONDIZIONI DI TENSIONE E DI DEFORMAZIONE	DENOMINAZIONE DELLA PROVA	SCHEMA DELLA PROVA
$\sigma_x = \sigma_y = \sigma_z = \sigma$	Compressione isotropa	
$\sigma_x \neq \sigma_y \neq \sigma_z$	Compressione triassiale vera	
$\epsilon_x = 0$	Deformazione piana	
$\sigma_x = 0$	Tensione piana	
$\sigma_x = \sigma_y = \sigma_r = 0$	Compressione uniassiale libera	
$\epsilon_x = \epsilon_y = \epsilon_r = 0$	Compressione edometrica	
$\sigma_x = \sigma_y = \sigma_r$	Compressione cilindrica o "triassiale"	

Figure 6.1: Types of tests carried out on samples to evaluate the mechanical behavior.

### 6.1 Triaxial test: methods and purpose

Conventional triaxial test is a common laboratory test widely used for obtaining the strength of the soil, or rather the shear strength parameters. The cylindrical soil specimen has a diameter of 38 mm and an height 75 mm. The specimen is vertically enclosed with a thin rubber membrane and placed between two rigid ends inside a pressure chamber, in which it is possible to apply a radial stress or confining pressure ( $\sigma_r$ ) and an axial load ( $\sigma_a$ ). In triaxial test the specimen it is subjected to isotropic stress ( $\sigma_a = \sigma_r$ ) or consolidation phase and then, with a constant velocity is applied an axial stress ( $\sigma_a - \sigma_r$ ) until failure. Since there is no shear stress on the sample, the confining and axial pressure are the minimum and maximum stresses respectively, and the increase of the axial stress is indicates like maximum principal stress difference ( $\sigma_a - \sigma_r = (\sigma_1 - \sigma_3)$ ).

Depending on the values assigned to  $\sigma_r$  and  $\sigma_a$ , it is possible to realize compression or extension tests, in loading or unloading. Furthermore, it is possible to control the drainage and the measure the pore pressure.

The triaxial tests differ mainly in respect of drainage conditions that occur during the consolidation and compression phases:

- Consolidated – Drained: the drainage are open in both the steps;
- Consolidated – Undrained: the drainage are close only during the second step;

- Unconsolidated – Undrained: the drainage are close in both the steps.

Consolidated-drained conditions are the most critical for the long term stability, while the consolidated- undrained for the short-term. With reference to the coarse-grained materials, because of their high permeability, any variation in the soil water pressure, compared to the initial pressure, is dissipated in a very short time. Therefore for these materials the study of the material behavior in the static field can be analyzed in drained conditions.

In addition to the standard triaxial test, other loading conditions can be realized by this equipment. For what concerns the consolidation phase it is possible to realize:

- Isotropic consolidation  $\sigma_r = \sigma_a$ ;
- Anisotropic consolidation  $\sigma_r \neq \sigma_a$ ;
- unidirectional consolidation.

The loading conditions realized during the compression phase arriving at failure are (Figure 6.2):

- The loading compression can be simulated by increasing  $\sigma_a$  and taking constant  $\sigma_r$ ;
- The unloading compression can be realized taking constant  $\sigma_a$  and decreasing  $\sigma_r$ ;
- The loading extension can be simulated increasing  $\sigma_r$  and taking constant  $\sigma_a$ ;
- The unloading extension can be simulated decreasing  $\sigma_a$  and taking constant  $\sigma_r$ .

These two conditions correspond to some real or field situation:

- The loading compression is equivalent of the stress state presents in a soil after the realization of a foundation;
- The unloading compression is equivalent of the stress state presents in a the soil that pushes a retained wall;
- The loading extension is equivalent of the stress state presents in the ground at the foot of a bulkhead, and in correspondence of an anchor plate;
- The loading extension is equivalent of the stress state presents in the ground to the bottom of an excavation.



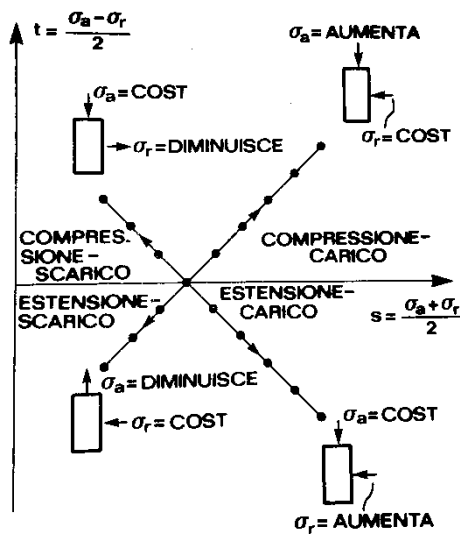


Figure 6.2: Stress path obtained by the triaxial apparatus.

## 6.2 Effect of grain breakage on the constitutive law

Grain ruptures on an isotropic or one-dimensional compression path produce an increase of compressibility, which is represented by a slope increase in the stress-strain plane (figure 6.3). Dimensionally this is the inverse of the stiffness parameter that evaluates the displacements and deformations under operating loads. The degree of crushed particles increases with the compressibility. In the case of identical grains, such as an assembly of glass balls of the same diameter, this parameters increases very abruptly since the ruptures occur simultaneously. The phenomenon is more progressive in sand on account of the grain's size and shape differences, which produces a less homogeneous division between the contact forces (Biarez and Hicher, 1994). In the case of well-graded material, instead, the contact forces between the particles are distributed heterogeneously and therefore, they show a lower compressibility. Indeed, it is observed that when the grains arrive at failure the stress path changes due to a reduction in void ratio: the amount of particles broken is reduced and then the tension transmitted by the grains decreases in intensity (Yamamuro and Lade ,1996).

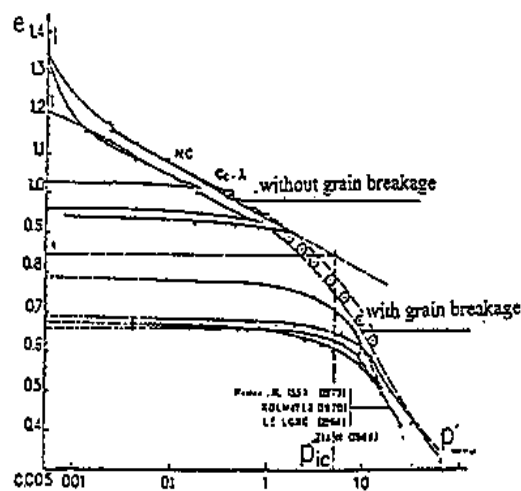


Figure 6.3: Effect of grains breakage due to uniaxial compression for a little well graduated sand.

Figure 6.4 shows the typical trend due to a one-dimensional cyclic compression plot for petroleum coke by Biarez and Hicher (1994). The plot also shows values of uniformity coefficient increasing to a constant value at lower void ratios, in which stage the curve starts to be concave (Einav, 2006). Indeed, at that point, the material is completely crushed: from that point the strain is minimal.

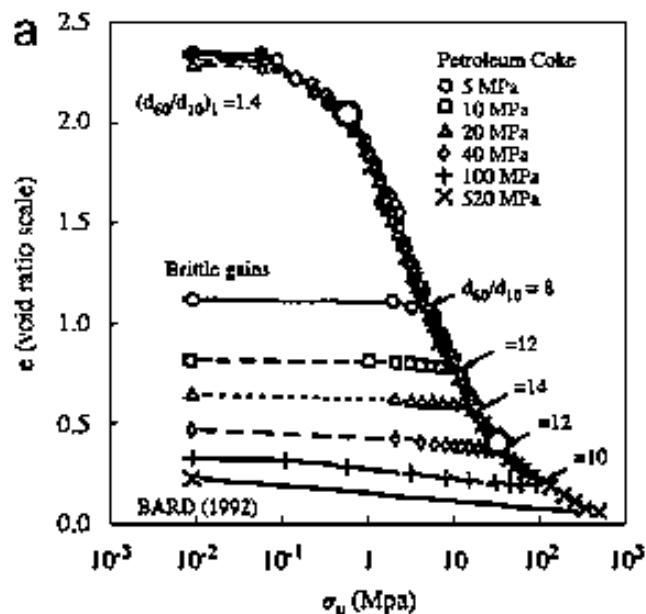


Figure 6.4: Effect of the breaking of the grains because of uniaxial compression for "petroleum coke" (Itai Einav, 2006).

On deviatoric path, first of all, it is observed a significantly bigger contradiction. This may be explained by the displacement of the perfect plasticity relation in the stress strain plane (Figure 6.6): at constant stress it develops continuing and increasing deformation. The maximum and minimum void ratio decreases when the uniform coefficient ( $C_u$ ) increases (figure 6.5). One can see that an increase of  $C_u$  due to grain ruptures, will produce a slip of the critical state line towards smaller void ratios.

In order to reach the critical state during a triaxial test, a bigger volume change will be needed in case of significant grain breakage. Therefore a significant change takes place in the global behavior of granular media due to grain breakage, which needs to be taken into account in a constitutive model.

The constitutive law of granular material subject to crushing, in the first instance is analogous to that of a dense sand, then in a second time, when it arrives at failure appears similar to that of a loose sand in the absence of crushing (Ali Daouadji,2000) (Figure 6.7).

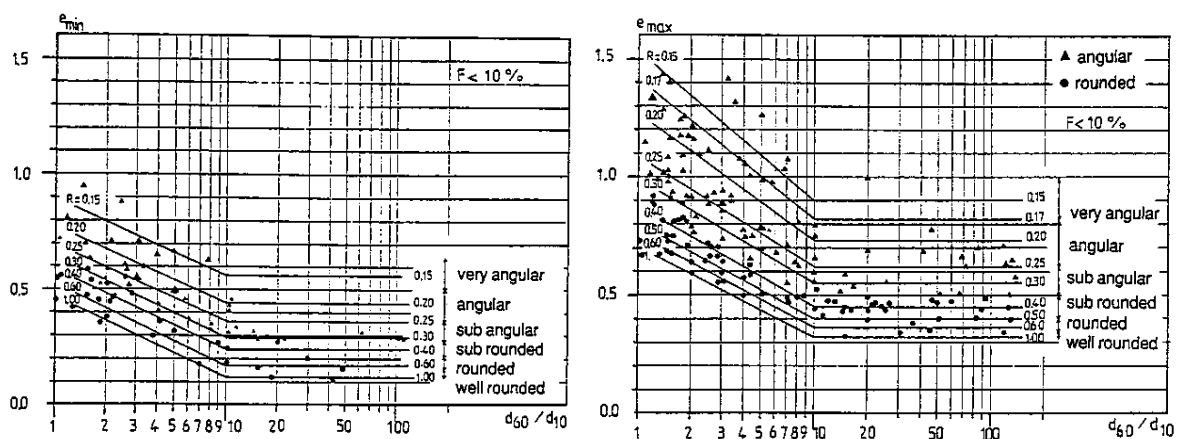


Figure 6.5: Assessment of the void ratio with the uniformity coefficient ( $d_{60}/d_{10}$ ) and its shape; It is reported the values for which the percentage of the fine fraction is less than 10% ( $F < 10\%$ ) (Biarez and Hicher, 1997).

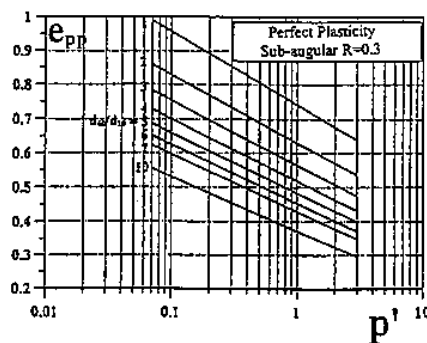


Figure 6.6: Perfect plasticity relation as a function of the grain size distribution (Biarez and Hicher, 1997).

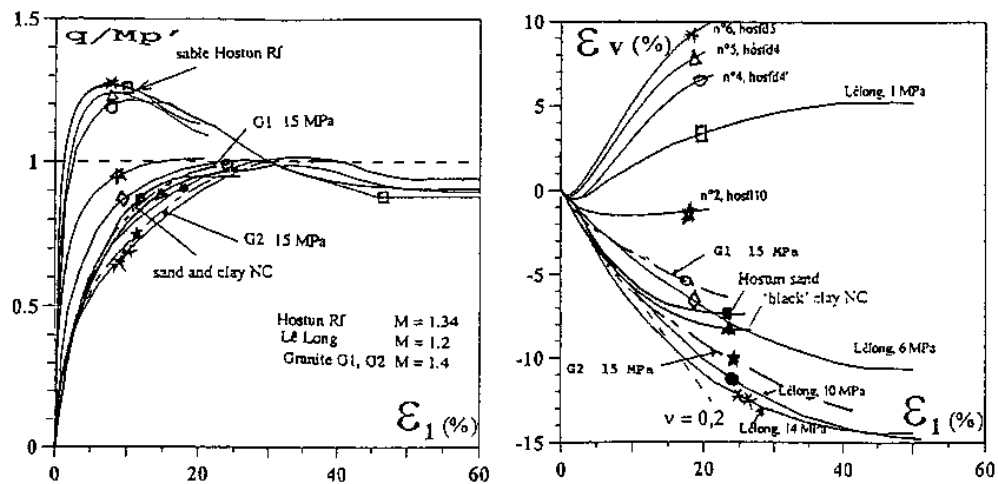


Figure 6.7: stress- strain path of a Huston sand subjected to grain breakage (Biarez and Hicher, 1997).

### 6.3 Parameters affecting the grain rupture

The grain rupture is influenced by two main categories (Ali Daouadji et al, 2001):

- Natural parameters: factors related to characterizing the discontinuous medium. They are invariant parameters, like the strength of a grain, dimension, grain size and shape;
- Mechanical parameters: factors characterizing the mechanical state of a medium supposed to be continuous: stress and strain. In this case the strength of the material is evaluated considering the loading conditions.

The mechanical parameters illustrate the effect of the level and path of stress, the amplitude of strains during mechanical loading. The level of stress from which they appear in a significant manner depends on the preceding parameters. However, the stress path also plays an important role. Experimental studies on this subject allow us to conclude that the stress deviator plays a major role and that the triaxial tests, for example, generate more ruptures than the isotropic or one-dimensional compression tests of the same average stress (figure 6.8) (Hicher et al., 1995). This may very well be explained by the relative displacements of particles, induced by lateral movements, which encourage grain rupture (Ali Daouadji et al, 2001).

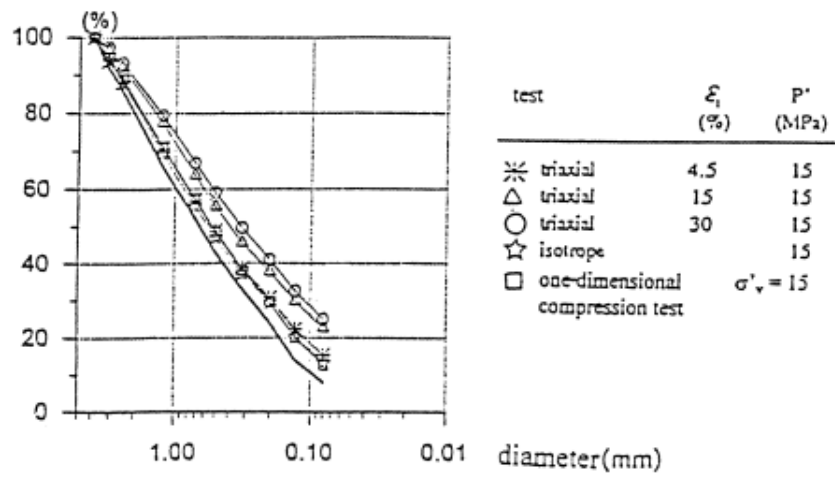


Figure 6.8: Influence on stress strain path on the grain size (Hicher et al., 1995)

## ***CHAPTER 7: Effect of particles breakage on the grain size distribution curve***

The fracture and friction grain breakage, can alter the particle size distribution of the material forming the granular medium. Then, in analogy with what described in section 4.3, may also modify the characteristics of that forming the biogas drainage layer. Therefore, the original engineering requirements with which a structure was designed will change during its engineering life. This phenomena could jeopardy the stability of such structure and make it unsafe during its design life . Consequently, understanding the crushing in granular materials is of highly needs (Al Hattamleh et. al., 2013) .

The most important engineering properties of granular materials such as stress-strain and strength behavior, volume change and pore-pressure developments, and variation in permeability depend on the integrity of the particles or the amount of particle crushing that occurs due to changes in stress (Lade and Yamamuro, 1996). To understand the effects and to quantify the amount of particle crushing were performed tests able to simulate some field conditions.

The amount of particle crushing is affected by the stress level (proximity to failure), the stress magnitude, and the stress path. For example it is reported the results obtained by Lade and Yamamuro (1996) on dense sand by using high-pressure triaxial tests (confining pressures from 0.5 to nearly 70 MPa). After testing, the specimens were recovered and a sieve analysis was performed on the dried soil to evaluate the grain-size distribution. The results of some of these

sieve analyses are shown in figure 7.1 (Lade e Yamamuro, 1996). The most important results can be summarized as follow:

- The regular pattern of the curves indicates consistent behavior: since the curves do not cross one another, it indicates a relatively low level of scatter in the data;
- The gradations shift toward a more well-graded condition after shearing: crushing induced by lateral forces of friction reduces the size of the material analyzed;
- The particle crushing increases with an increasing initial confining pressure: compression leads to the disintegration of the material analyzed;
- For similar initial effective confining pressures the drained tests appear to produce more particle crushing than the undrained tests: when the drainage are closed the sample do not have any deformation, and therefore, the energy to arrive at failure is not considered;
- The gradation curves indicates that extension tests do not exhibit as much particle crushing as compression tests;
- Compression in drained conditions is the most unfavorable loading condition.

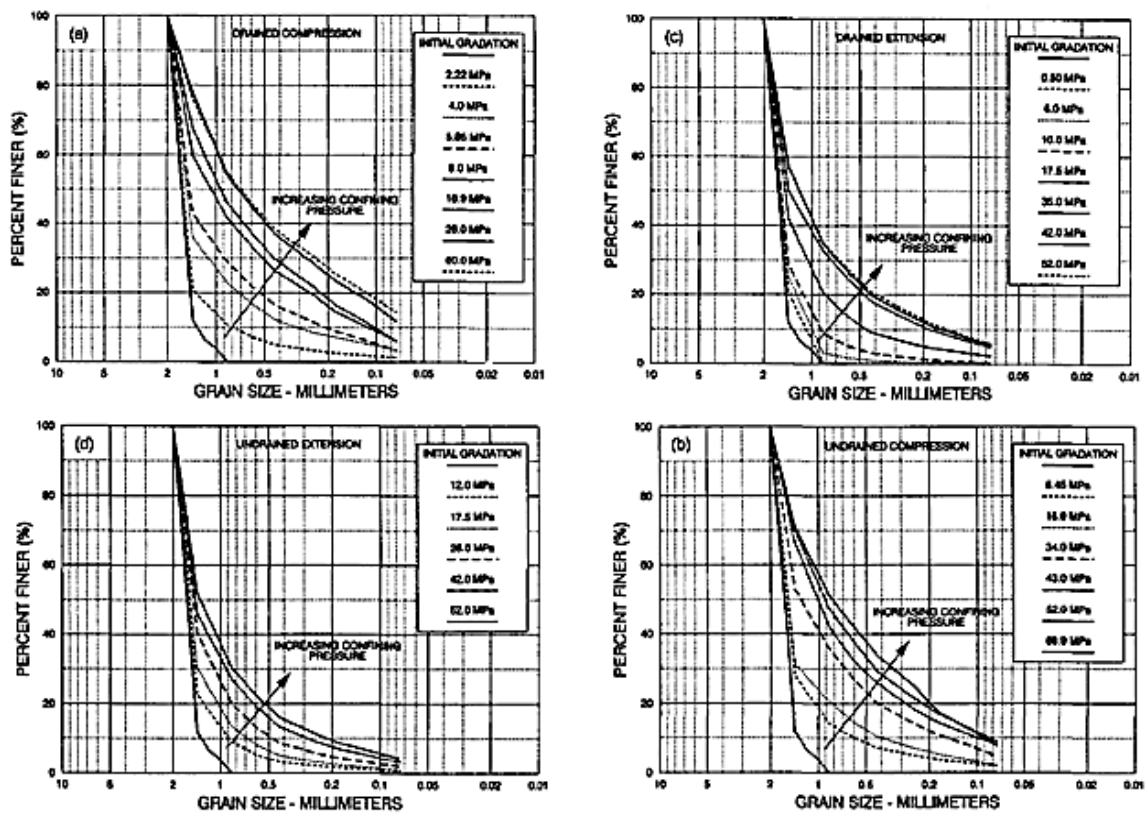
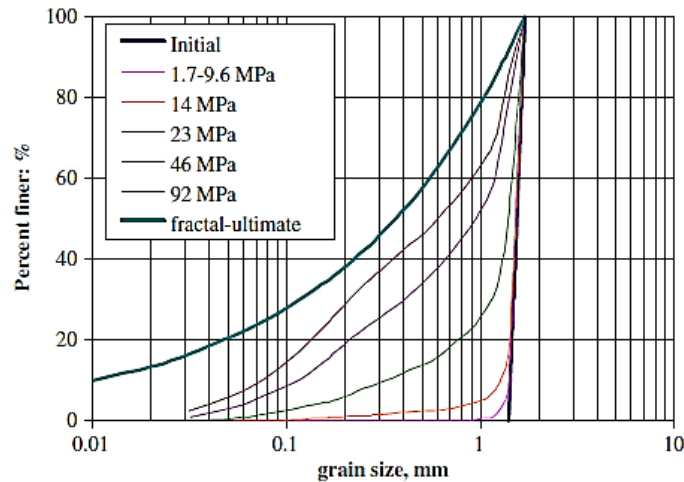


Figure 7.1: Effect of compression tests on the particle by applying a confining pressure of 5 to 70 MPa: a) drained compression, b) undrained compression, c) drained extension, d) undrained extension (Lade and Yamamuro, 1996).

Similar results can be obtained by Nakata (2001). As show in figure 7.2, the grain size distribution remains more or less the same till the vertical stress exceeds a threshold of more than 9.6MPa. From this point onwards the curves start to deviate from the initial distribution consistently towards an ultimate state.



**Figure 7.2: Evolution of grain size distribution with applied vertical stress for uniformly graded sand under one-dimensional compression (after Nakata et al., 2001).**

### 7.1 Particles breakage factors

The amount of particle breakage during loading of a soil sample is defined by the particle size distribution curves measured before and after loading (Hardin, 1984). Therefore, for quantifying the amount of particles breakage many particle breakage factors have been proposed. The principal significant use of these coefficients may be related to permeability estimates when there are changes in gradation due to particle breakage. Particles crushing can decrease the hydraulic conductivity by up to two orders of magnitude (T. DeJong, 2009).

Particles breakage factors are empirical in nature, and are based on changes in particle sizes as the key measurement. The most widely used breakage indices are:

- Marsal (1967),  $B(\%)$ ;
- Lee and Farhoomand (1967),  $B$ ;
- Hardin (1985),  $Br$ ;
- Lade e Yamamuro (1996),  $B_{10}$ .

Some are based on a single particle size, while others are based on aggregate changes in the overall grain-size distribution (i.e. Hardin). Their graphical representation is reported in figure 7.3.



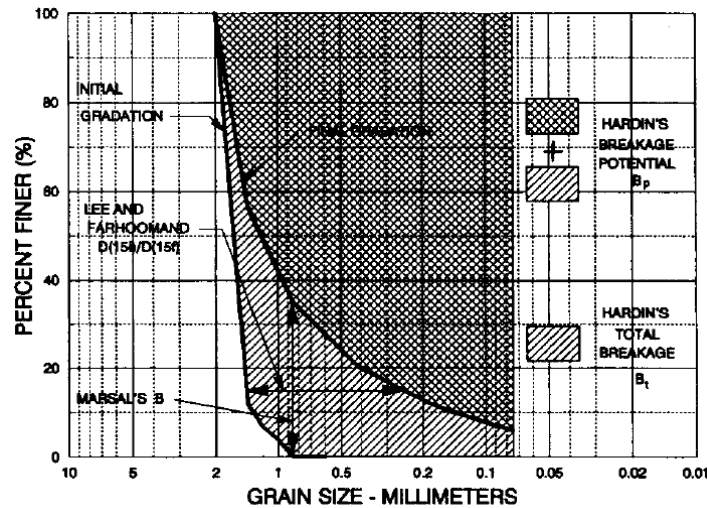


Figure 7.3: Graphical explanation of the breakage factors: Marsal (1967), Lee and Farhoomand (1967), and Hardin (1985); Lade e Yamamuro (1996).

- **Marsal breakage factor (1967) ,  $B(\%)$**

The Marsal (1967) breakage factor is calculated from the changes in the amounts of material retained on each sieve size.

Marsal's method involves the change in individual particle sizes between the initial and final grain-size distributions. The difference in the percentage retained is computed for each sieve size. This difference will be either positive or negative. Marsal's breakage factor,  $B$ , is the sum of the differences having the same sign.

$$B (\%) = \frac{1}{M_i} \sum_{d_i}^{df} [(M_i - M_f)] \quad (7.1)$$

Where:  $B$  is the Marsal's index,  $M_i$  e  $M_f$  are the percentage retained on different sieves after and before grain breakage.

The lower limit of Marsal's index is zero percent, and has a theoretical upper limit of 100%. However, when particle crushing is extensive, the gradation curve shifts substantially from the larger to the smaller sieve sizes and there tends to be very little material left for comparison on the original, larger sieves.

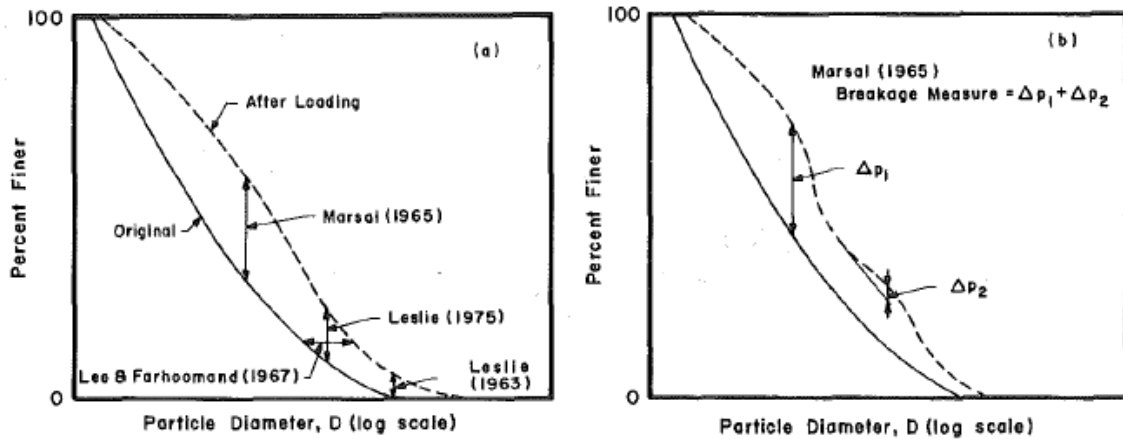


Figure 7.4. Graphical explanation of the breakage factors: Marsal (1967), Lee and Farhoomand (1967), and Hardin (1985); Hardin (1985).

Marsal (1967) developed his measure of particle breakage in connection with the design and construction of earth and rockfill dams. While performing large-scale triaxial compression tests, he noticed significant amounts of particle breakage. He subsequently developed a breakage index,  $B$ , to quantify this breakage.

- **Lee and Farhoomand breakage factor (1967),  $B$**

Lee and Farhoomand (1967) developed their measure of particle crushing while investigating earth dam filter materials. Their concern was whether extensive particle crushing could effectively plug dam filters. They proposed a breakage factor expressing the change in a single particle diameter, namely that corresponding to 15% finer on the grain-size distribution curves before and after testing. These grain sizes were chosen because gravel filter drainage requirements were commonly based on this particle size.

$$B = \frac{d_{15\text{ initial}}}{d_{15\text{ final}}} \quad (7.2)$$

Where:  $B$  is the Lee and Farhoomand index,  $d_{15\text{ initial}}$  and  $d_{15\text{ final}}$  the grain size that only 15% of the grains are finer than. The lower limit of this ratio is unity and there is no upper limit.

Lee and Farhoomand performed a series of isotropic and proportional loading tests on sands to study particle breakage. The particle breakage factor here described (1967) originally developed to evaluate plugging in gravel filters in earth dams.

- **Hardin breakage factor (1985),  $Br$**

Hardin's (1985) relative breakage factor is based on the area between the original and final grain-size curves, normalized by the area between the original grain-size curve and the No. 200 sieve size (0.0074mm). Hardin's measure of particle breakage is therefore stable and robust, and not unduly sensitive to small variations in individual measurements. He based his measure of particle breakage on changes in the entire particle-size distribution defining two different quantities: the breakage potential ( $B_p$ ) and the total breakage ( $B_t$ ). The first one is defined as the area between the original grain-size distribution curve of the soil and the No. 200 sieve size, as shown in figure 7.5. The breakage potential represents the total possible change in gradation obtained if every grain is broken down from its original size to particles smaller than a certain diameter. Hardin used the No. 200 U.S. sieve size as a limit because there is limited amount of crushing below this size. It is also more difficult to obtain particle-size distributions below this particle size using a standard sieve analysis. The total breakage,  $B_t$ , is defined as the area between the original grain size distribution curve and the final grain-size distribution curve, as shown in figure 7.5. Hardin then defined the relative breakage as the ratio of total breakage divided by the potential breakage:

$$Br = \frac{B_t}{B_p} \quad (7.3)$$

Where:  $Br$  is the relative breakage factor,  $B_t$  and  $B_p$  the total and potential breakage factor respectively. The relative breakage has a lower limit of zero and a theoretical upper limit of unity.

Hardin proposed his index in order to estimate the total breakage expected for a given soil subjected to a specified loading. He performed triaxial and one dimensional compression test on single mineral soils and rockfill like materials.

- **Lade breakage factor (1996),  $B_{10}$**

The Lade index was determined in order to correlate the particle breakage factors with the total energy input and, it can be used as the basis for the evaluation of permeability of soils in earth and rockfill dams or other earth structures in which the effect of particle breakage on permeability is important for seepage analyses.

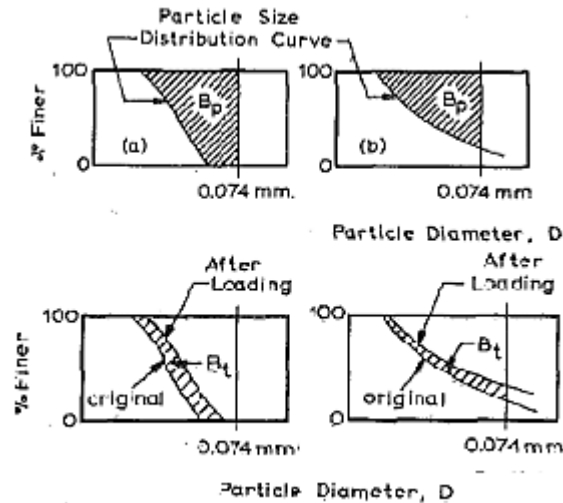


Figure 7.5: Graphical meaning of the relative breakage factor and potential breakage factor (Hardin, 1985).

In order to correlate permeability to a breakage factor, Lade has proposed an index that uses the percent of a soil passing the 10% in weight:

$$B_{10} = 1 - \frac{d_{10} \text{ final}}{d_{10} \text{ initial}} \quad (7.4)$$

Where:  $B_{10}$  is particle breakage factor;  $d_{10f}$  effective grain size of the final gradation; and  $d_{10i}$  effective grain size of the initial gradation. The formulation of this particle breakage factor is based on the lower limit being zero when there is no particle breakage, and the upper limit being unity at infinite particle breakage.

Lade e Yamamuro(1996) performed a series of extension and compression triaxial tests to study particle breakage.

The choice of  $d_{10}$  was made in order to obtain a connection with the empirical formula for determining the hydraulic conductivity given by Hazen (1982). Indeed, known the Lade index ( $B_{10}$ ), it is possible to evaluate how the permeability changes due to crushing.

## 7.2 Correlation between particles breakage factor and the and other engineering parameters

The Marsal, Lade, Lee and Farhoomand and Hardin breakage indices were determined by multiple tests. The correlation between these parameters and the total energy or plastic work, shows that the amount of crushed material increasing with the applied stress. Studies conducted by Lade and Yamamuro (1996), HU Wei et al (2011) and Bopp (2005) evaluated that their relationship is hyperbolic, as shown in figure 7.6 and 7.7. These parameters have been chosen

because independent to the stress path that lead at failure the specimen. The plastic work and energy represent the area under the stress-strain curve, used to describe the constitutive material. The total energy is the sum of the isotropic compression and shearing energy, while the plastic work is the energy that leads to non-recoverable deformation of the material analyzed (Lade and Yamamuro, 1996).

Breakage can significantly alter the engineering properties of the materials. Chuhan (2000), Valdes and Caban (2006), observed that the particles crushing can reduce the hydraulic conductivity until two orders of magnitude. In the same way, studies conducted by Jason T. DeJong (2009) determined that the hydraulic conductivity decreases by several orders of magnitude whit the increasing of the Hardin and Lee and Farhoomand (B) breakage indexes (Br), (Figure 7.8).

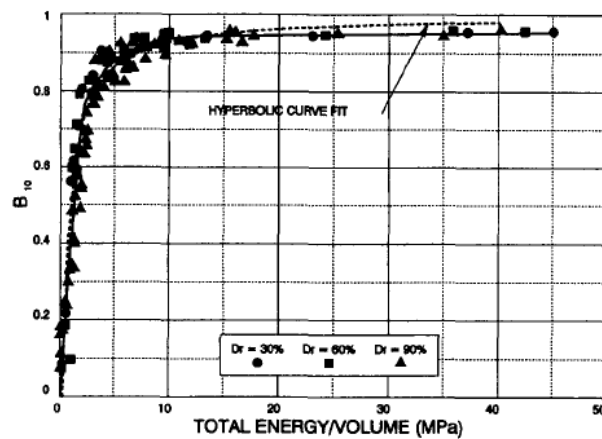


Figure 7.6: Correlation between the Lade coefficient (B10) and the total energy (sum of the of isotropic compression and shearing energy that leads at failure the specimen) per unit volume of specimen during a triaxial test on standard sand (sand Cambria ) having different values of relative density (Dr); (Lade and Yomamuro, 1996).

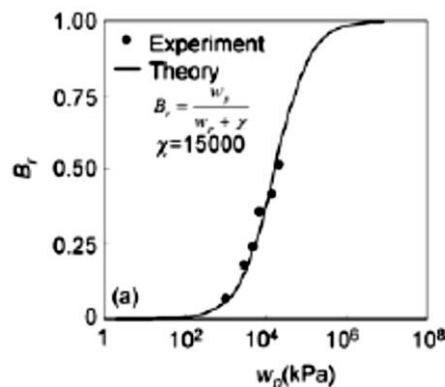


Figure 7.7: Correlation between the coefficient of Hardin (1985) and the plastic work for a standard sand (Cambria sand); HU Wei et al (2011);

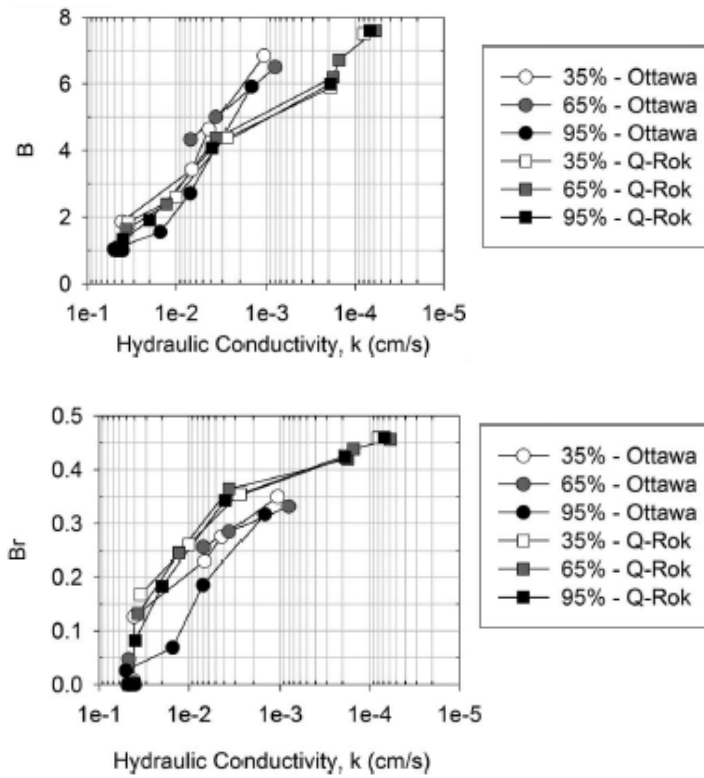


Figure 7.8. Correlation between the hydraulic conductivity and Hardin and Lee and Farhoomand breakage indexes; (Jason T. DeJong , 2009).

## ***CHAPTER 8: Tests used to determine the characteristics of the material forming the biogas drainage layer***

The material used for the biogas drainage layer must be characterized by the following geotechnical requirements:

- Hydraulic conductivity higher than or equal to  $10^{-4}$  m/s and hence, of a material consists of coarse sand or larger grain size (paragraph 2.6);
- Particle size in order to be internally stable and compatible with the neighboring layers (section 4.3).

To define the properties above, it is fundamental to determine the grain size and the variety of the particles that constitute the material. A possible increase of the fine fraction could seriously compromise the proper functioning of the biogas drainage layer and then, jeopardize the final landfill cover stability. Indeed, according to the Thiel relationships, it is possible to observe that if the hydraulic conductivity decreases, the pore gas pressure increases with a consequent reduction of the safety factor obtained from the cover slope stability analysis (chapter 2). Furthermore, due to seepage or simply vibration, this fine particles may migrate into the underlying body waste making internally unstable the material forming the biogas drainage layer (chapter 3).

### 8.1 Criteria analyzed for evaluating the type of tests

For the realization of the biogas drainage layer the material is subjected to different dynamic actions, like:

- An impact for falling when it is transported;
- Several actions of compression and sliding due to friction when it is stretched by work means.

Whereas, after the realization the biogas drainage layer must bear static loads, as:

- High pressure due to the sheep foot roller used for the compaction of the hydraulic barrier;
- The weight of the upper layers.

Moreover, as noted in paragraph 4.3, the drainage is not affected by thermal loads as freezing and thawing, therefore it is not necessary to determine the durability of the material, defined in Chapter 5.

For determining how these actions can influence the requirements of the material formed the biogas drainage layer, it is necessary to perform tests that are able to represent the field conditions and, verify if the properties for which it is chosen remains almost unchanged. More specifically, in order to identify if it modifies its external surface due to rupture, they must be capable to test the mechanical resistance of the material for similar or equivalent efforts. Moreover, the results obtained, must be determined by using the particle size distribution. Therefore, it is necessary to perform grain size analysis and permeability test before and after the application of external loading conditions. Consequently, the tests must be carried out directly on the material. Hence, the attention lies on the laboratory tests, able to represent the field situations and capable to assess the mechanical resistance and the behavior of the material for the actions describe in the section 4.3. The choice must be done according to criterion still present in literature in order to determine with accuracy and sensibility how the material behaves due to different actions.

Generally the laboratory instrumentation is calibrated for samples having certain dimensions and characteristics. Therefore and in accordance with the “scale factor”: the particle size of the analyzed material must be suitable for the equipment used.



### 8.1.1 Permeability test

Laboratory permeability tests are generally performed using an instrument called permeameter and capable of measuring the permeability coefficient of a given soil. The types of probes generally include:

- Constant head tests, used for granular material having permeability of the order of  $10^{-5}$  m/s;
- Falling head test, used to evaluate the permeability for granular material having permeability between  $10^{-5}$  and  $10^{-8}$  m/s.

In constant-head tests, the hydraulic head ( $h$ ) is maintained constant through a sample of a length ( $L$ ) and area ( $A$ ). The total volume of fluid ( $V$ ) is measured during a time period ( $t$ ). The hydraulic conductivity ( $kf$ ) is then determined by using the following relationship:

$$kf = \frac{Q}{A} \cdot i \quad (8.1)$$

Where:  $Q$  is the flow rate,  $A$  is the section and  $i$  is the hydraulic gradient. This test method is generally suitable for pervious or coarse-grained soils.

In falling-head tests, the hydraulic head varies over time for the entire duration of the test. It is applied for fine-grained soils having a low permeability, since the characteristics of the apparatus allow to easily perform the measurements of the hydraulic load and the time for a wide range of values of the coefficient of permeability. The value of  $kf$  is given by the relation:

$$kf = \frac{A \cdot L}{a \cdot t} \cdot \ln \frac{h1}{h2} \quad (8.2)$$

Where:  $a$ , area of pipet or burets;  $L$ , length of the sample;  $A$ , section of the sample;  $t$ , time required to lower the heads to a starting position  $h1$  and final position  $h2$ .

### 8.1.2 Mechanical resistance and grain size

During the realization of the biogas drainage layer, the material must resist to impacts, sliding, crushing and hence, it should possess a certain mechanical resistance. As defined in the chapter 5, this property is strictly associated to the parent material and to mineralogical composition of the grains. It is expressed in terms of hardness, toughness or ability of the material to support the imposed loads over a strata without breakage, and evaluated as resistance to wear, impact

and friction. Therefore, this property can be determined performing standard tests, like Los Angeles Abrasion or similar (sections 5.2).

After the realization, the particles are disposed in a strata and are subjected to efforts of different entities. The passage of roller for the realization of the hydraulic barrier, transmits compressive and attrition loads, that tend to desegregate and fracture the material. For resisting to this action, it is necessary to evaluate in which way the grains transmit the imposed loads over the surface of the strata and how it is transmitted on the underlying material. Given the disposition of the aggregates, the loads will be carried out by the grains of the material forming the biogas drainage layer. The capacity of the layer to support this kind loads is one of the most important properties of the strata. The erosion and the crushing of the grains, can change the particle size distribution, with consequence effects on the minimum design permeability. Also, this can lead to a variation of the mechanical resistance of the material, which can be re-estimated by testing the quality of grains (i.e. abrasion test) (section 4.3 and 5.2).

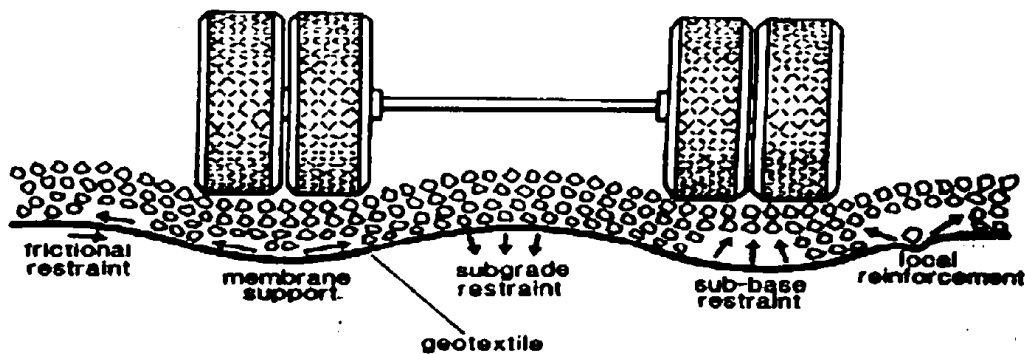


Figure 8.1: Effect of grains sliding when the material is subjected by work means.

As reported in the section 5.2, to perform aggregate quality tests, the material must possess specific grain size requirements. This can be explained considering that, generally, the resistance of the material increases with decreasing its size (Mitchell, 1993; Lee and Farhoomand, 1967). Therefore, grain breakage due to crushing, abrasion and friction can be more likely in coarse materials, rather than in fine materials (section 5.1). For these reasons, aggregate impact and crushing tests are done with grains of dimension between 9.52 mm and 12.70 mm (sections 5.2.2 and 5.2.3). For what concern the Los Angeles Abrasion Test, the analysis of the abrasion, friction and impact resistance, is performed on aggregates retained on a sieve of 19 mm or passing a sieve of 38 mm. For the last category, the smallest grain size analyzed is represented by material ranging between 2.3 mm and 4.7 mm (ISRM, 1998). Instead, in accordance with the UNI 1097-2, the aggregate used for the standard Los Angeles abrasion

test must pass a sieve of 14 mm and have to be retained on another of 10 mm (section 5.2.1). In all cases, the result obtained is closely related with the maximum compressive strength of the material tested (paragraph 5.3).

According to the Thiel procedure, described in the chapter 2, and the filter design criteria, described in the chapter 3, the material used have to possess an equivalent diameter ( $d_{10}$ ) equal or higher than 0.1 mm. Therefore, according to the dimensions involved, the abrasion test appears the most suitable to simulate what happens during the installation and realization of the biogas drainage layer. Through it, is possible to determine the quality of the material under different loading conditions or actions, such as abrasion, impact and friction. The results obtained is expressed in terms of hardness, toughness, and hence, in the ability of the grains to preserve its external surface. Moreover, through the coefficient Los Angeles (LA), it is possible to estimate indirectly the compression strength of the material, which may be comparable with the maximum vertical stress transmitted by the quasi-static load induced by the compaction means (sections 5.3 and 4.2). For these reasons, this test can provide important information about the quality of the material used under dynamic actions.

### **8.1.3 Static loads and deformation at failure**

As reported in chapter 4, the effort transmitted by compaction is considered quasi static. The compaction takes place slowly and developing great pressure; hence, the transmission rate of the load results greater than that required for the passage of the roller. Consequently, the entity of the vertical stresses developed in the granular medium forming the biogas drainage layer, can be determined through the elastic theory that assess the soil-foundation interaction. The compressive load is diffused with depth by the contacts between the grains and then, must be higher in the upper parts of the biogas drainage layer.

Generally when a load is applied on the ground, it is possible to observe a vertical displacements measured respect to a reference plane, or settlement. In the present case, the strata in question, will not change its thickness because rests on a very compressible layer: the waste body is more deformable than the granular material formed the biogas drainage layer, which for its function and position must have a certain stiffness. Therefore, the pressure is transmitted at first to the grains of the granular material, and then to wastes, which due to their deformability will undergo a settlement (Figure 8.2). According to this hypothesis, hence, the evaluation of the stiffness appears secondary respect to the hardness. The possible fragility of the material can be determined indirectly by fractring analysis of the material in question.

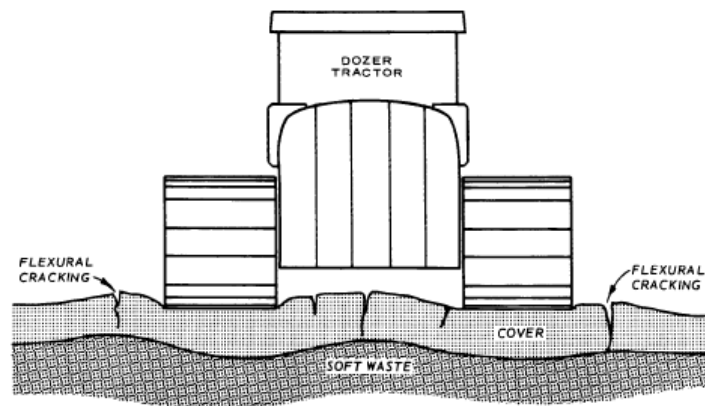
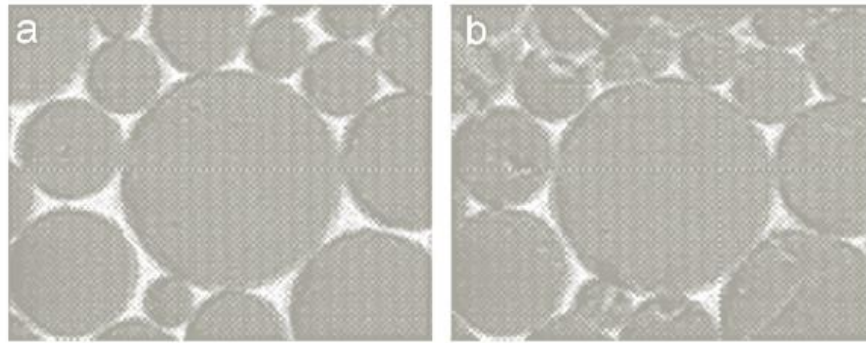


Figure 8.2: Effect of the work means passage on a soft layer, such as waste.

In geotechnical engineering to evaluate the mechanical behavior at failure and the shear strength parameters of a material when compressed by a structure, foundation or an embankment, are used triaxial tests because capable of simulating axial loads with or without the intervention of lateral friction, exactly as occurs in situ. Through these tests, the drainage can be controlled and therefore, it is possible to define the strength parameters of the material analyzed at short and long term (chapter 6.1).

Pointing out that the speed of the load transmission results greater than that of the passage of the roller on the medium and, recovering the analogy carried out from the calculation of the vertical stresses, it is possible to affirm that even in this case could be used the triaxial test. More specifically, the effect of the compacting means on the biogas drainage layer, may be comparable to that obtained through the realization of a foundation in a short time (section 6.1). As said before, to evaluate this type of action it is used an un-drained and unconsolidated triaxial test. In the case of material having high permeability, the consolidation or isotropic compression, and the failure or axial compression, can be performed with open drainage. Indeed, by this modality, the sample breaks more than the un-drained conditions and in addition simulates what happens in field because as reported in the chapter 2 the biogas drainage layer is dry (chapter 7). Then, it is possible to assess whether the material due to static loads may fracture, splitting the grains into smaller pieces or of similar size (Figure 8.3). Consequently, it should be done on a sample that has already undergone the effects of the installation or dynamic actions. In this way, it is possible to have a wide representation of how the material can change its grain size distributions.

The grain size of the sample may be a limit on the application of this type of test. As discussed in chapter 6.1, the standard triaxial cell has a height of 75 mm and a diameter of 38 mm. Consequently, the material analyzed can have a dimension similar or lower than those of the coarse sand.



**Figure 8.3 : Effect of grain breakage when confined and subjected to compressive load.**

## **8.2 Types and characteristics of the material chosen**

As shown in the section 1.2, the biogas drainage layer is placed below the hydraulic barrier. Considering this, it is not exclude the possibility of using a waste material properly chosen and complies with the requirements for the acceptance of non-hazardous waste landfills. In this context, among the materials that produce more interest, there is the building demolitions debris, exhausted foundry sand, waste incineration, ecc. The disadvantages in the use of these materials are mainly related to their availability, which can be inconsistent, and their non-uniformity engineering properties, because of coming from different sites and production plants. Therefore, before being employed is necessary to estimate their geotechnical properties. In the present case and in the following chapters, it will be analyzed a selected waste from incineration screening.

### **8.2.1 Characteristics of the sample classified as selected waste**

To evaluate the grain size of the sample classified as selected waste, is carried out sieve analysis. It is used sieves of square mesh, of increasing size and classified according to the ASTM system. The grain size distribution is determined using the mass retained in each sieve. The material in question is not subjected to the preliminary analysis and is not washed. It has a net weight of 19.4 kg, size slightly greater than 25.4 mm and not less than 0.0074 mm (Table 8.1 and Figure 8.5). Moreover, due to its non-homogeneity is characterized by particles of different origin, properties and shapes (figure 8.4).



Figure 8.4: Natural sample.

Table 8.1: Grain size analysis of the natural sample

Sieve size [mm]	Percentage of weight passing the sieve (%)
0.074	1.67
0.105	1.70
0.177	1.75
0.25	1.79
0.42	1.84
0.84	1.89
2	1.96
4.76	2.17
10	7.16
12.5	20.51
14	37.88
19.1	80.43
25.4	95.22

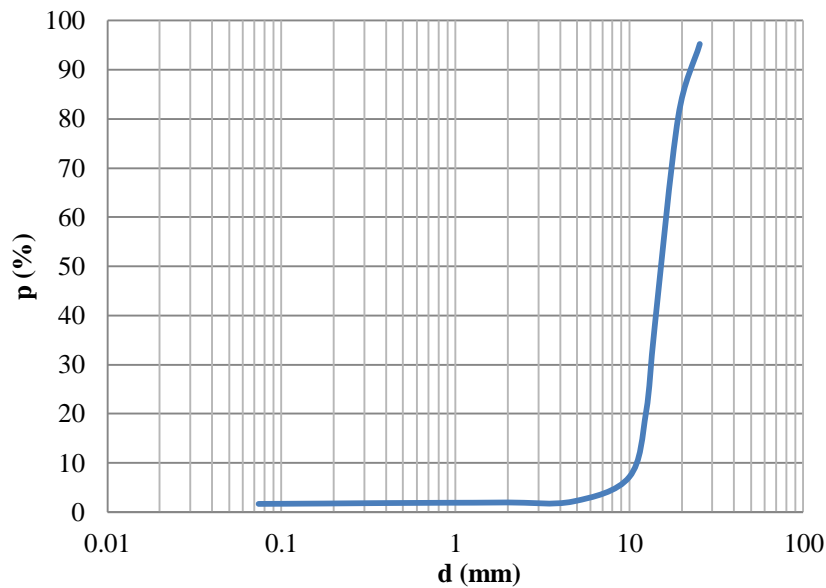


Figure 8.5: Grain size distribution (GSD) of the natural sample.

From the grain size distribution curve it is possible to determine the uniform ( $C_u$ ) and the curvature ( $C_c$ ) coefficient, defined in the section 3.1.1, which are respectively equal to 1.6 and 1. Therefore the material is uniform and, as it shown in figure 8.5, gravelly. Consequently, its permeability can be higher than minimum required for the biogas drainage layer. However, given the size of analyzed sample, it is difficult to quantify this properties using a laboratory test. Indeed, as reported in previous section (8.1.1), constant or falling head equipment is calibrated for material having dimension lower than coarse sand (section 8.1.2). Therefore, due to the “scale factor” the permeability of sample in question is evaluated by empirical relationship, like the Hazen’s equations (1892), that does not include the parameters characteristic of the material (section 2.5; equations 2.12). Through linear interpolation of the particle size distribution curve it is possible to determine the effective diameter, which results  $d_{10} = 10.5$  mm. Using this value and applying the over mentioned relationship, it is obtained an hydraulic conductivity equal to 110.9 cm/s (1.1 m/s). As expected, higher than  $10^{-4}$  m/s and therefore fully verified. Based on this value, it can be said that the material here analyzed is suitable for the realization of the biogas drainage layer.

As mentioned in the paragraph 3.4, aimed to the determination of the particle size distribution of the foundation and biogas drainage layer, it is observed that the analyzed sample can also be used for the installation of the foundation strata because it is compatible with the underlying waste (figure 8.8). Indeed, applying the Terzaghi’s clogging criterion (section 3.2, equation 3.3), the ratio between  $d_{15}/d_{85}$  is 0.08, lower than 4 and hence verified.

For completeness, it is determined the internal stability according to the methods proposed by Kezdi (1979) and Kenney and Lau (1988), described in the section 3.3. Observing the figure 8.6, for particles size less than 3 mm the  $d_{15}/d_{85}$  ratio is higher than 4 (figure 8.6). Implementing the Kenney and Lau criterion (1986), for  $F$  between 0 and 2, the portion of the curve represented by  $H$  is above the line  $H=F$  (figure 8.7). Despite the negative outcome of these checks, the material has a structure able to ensure the minimum design permeability for the biogas drainage layer. The percentage of fine and very fine is very low and hence, the skeleton is prevalent formed by coarse grains of large diameter. Then, in presence of flow, the finer particles can easily pass through its skeleton without producing modifications to the structure of the layer, or reduce the permeability of the material.

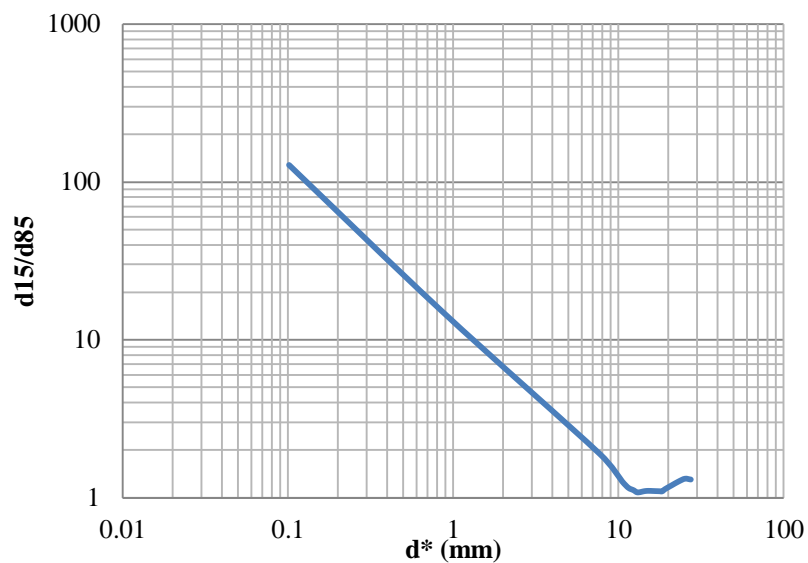


Figure 8.6: Kezdi (1979) internal stability analysis on the natural sample.

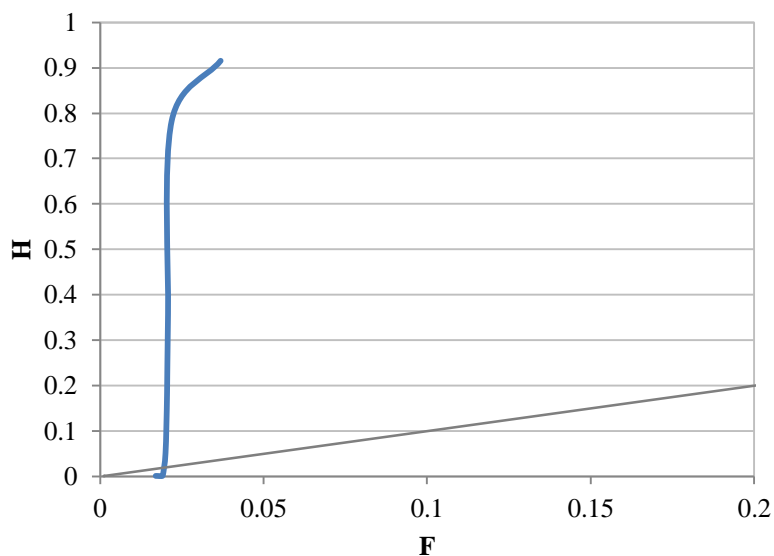


Figure 8.7 : Kenney e Lau (1986) internal stability analysis on the natural sample.



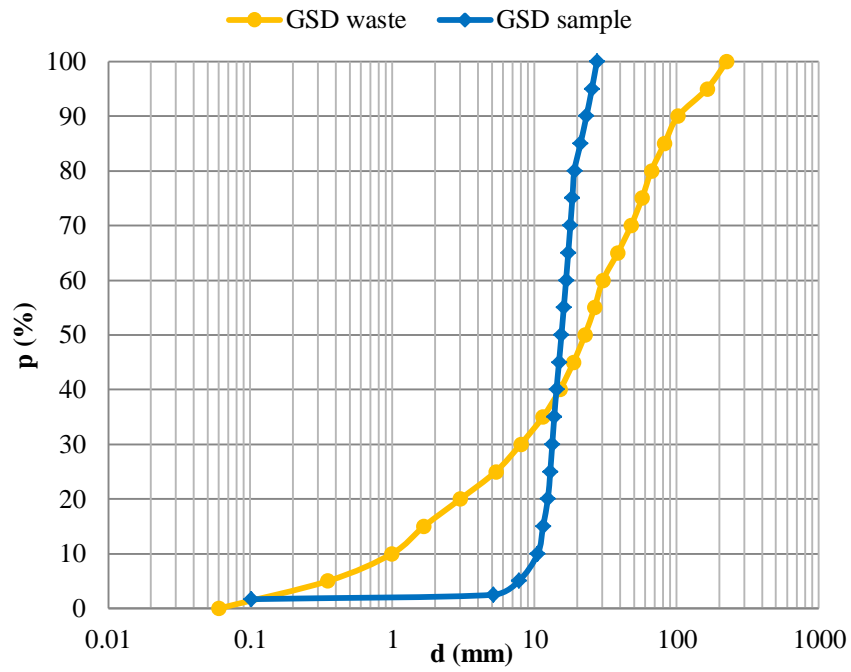


Figure 8.8 : Comparison between the grain size distribution of Jessberger (1994) and that of the sample analyzed.

## ***CHAPTER 9: Analysis of the results obtained by laboratory test***

In analogy with the time sequence of the applied loads, described in the chapter 4, the sample analyzed should be subjected to impacts, sliding, crushing and subsequently, to a static compression. In other words, and in accordance with the description given in the chapter 8, for evaluating its mechanical resistance should be carried out the Los Angeles abrasion test, reported in the section 5.2, while for determining the mechanical behavior at failure should be performed a triaxial test. As reported in chapter 8.1, before carrying out these test, it is necessary to assess whether the material analyzed complies with the particle size requirements. From sieve analysis the sample is gravelly and in proportion not suitable to perform the standard Los Angeles abrasion test. Indeed, and in accordance with standards UNI 1097-2 (section 5.2.1), the percentage passing through the sieve of 12.5 mm is not between 60% and 70% (figure 8.5 and table 8.1). Moreover, it is not possible to determine the effect of the static load on the analyzed sample due to the absence in laboratory of a large scale triaxial cell (section 6.1). Considering as reported above, to estimate the mechanical resistance of the material used for the biogas drainage layer, it is performed a test using the Los Angeles apparatus. Moreover, the hydraulic conductivity will be determined by the Hazen (1892) empirical formula (paragraph 2.6, equation 2.12), given the impossibility of carrying out permeability tests on sample.

### 9.1 Procedure adopted for determining the mechanical resistance of the analyzed sample

In function of what reported in the introduction of the previous chapter, it is not possible to perform the Los Angeles abrasion test, whose procedure is described in paragraph 5.2.1. Therefore, in order to identify if shock, crushing and impacts between the grains influencing the mechanical resistance and the particle size distribution of the material used for the biogas drainage layer, it is tested a material that is representative of that used in the field and of grain size reported in paragraph 8.2.1. The objective is to presume through the Los Angeles apparatus (Figure 5.2), what happens during the installation of the biogas drainage layer.

Consequently, in accordance with the previous statement and the Los Angeles abrasion test procedure, will be carried out a modified test according to the following criteria:

- The abrasive effect is induced by 10 spheres: because of the availability of the geotechnical laboratory at the University of Padua, the steel balls used are not 11;
- The analyzed sample (Table 9.1), formed by the balls and the material (Figure 8.5), is placed in the Los Angeles apparatus;

**Table 9.1: Characteristics of the sample used to perform the modify Los Angeles abrasion test.**

<b>Sample</b>	<b>Weight (kg)</b>
Material weight	16±0.5
Abrasive charge weight (10 spheres)	4,0±0.5

- It is chosen to perform 100, 200 and 500 revolutions with the Los Angeles apparatus: the energy levels transmitted on the sample grows and arrive up to 500 revolutions, required for the standard Los Angeles abrasion test (section 5.2). In this way, the material modifies its outer surface for abrasion and fracture, which are respectively induced by wear and impact, like seen in section 4.3;
- Removed the material from the Los Angeles apparatus, it is carried out particle size analysis for each energy level;

The comparison between the procedure adopted and the Los Angeles abrasion test is shown in Table 9.2.

**Table 9.2: Comparison between the procedure adopted and the Los Angeles abrasion test;**

<b>Requirements</b>	<b>Los Angeles Abrasion test</b>	<b>Test realized by using the Los Angeles apparatus</b>
Weight	5±0.5kg	16±0.5kg
Abrasive effect	11 balls	10 balls
Revolutions	500	100; 200; 500
Speed	31-33 rpm/minute	31-33 rpm/minute
Results	Material retained on a sieve of 1.68 mm	Material sieved on a sieves reported in the sections 8.2.1

By the procedure adopted here, it is possible to define the grain size distribution for each energy level and indirectly, estimate the mechanical resistance of the material. However, this analysis determines only an order of magnitude of the maximum allowable pressure on the material: as seen in section 5.3, the correlation between this pressure and the LA bulk index, is possible only if it is performed the standard Los Angeles abrasion test.

### **9.1.1 Grain size distribution of the sample after 100 revolutions**

After being appropriately washed and dried, the sample is subjected to 100 revolutions using Los Angeles apparatus. As previously mentioned, this test wants to test a material that is representative of that used for the biogas drainage layer. Then, it is possible to observe how all the particles belonging to different grain classes modify their outer surface due to the test procedure described in section 9.1. The weight of the sample inclusive of the steel balls is close to 20 kg (Table 9.1).

Made 100 revolutions, the sample is sieved in order to define the new grain size distribution (Table 9.3 and Figure 9.2).

From the grain size distribution curve it is possible to determine the uniform (Cu) and the curvature (Cc) coefficient, defined in the section 3.1.1, which are respectively equal to 3.03 and 1.7. Therefore the material can be considered still uniform and, as it shown in figure 9.2, gravelly. Consequently, the permeability its associated will be greater than the minimum required for the biogas drainage layer. Therefore, the material should present a structure able to ensure the minimum design permeability.



Figure 9.1: Appearance of the crushed sample after 100 revolutions and 10 steel balls;

Table 9.3: Grain size analysis of the sample after 100 revolutions and 10 steel balls;

Sieve size [mm]	Percentage of weight passing the sieve (%)
0.074	3.72
0.105	3.95
0.177	4.76
0.25	5.37
0.42	5.85
0.84	6.42
2	7.37
4.76	9.57
10	21.99
12.5	39.48
14	53.60
19.1	86.57
25.4	96.77

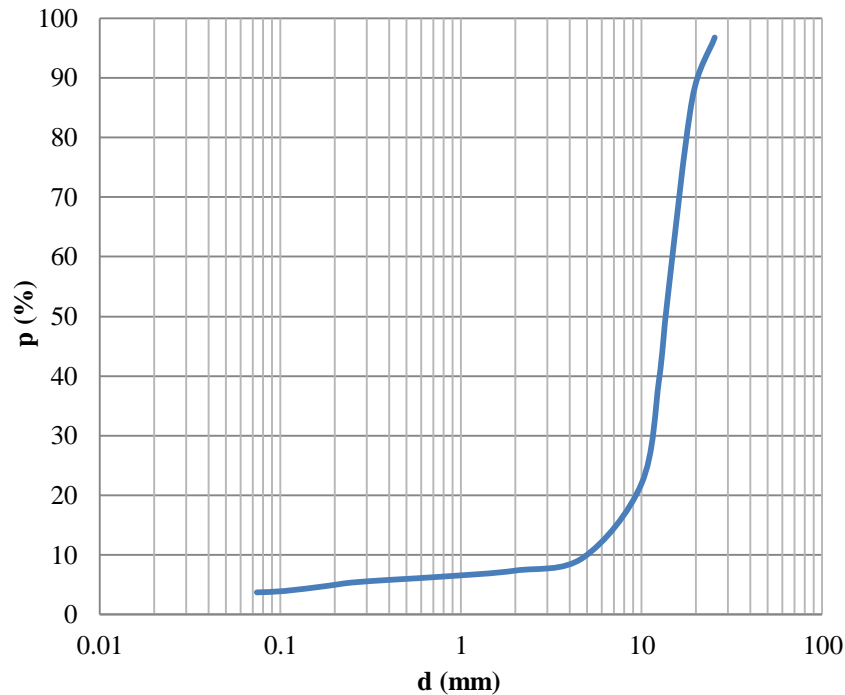


Figure 9.2: Grain size distribution of the sample after 100 revolutions and 10 steel balls.

### 9.1.2 Grain size distribution of the sample after 200 revolutions

Following the particle size analysis downstream 100 revolutions, the same sample is subjected to an additional 100 revolutions. . Since is not washed this weight was unchanged (Table 9.1). As shown in the figure 9.3, as a result of this test the sample is further crushed and fractured. Through sieve analysis of this material, it is determined the new particle size distribution curve, which is shown in table 9.4 and figure 9.4.

From the grain size distribution curve it is possible to determine the uniform ( $C_u$ ) and the curvature ( $C_c$ ) coefficient, defined in the section 3.1.1, which are respectively equal to 7.61 and 3.8. Therefore the material can be considered poor graded and, as it shown in figure 9.7, gravelly. Consequently, the permeability its associated will be greater than the minimum required for the biogas drainage layer. Therefore, the material should present a structure able to ensure the minimum design permeability.



Figure 9.3: Appearance of the crushed sample after 200 revolutions and 10 steel balls;

Table 9.4: Grain size analysis of the sample after 200 revolutions and 10 steel balls;

Sieve size [mm]	Percentage of weight passing the sieve (%)
0.074	3.34
0.105	3.58
0.177	4.38
0.25	5.33
0.42	6.50
0.84	8.54
2	10.28
4.76	13.89
10	30.79
12.5	47.05
14	62.08
19.1	90.12
25.4	98.11

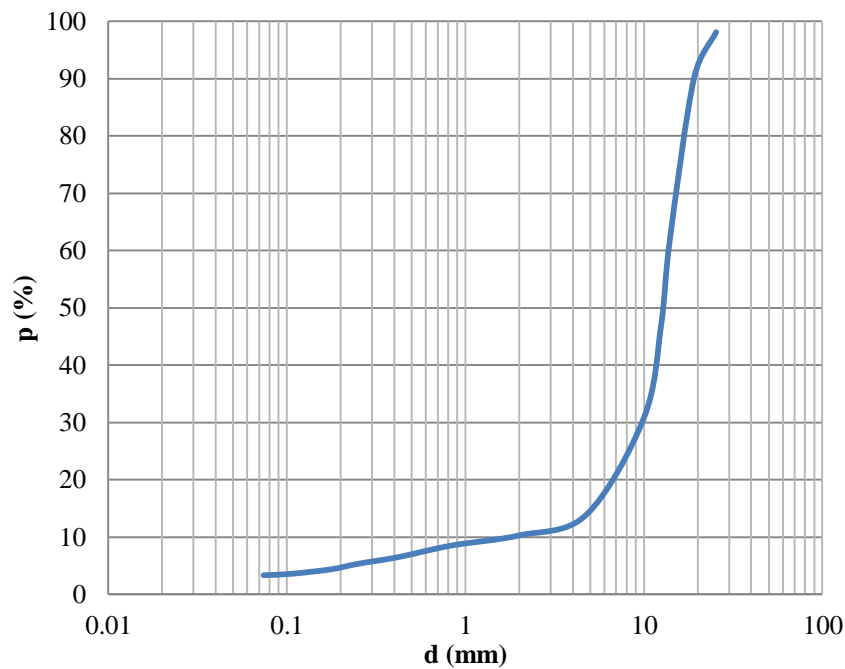


Figure 9.4: Grain size distribution of the sample after 200 revolutions and 10 steel balls.

### 9.1.3 Grain size distribution of the sample after 500 revolutions

Following the sieve analysis downstream 200 revolutions, the same sample is subjected to an additional 300 revolutions. Since is not washed this weight was unchanged (Table 9.1). As shown in the figure 9.5, as a result of this test the sample is further fractured and crushed. Through the sieve analysis of this material, it is determined the new particle size distribution curve, which results are shown in table 9.5 and figure 9.6.

Performing 500 revolutions using Los Angeles apparatus, can be estimated Los Angeles bulk index, LA (%). As mentioned in section 9.1, it is correlated with the allowable pressure acted on the material and thus, comparable with the maximum vertical stress induced by the compaction of the material forming the hydraulic barrier (section 4.2).

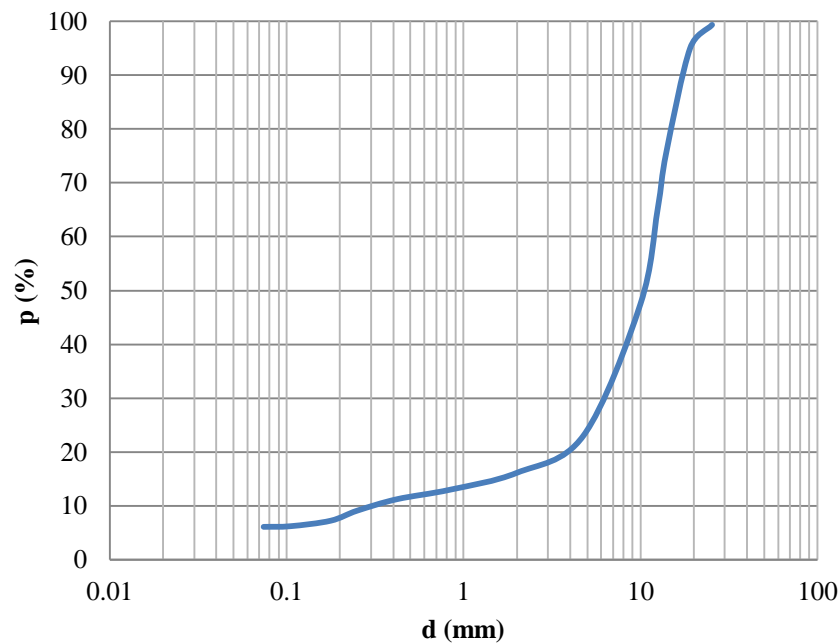




Figure 9.5: Appearance of the crushed sample after 500 revolutions and 10 steel balls;

Table 9.5: Grain size analysis of the sample after 500 revolutions and 10 steel balls;

Sieve size [mm]	Percentage of weight passing the sieve (%)
0.074	6.09
0.105	6.21
0.177	7.23
0.25	9.10
0.42	11.23
0.84	13.00
2	16.13
4.76	23.03
10	47.52
12.5	65.05
14	75.67
19.1	95.04
25.4	99.36



**Figure 9.6: Grain size distribution of the sample after 500 revolutions and 10 steel balls.**

From the grain size distribution curve it is possible to determine the uniform ( $C_u$ ) and the curvature ( $C_c$ ) coefficient, defined in the section 3.1.1, which are respectively equal to 36.6 and 10.3. Therefore the material can be considered well graded and, as it shown in figure 9.6, gravelly. Consequently, the permeability its associated will be greater than the minimum required for the biogas drainage layer. Therefore, the material should present a structure able to ensure the minimum design permeability.

## 9.2 Mechanical resistance of the analyzed sample

From the particle size distribution curve of the sample obtained after 500 revolutions (Figure 9.6) it is possible to estimate the bulk index LA, defined in paragraph 5.2. In accordance with the modality of the test here performed and explained in section 9.1, this index defines only an order of magnitude of the maximum allowable pressure of the tested material (UCS).

Given the unavailability in the university laboratory of the sieve of dimension equal to 1.68 mm (required for the determination of the bulk index LA, Table 9.2), the LA index it is assume equal to the percentage by weight passing through a sieve sized of 2 mm and therefore to 16% (Figure 9.6 and table 9.4). Using this value and the equation 5.7 ( section 5.3) it is possible to obtain a value of the maximum allowable pressure (UCS) equal to:

$$UCS = \exp \left( \frac{88.01 - 16}{12.35} \right) = 337MPa \quad (5.7)$$

This value of UCS is a function of the intrinsic characteristics of the material analyzed, and therefore, independent of its size (section 5.3). Then, the results here obtained may be associated with a particle having a diameter equal to the thickness of the biogas drainage layer and hence, comparable with the maximum vertical stress induced by the compaction of the material forming the hydraulic barrier. As seen in section 4.1, this pressure has intensity equal to 1750 kPa (1.75 MPa) lower than 337 MPa. Therefore, according to this result, the material bears the static load without failure. This result is only indicative because: the modality of the test used is not standard (section 9.1), the analyzed material does not have a uniform and homogenous properties (section 8.2). Therefore, to observe these conclusions it is appropriate performing in situ test, identifying a portion of the landfill cover in which it is applied loads higher than that induced by the maximum compaction pressure. Then, it will be necessary to define the new grain size of the material used for the biogas drainage layer and contextually, will be verified the behavior of geotextile used to separate the biogas drainage layer and the hydraulic barrier.

### **9.3 Effect of the different energy levels on the grains size distribution of the analyzed sample**

According to the results obtained and reported in the sections 9.1.1, 9.1.2, 9.1.3, after 100, 200 and 500 revolutions by Los Angeles apparatus, the different grain size distribution are comparable because:

- The sample tested is always the same: the material weight remains constant because it is not washed (table 9.1);
- The abrasive charge is always represented by 10 steel spheres (table 9.2);
- The energy imprinted increases gradually up to its maximum, characterized by 500 revolutions (section 9.1);
- The revolutions speed is constant and varies between 31 and 33 rpm/minute (table 9.2);
- The grain size analysis is performed by using the same sieve (table 9.2).

In this way, it is possible to have a direct comparison among the energy, the original grain size distribution and the breakage material (figure 9.7).

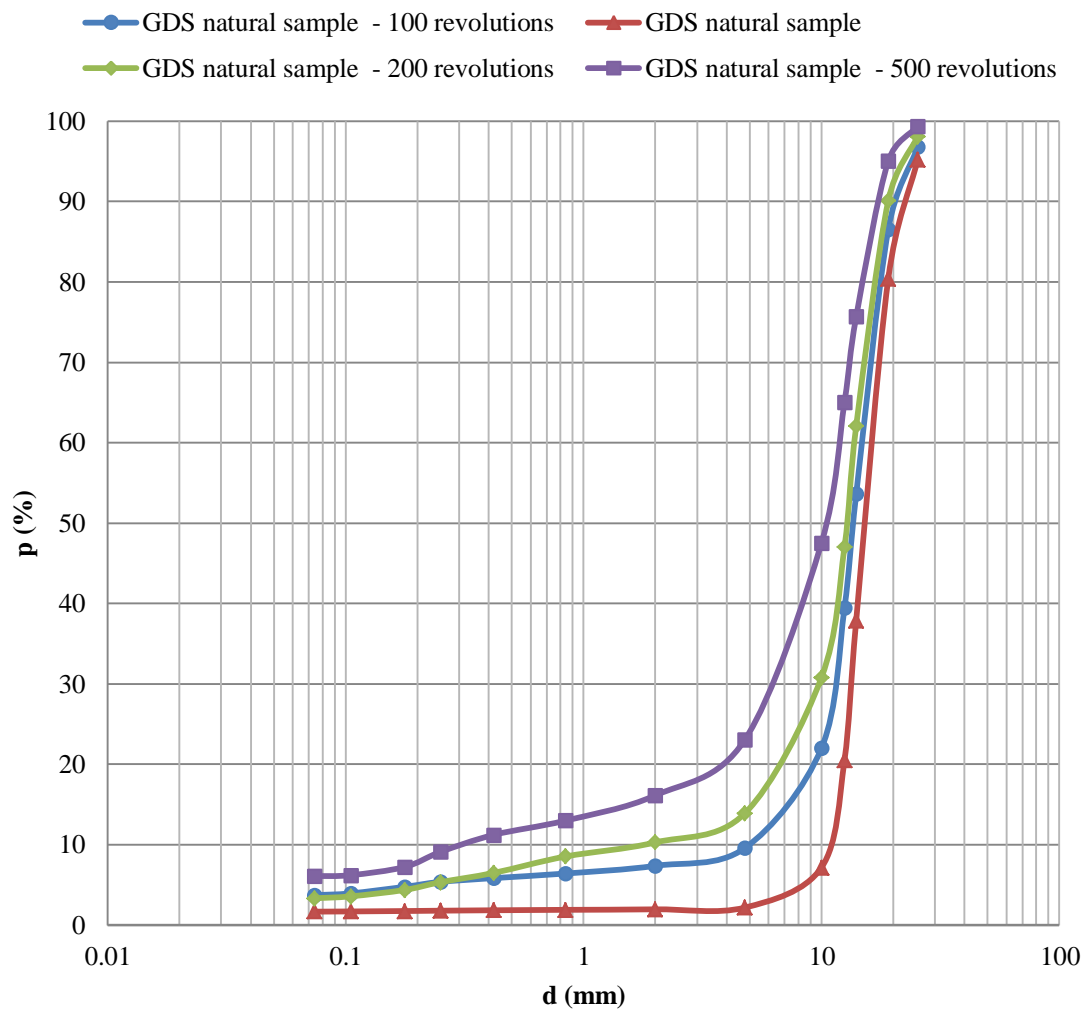
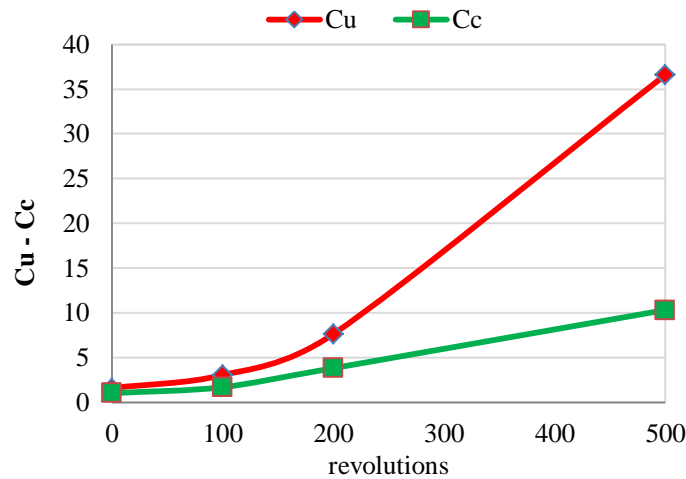


Figure 9.7 : Comparison of the grain size distribution obtained after 100, 200 and 500 revolutions.

When comparing these curves obtained for each energy level, it is observed that:

- As expected, the amount of the material breakage increase with the energy: the grain size distributions shift toward lower diameter increasing the percentage of fine fraction;
- The uniform material becomes well graded (figure 9.8): abrasion and attrition erodes the external surface of the grains, reducing its dimension, as explained in the section 4.3;



**Figure 9.8: Trend of the uniformity coefficient (Cu) and curvature (Cc) as a function of the energy level imparted to the material.**

- The dimension of the material remain almost the same and as said before of the gravel: the material has a good mechanical properties;
- The fine fraction increase more rapidly than the intermediate ones (Figure 9.9): fracture and attrition reduces coarse particles into smaller parts, which are generally brittle (section 5).

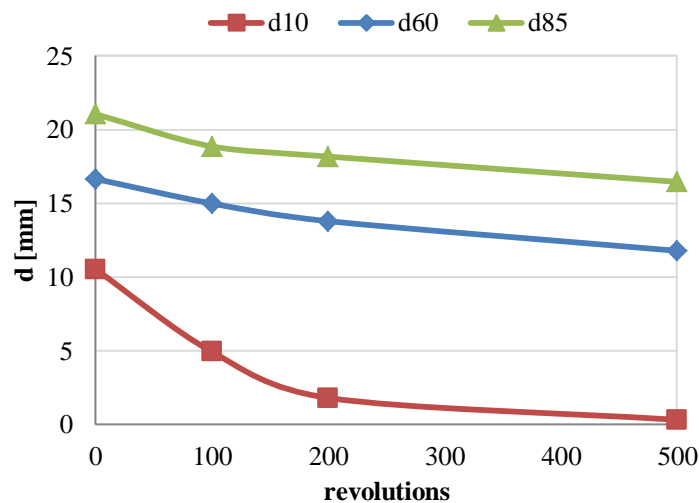


**Figure 9.9: Trend of the effective diameter (d10), the d60 and d85 in function of energy level imprinted.**

#### 9.4 Effect of grains breakage on the hydraulic conductivity of the sample analyzed

The hydraulic conductivity, obtained through the Hazen equations (1892) (section 2.5), is calculated for each particle size distribution (Section 9.1) curve obtained for any energy levels. In table 9.6 are given the results obtained from this calculation. In Figure 9.10 is shown the

trend of the hydraulic conductivity as a function of the energy content. It is observed that in the very extreme energy, represented by 500 revolutions, the hydraulic conductivity is equal to  $10^{-2}$  m/s. This value is higher than the minimum required, calculated in the section 2.6, and then the material tested is suitable for the biogas drainage layer.

**Table 9.6: Hydraulic conductivity calculated by the Hazen relationship (1892) in function of the energy imprinted.**

Revolutions	d10 [mm]	Hazen K [m/s]
0	10.53	1.10
100	4.94	0.24
200	1.81	0.033
500	0.32	0.0010

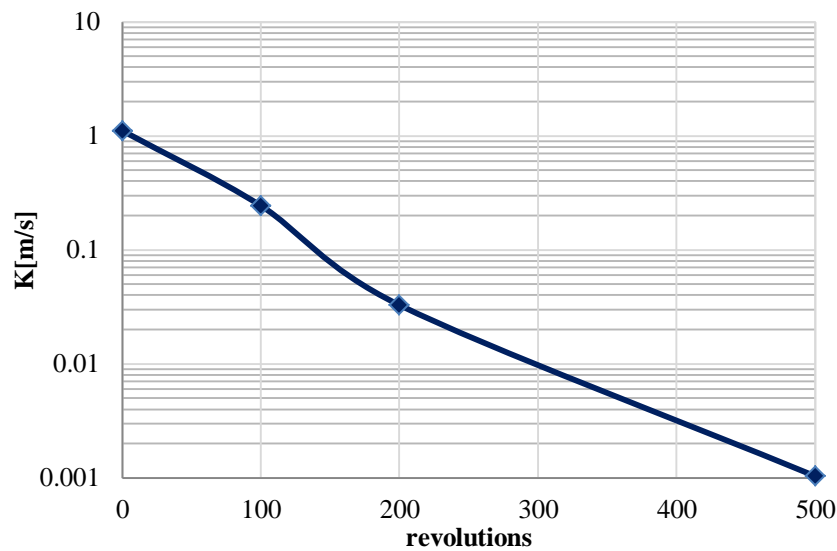


**Figure 9.10: Trend of hydraulic conductivity as a function of the energy imparted to the material.**



**Figure 9.11: Comparison between the natural sample a) and that obtained after 500 revolutions b).**

#### 9.4.1 Determination of the particle breakage factors and their correlation with the energy and the hydraulic conductivity

To quantify the amount of breakage material are determined particle breakage factors, described in Chapter 7, and evaluated in function of grain size distribution (Section 9.1), obtained following the different energy levels imparted on the material (Table 9.7).

As expected, for each energy level the amount of material breakage increase with the energy imprinted. The Marsal index (1967), equation 7.1, shows a variation in percentage for each diameter belonging to the particle size distribution of 2.29%. This value, as represented in Figure 7.4, indicates the variation in percentage by weight of a diameter representative of the sample tested that, in the present case, is around to 10 mm (Figure 9.7). Therefore the gradations curve does not shift substantially from the larger to the smaller sieve.

The Lee and Farhoomand index (1967), equation 7.2, expresses the change in the diameter corresponding to 15%,  $d_{15}$ . It is observed that after 500 revolutions, this diameter is increased 7.25 times.

The Hardin index (1985), equation 7.3, identifies a ratio between areas (Figure 7.5). In the present case, the area between the curve crushed (500 revolutions) and the original one is equal to 0.24. Therefore, the original grain size distribution is reduced of this quantity.

Finally, the Lade index (1996), equation 7.4, shows that the diameter  $d_{10}$ , also used for the Hazen's empirical formula (1892), is reduced of 0.97: it has almost reached the maximum limit value, which is 1. Consequently a further crushing, induced by a higher energy content, result in a ratio between the diameter  $d_{10\text{final}}$  (crushed) and  $d_{10\text{initial}}$  (original) very small. It can be explained observing that the  $d_{10\text{final}}$  assumes values lower than 0.074 mm.

**Table 9.7: Values of Marsal (1967), Lee and Farhoomand (1967), Hardin (1985) and Lade (1996) breakage factor in function of the energy imprinted.**

<b>Revolutions</b>	<b>B(%) Marsal (1967)</b>	<b>B Lee and Farhoomand (1967)</b>	<b>Br Hardin (1985)</b>	<b>B10 Lade (1996)</b>
0	0	0	0	0
100	0.94	1.63	0.095	0.53
200	1.35	2.25	0.15	0.83
500	2.29	7.25	0.24	0.97

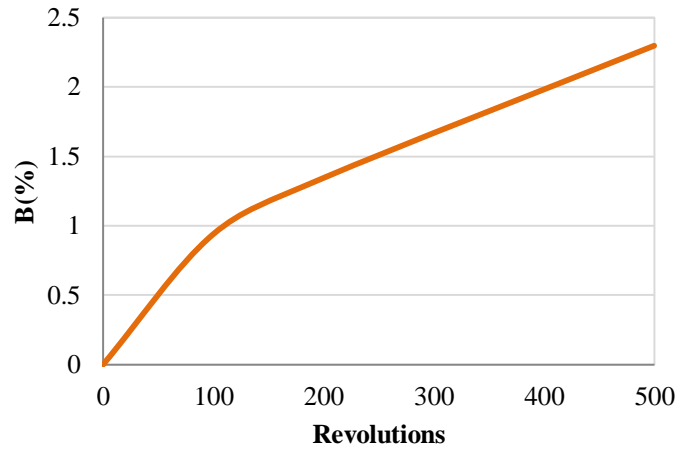


Figure 9.12: Trend of Marsal breakage factor, B (%), in function of the imparted energy.

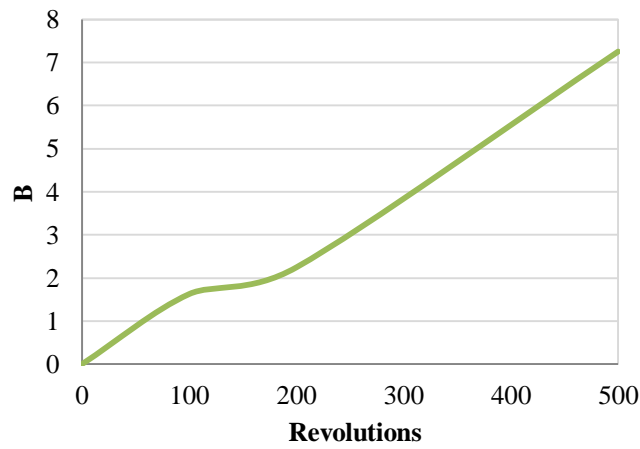


Figure 9.13: Trend of The Lee and Farhoomand breakage factor (1967) ,B, in function of the imparted energy.

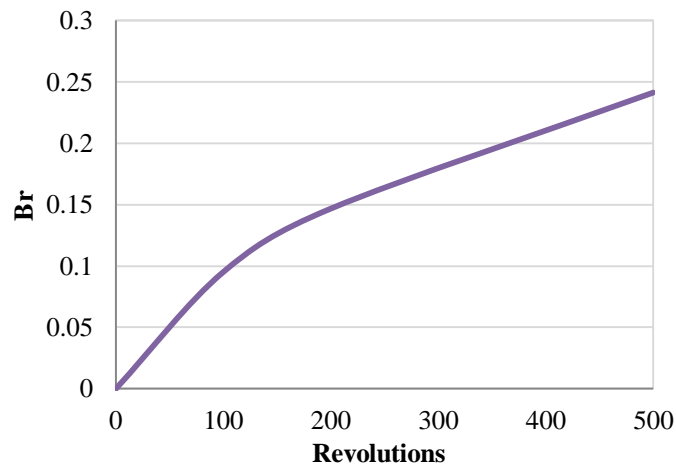


Figure 9.14: Trend of Hardin breakage factor (1985), Br, in function of the imparted energy.



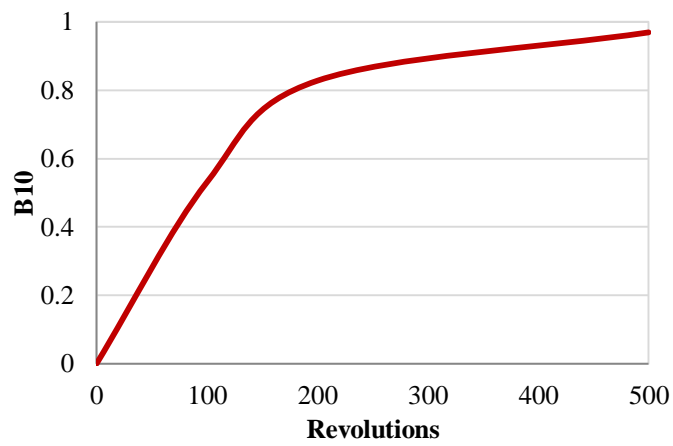


Figure 9.15: Trend of Lade breakage factor, B10, in function of the imparted energy.

As expected, the hydraulic conductivity decreases with the amount of breakage material (Figure 9.26).

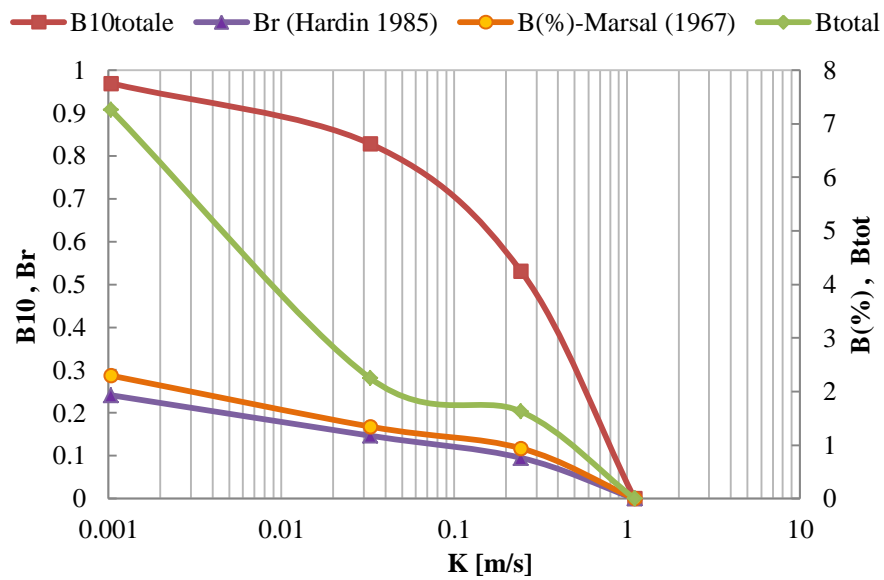


Figure 9.16: Trend between the breakage factor indexes and the hydraulic conductivity.

## **CHAPTER 10: Conclusions**

The material used for the biogas drainage layer for the nonhazardous waste landfill of Torretta, should possess the following minimum geotechnical requirements (section 2.6 and 3.4):

- Hydraulic conductivity higher than or equal to  $10^{-4}$  m/s;
- Grain size typical or higher than that of coarse sands.

As reported in the introduction and chapter 2, these properties are determined with the aim to preserve the final landfill cover slope stability against the excess of pore gas pressure. In order to determine the hydraulic conductivity must be carried out the permeability tests of the sample; instead, to define the particle size characteristics it is necessary to perform sieve analysis.

The biogas drainage layer, as reported in the Chapter 4, is subject to various types of actions, which can be summarized as follow:

- Fracturing, attrition and wear induced by dynamic efforts explicated during the installation and induced by grains contacts, sliding and impacts;
- Compression induced by quasi-static and static load, respectively due to compaction of the material forming the hydraulic barrier and for the weight of the overlying layers.

Due to these loads, the material forming the biogas drainage layer can arrive at failure and can change the geotechnical requirements for which is chosen: permeability and grain size distribution. Therefore, in order to observe if the particles of the material, due to shocks, impacts, friction and compressions, break for fracture, attrition and abrasion, should be

necessary to carried out tests able to determine its mechanical resistance (Chapter 4). Therefore, and by the study reported in chapter 8, in order to support the efforts explicated during the installation phase, the material must possess a certain quality which is expressed in terms of hardness, toughness and abrasion resistance (Chapter 5). Consequently, for this purpose and in function of the minimum grain size requirements reported in chapter 2 and 3, the Los Angeles abrasion test appears the most suitable (section 5.2). This test is used to design roads, which for their function and loads, are more stressed than the biogas drainage layer. Therefore, through it, the energy transmitted to the material will be presumably greater than that present in the field.

In order to assess the ability of the material to bear stresses induced by the compaction of the hydraulic barrier, and by the weight of the strata placed above the biogas drainage layer, should be carried out a loading compression triaxial test (Chapter 6). In this way, it is possible to observe whether the grains of the material due to isotropic (consolidation phase) and axial pressure (compression phase) break changing its structure. This assumption can be made considering that, in this second phase, the biogas drainage layer is confined and then, because of pressure induced by the foot sheep roller, it develops vertical stresses which are comparable to those induced by a structure on a ground and hence, solved by soil-foundation elastic theory (section 8.1.3).

The layer in question is placed below the hydraulic barrier and then, it is not excluded the possibility of employing a waste material, suitably selected and complies with the requirements of acceptability of non-hazardous waste landfill. For example, in the case of exam, it is chosen a waste incineration material (paragraph 8.2). As shown in chapter 8.2.1, is gravelly and therefore its hydraulic conductivity is greater than the minimum required. This material, as reported in Chapter 9, does not have a grain size for which it is possible to carry out the standard Los Angeles abrasion and triaxial tests. Then, in order to identify its mechanical and breakage resistance, is performed a test using the Los Angeles apparatus (chapter 9). The good results, obtained from the acceptability analysis of the sample conducted in the laboratory, show that the material after different shocks and dynamic stresses, of entity higher than those observed in the situ, is able to ensure the minimum design permeability. Concluding the analyzed material can be used as a granular medium for the biogas drainage layer: it supports the efforts explicated during the realization of that layer and the installation of the overlying hydraulic barrier.



**REFERENCES**

- Alamgir, M., McDonald, Ch., Roehl, K.E., Ahsan A. (Eds.) (2005). Integrated Management and Safe Disposal of Municipal Solid Waste in Least Developep Asian Countries. A Feasibility Study. p 83. Khulna University of Engineering and Technology, Khulna,Bangladesh;
- Al-Harti, A.A. (2001), "A field index to determine the characteristics of crushed aggregate", Derpartment of Engineering and Environmental Geology, Faculty of Earth Sciences, King Abdulaziz University, Bull Eng Geol (2001) 60:193-200;
- Al Hattamleh O. et al. (2013), "The Consequence of Particle Crushing in Engineering Properties of Granular Materials", International Journal of Geosciences, 2013, 4, 1055-1060;
- Andrianatrehina et al. (2012), "Internal stability of granular materials in triaxial tests", ICSE6 Paris - August 27-31;
- Biarez J., Hicher P.-Y., (1997). Influence de la granulométrie et de son évolution par ruptures de grains sur le comportement mécanique de matériaux granulaires. Revue française de génie civil 1 (4), 607–631;
- Daouadj A., Hicher y.(2010), "An enhanced constitutive model for crushable granular materials", International journal for numerical and analytical methods in geomechanics, 34:555–580;
- Daouadji A, Hicher PY, Rahma A. (2001) "An elastoplastic model for granular materials taking into account grain breakage", European Journal of Mechanis Solids 2001; (20):113–137;
- de Graauw, A.F., van der Meulen, T., van der Does de Bye, M.R. (1984), "Granular Filters: Design Criteria", Journal of Waterway, Port, Coastal and Ocean Engineering, 110(1), 80-96;
- DeJong J.T., Geoffrey C. (2009), "Influence of Particle Properties and Initial Specimen State on One-Dimensional Compression and Hydraulic Conductivity", Journal of Geotechnical and Geoenvironmental Engineering, Vol. 135, ASCE, 3-449–454;
- Dixon, N., Russell, D., Jones, V. (2005), "Engineering properties of municipal solid waste", Geotextiles and Geomembranes, 23(3), 205-233;

- Einav, I., (2007). “Breakage mechanics—Part II: Modelling granular materials”, *J. Mech. Phys. Solids*, 55 (2007) 1298–1320;
- Fernlund J.M.R. (2005), “3D image analysis size and shape method applied to the evaluation of the Los Angeles test”, Department of Land and Water Resources Engineering, KTH, 100 44 Stockholm, Sweden, *Engineering Geology*, 77, 57–67;
- Giroud, J.P., Bachus, R.C. and Bonaparte, R. (1995) “Influence of Water Flow on the Stability of Geosynthetic-Soil Layered Systems on Slopes”, *Geosynthetics International*, Vol. 2, No. 6, pp. 1149-1180;
- Göktepe A. B., A. Sezer ,(2009),“Effect of particle shape on density and permeability of sands”, *Geotechnical Engineering* 163, 307-320;
- Hardin, B. O. (1985). "Crushing of soil particles", *Journal of Geotechnical Engineering*, ASCE, 111(1 0), 1177- 1192;
- Hicher P.-Y., Kim M.S., Rahma A., (1995). “Experimental evidence and modelling of grain breakage influence on mechanical behavior of granular media”, International Workshop, “Homogenization, Theory of Migration and Granular Bodies”, Gdansk–Kormoran, pp.125–133;
- Hu W, Yin Z Y, Dano C, et al. (2011) “A constitutive model for granular materials considering grain breakage”, *Sci China Tech Sci*, 54: 2188–2196;
- Hyun Il, P., Borinara, P., Hong, K.D. (2011), “Geotechnical Considerations for End-Use of Old Municipal SolidWaste Landfills”, *International Journal of Environmental Research*, 5(3), 573-584;
- Jessberger, H. L. (1994). “Design Procedures of Engineered Waste Landfills. Proc”., Meeting of Geotechnical Engineering Geotechnics in the Design and Construction of Controlled Waste Lnadfills, Milazzo (ME), Associazione Poligeotecnici Riuniti;
- Justine Odong, (2013), “Evaluation of Empirical Formulae for Determination of Hydraulic Conductivity based on Grain-Size Analysis”, *International Journal of Agr. & Env.* [01];
- Kahraman S., Fener M. (2007), “Predicting the Los Angeles abrasion loss of rock aggregates from the uniaxial compressive strength”, Mining Engineering Department, Nigde University, 51100 Nigde, Turkey, Geological Engineering Department, Nigde University, 01330 Nigde, Turkey, 4861–4865;
- Kenney, T.C., Lau, D. (1986), “Internal stability of granular filters: Reply”, *Canadian Geotechnical Journal*, 23(3), 420-423;
- Kezdi, A. (1969), “Increase of protective capacity of flood control dikes”, Department of Geotechnique, Technical University, Budapest, Hungary;

- Lade P.V., Yamamuro A., Bopp Paul A., (1996), “Significance of particle crushing in granular materials”, *Journal of Geotechnical Engineering, ASCE*, 122:309-316;
- Lee K.L., Farhoomand I., (1967). “Compressibility and crushing of granular soils in anisotropic triaxial compression”, *Canadian Geotechnical Journal*, Vol. 4, No. 1, 1967, pp. 68-86;
- Marsal R.J., (1967). “Large scale testing of rockfill materials”, *Journal of the Soil Mechanics and Foundations Division* 93 (SM2), 27–43;
- Millard, R.S. (1993). *Road building in the Tropics*. Transport Research Laboratory State-of-the-art Review 9, HMSO, London;
- Moraci, N., Tondello, M. (1996), “La progettazione dei filtri nell’ingegneria marittima”, *Atti IV Convegno AIOM, Padova*;
- Musso, A., Federico, F. (1983), “Un metodo geometrico-probabilistico per la verifica dei filtri”, *Rivista Italiana di Geotecnica*, 4, 177-193;
- Raut, A.K. (2006), “Mathematical modelling of granular filters and constriction-based filter design criteria”, PhD Thesis, University of Wollongong, Australia;
- Thiel, R.S. (1998), “Design and Testing of a NWNP Geotextile Gas Pressure Relief Layer Below a Geomembrane Cover to Improve Slope Stability”, *Geosynthetics International*;
- Thiel, R.S. (1998), “Design Methodology for a Gas Pressure Relief Layer Below a Geomembrane Landfill Cover to Improve Slope Stability”, *Geosynthetics International*, 5(6), 589-617;
- Ugur et. al.(2010) “Effect of rock properties on the Los Angeles abrasion and impact test characteristics of the aggregates”, *materials characterization*,61 ,90-96;
- Wan, C.F., Fell, R. (2008), “Assessing the Potential of Internal Instability and Suffusion in Embankment Dams and Their Foundations”, *Journal of Geotechnical and Geoenvironmental Engineering*, 134(3), 401-407.
  
- Decreto legislativo 36 del 13/01/2003;
- Decreto Legislativo 13 gennaio 2003, n. 36: [www.camera.it](http://www.camera.it);
- Decreto ministeriale 11 marzo 1988: [www.attiministeriali.miur.it](http://www.attiministeriali.miur.it);
- Bonaparte et. al. (2004), “(Draft) Technical Guidance, For RCRA/CERCLA Final Covers, EPA
- ISRM (1998). “Metodi suggeriti per a determinazione della durezza e dell’abrasività delle rocce”, *Rivista italiana di geotecnica* 2, 64-70;

- SS (1974). SS73:1974 “Specification for methods for sampling and testing of mineral aggregates, sand and fillers” - Determination of aggregate impact value, aggregate crushing value and ten percent fines value. Singapore Standard, Singapore.
- UNI EN 1097-2:2010;
  
- Colombo P. e Colleselli F., (2012), “Elementi di geotecnica” , Zanichelli;
- Harold N. Atkins, (2003), “Highway materials, Soils and Concretes”, Prentice Hall;
- Yang H. Haung, (2003), “Pavement Analysis and Design (3<sup>rd</sup> edition)”, Prentice Hall.
  
- Favaretti M.: “Environmental geotechnics”. Academic year 2012-2013, Università degli studi di Padova.
  
- Busana S. : Progetto preliminare della copertura superficiale finale della discarica di rifiuti urbani e/o non pericolosi di Torretta (Legnago), 2015;
  
- Cover Slope Stability: Landfill Gas Pressure: [www.ladfilldesign.com](http://www.ladfilldesign.com);
- Landfill gas pressure relief layer: [www.ladfilldesign.com](http://www.ladfilldesign.com);
- Slope stability sensitivities of final covers: [www.geosyntheticmagazine.com](http://www.geosyntheticmagazine.com) .